GEOLOGICA ULTRAIECTINA

Mededelingen van de
Faculteit Aardwetenschappen
Universiteit Utrecht

No. 122

# Magnetic Minerals in Pliocene and Pleistocene Marine Marls from Southern Italy

## Rock Magnetic Properties and Alteration during Thermal Demagnetization

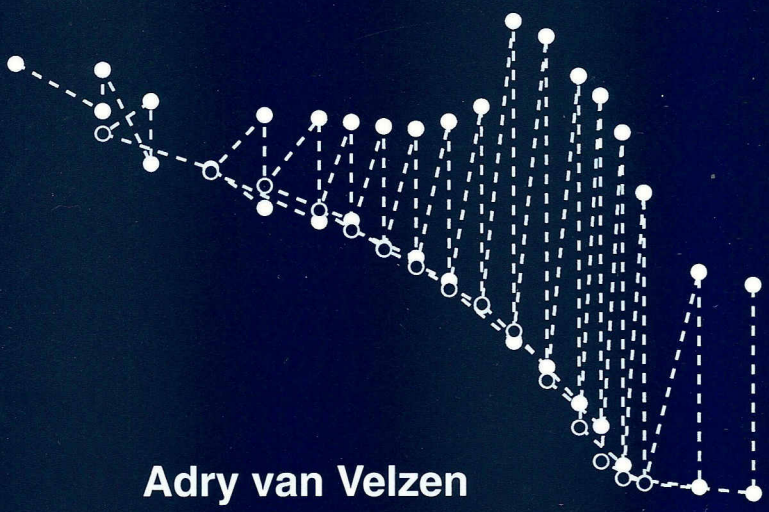

**Adry van Velzen**

GEOLOGICA ULTRAIECTINA

Mededelingen van de
Faculteit Aardwetenschappen
Universiteit Utrecht

No. 122

# Magnetic Minerals in Pliocene and Pleistocene Marine Marls from Southern Italy

## Rock Magnetic Properties and Alteration during Thermal Demagnetization

CIP-GEGEVENS KONINKLIJKE BIBLIOTHEEK, DEN HAAG

Velzen, Adrianus Johannes van

Magnetic minerals in Pliocene and Pleistocene marine marls from southern Italy: Rock magnetic properties and alteration during thermal demagnetization / Adrianus Johannes Van Velzen. - Utrecht: Faculteit Aardwetenschappen, Universiteit Utrecht. - (Geologica Ultraiectina, ISSN 0072-1026 ; no. 122)
Proefschrift Universiteit Utrecht. - Met lit. opg. - Met samenvatting in het Nederlands.
ISBN 90-71577-76-7
Trefw.: sedimentologie ; Zuid-Italië / paleomagnetisme

# Magnetic Minerals in Pliocene and Pleistocene Marine Marls from Southern Italy

## Rock Magnetic Properties and Alteration during Thermal Demagnetization

Magnetische mineralen in Pliocene en Pleistocene mariene mergels uit Zuid-Italië - Gesteentemagnetische eigenschappen en omzettingen tijdens thermische demagnetisatie
(met een samenvatting in het Nederlands)

PROEFSCHRIFT

TER VERKRIJGING VAN DE GRAAD VAN DOCTOR AAN DE UNIVERSITEIT UTRECHT OP GEZAG VAN DE RECTOR MAGNIFICUS PROF. DR. J. A. VAN GINKEL INGEVOLGE HET BESLUIT VAN HET COLLEGE VAN DEKANEN IN HET OPENBAAR TE VERDEDIGEN OP DONDERDAG 16 JUNI 1994 DES MIDDAGS TE 12.45 UUR

DOOR

Adrianus Johannes Van Velzen

geboren op 10 januari 1959 te Geleen

| | | |
|---|---|---|
| Promotor: | Prof. Dr. J.D.A. Zijderveld | Faculteit Aardwetenschappen |
| Co-promotor: | Dr. M.J. Dekkers | Faculteit Aardwetenschappen |

*Caminante no hay camino*
*se hace camino al andar,*
*al andar se hace camino*
*y al volver la vista atrás*
*se ve la senda que nunca*
*se ha de volver a pisar.*

Antonio Machado

# Contents

Research was conducted at:
Paleomagnetic Laboratory 'Fort Hoofddijk'
Institute of Earth Sciences, Utrecht University
Budapestlaan 17,
3584 CD Utrecht
The Netherlands

## Bibliography

The following chapters have been published or are submitted for publication:

Chapter 2:
van Velzen A.J. and Zijderveld J. D. A.,
Rock magnetism of the Early Pliocene Trubi formation at Eraclea Minoa (Sicily). Geoph. Res. Lett., 17, 791-794,1990.

Chapter 3:
van Velzen A.J. and Zijderveld J.D.A.,
A method to study alterations of magnetic minerals during thermal demagnetization applied to a fine-grained marine marl (Trubi formation, Sicily). Geophys. J. Int., 110, 79-90, 1992.

Chapter 4:
van Velzen A.J. and Zijderveld J.D.A,
Effects of weathering on single domain magnetite in Early Pliocene marine marls. Submitted to Geophys. J. Int.

Chapter 5:
van Velzen A.J., Dekkers, M.J. and Zijderveld, J.D.A.,
Magnetic iron-nickel sulphides in the Pliocene and Pleistocene marine marls from the Vrica section (Calabria, Italy). Earth Planet. Sci. Lett., 115, 43-55, 1993.

# Summary

The rock magnetic properties of two different Pliocene to Pleistocene marine marls from southern Italy are studied. Different conditions during sedimentation have led to two completely different magnetic mineralogies in these marls. Chapters 2, 3 and 4 examine the rock magnetic properties of the Early Pliocene marine marls of the Trubi formation sampled at Eraclea Minoa in the Caltanissetta basin on southern Sicily (photo 1). These pelagic marls are characterized by a high carbonate content (60-80%), a sedimentation rate of 4-5 cm/ky and a cyclic lithology related to the Earth's orbital cycles. Magnetite is the primary remanence carrier in the Trubi marls. In chapters 5, 6 and 7 rock magnetic results for the Late Pliocene-Early Pleistocene marine marls of the Vrica section are presented (photo 2). The Vrica section is the Pliocene-Pleistocene boundary stratotype, situated in the Crotone-Spartivento basin of northern Calabria. The marls were deposited in shallower water with a sedimentation rate between 25 and 50 cm/ky and they have a carbonate content of only 15-25%. In these marls the climatic fluctuations caused by the Earth's orbital cycles are expressed as frequently occurring sapropelitic layers. Magnetic sulphides are the main magnetic minerals in the Vrica marls.

In chapter 2 rock magnetic properties of the Trubi marls are investigated. Measurements include acquisition of isothermal remanent magnetization (IRM), alternating field (AF) demagnetization and thermal demagnetization of IRM, hysteresis measurements and low-temperature cycling of IRM to liquid nitrogen temperature. Single domain (SD) magnetite is found to be the main remanence carrier in the Trubi marls.

In chapter 3 a method is presented to study alterations of magnetic minerals during stepwise thermal demagnetization. The method monitors changes in total IRM and the coercivity spectrum of the IRM in order to specify which magnetic fractions are affected by alterations. The results confirm that magnetite is the main carrier of the remanent magnetization. During heating above 390°C new grains with magnetite-like properties are formed in the marls, most likely by alteration of pyrite. The formation is indicated by an increase of magnetic susceptibility and total IRM and by the occurrence of viscous magnetizations. Part of the demagnetization above 500°C is shown to be the result of the alteration of magnetite to hematite, but this does not affect the analysis of the NRM directions.

At about 150°C an alteration is detected that is important for the analysis of the NRM. Almost all IRM with AF coercivities higher than 100 mT disappears after heating to 150°C whereas the IRM with AF coercivities lower than 100 mT increases. This alteration is attributed to a reduction of coercivity in SD magnetite grains due to the relaxation of stress. In chapter 4 the latter alteration is subject of a more comprehensive investigation. It appears that the major part of the variation in remanent coercivities in the marl sections has to be attributed to the effects of weathering. After heating to 150°C the higher coercivities are reduced to values that are normal for magnetite and the initial differences in coercivities virtually

disappear. Thermal demagnetization experiments indicate that magnetite with anomalously high coercivities is responsible for the observed variation in coercivities. It is suggested that low-temperature oxidation due to weathering has oxidized the surface of the magnetite grains. The resulting stress in the grains causes an increase of coercivities. When the marls are heated to 150°C the stress is reduced, presumably through the diffusion of Fe-ions and vacancies. It is demonstrated that the weathering induced increase of coercivities has a stabilizing effect on the primary component of the NRM as well as on the secondary overprint. After heating to 150°C, alternating field demagnetization is much more effective to separate the primary and secondary component than before heating.

Chapter 5 gives some rock magnetic parameters for the Vrica marls and reports the results of a microprobe study of magnetic concentrates from the marls. In the magnetic concentrates a large number of small iron sulphide grains of many different compositions are present. Compositions vary from pyrite to monosulphides and even sulphur deficient sulphides. A remarkable observation is the presence of a considerable amount of Ni in many sulphide grains. Ni contents up to 35% of the total metal content are measured. Processes during early diagenetic sulphate reduction are reviewed to explain the presence of magnetic monosulphides and the high Ni content. The rock magnetic properties of the marls confirm that magnetic sulphides are the main remanence carriers. The properties are compatible with the properties of monoclinic pyrrhotite, except for anomalously high maximum blocking temperatures for the sulphide remanence.

Chapter 6 examines the variation in rock magnetic properties in the Vrica section. The observations are used to further analyze the magnetic properties of the remanence carriers. The results point to a mixed magnetic mineralogy of varying amounts of monoclinic pyrrhotite and greigite and a smaller amount of magnetite. A distinct decrease in NRM and IRM intensities that occurs 15 m below the Pliocene-Pleistocene boundary is attributed to a reduction of sedimentation rate as a result of to changing climatic conditions.

In chapter 7 the method described in chapter 3 is used to study the thermal behaviour of the magnetic sulphides in the Vrica marls. After heating to 150 and 200°C, an increase of existing remanence occurs. In a number of samples of the samples this increase of remanence causes spurious magnetization during thermal demagnetization of the NRM. During thermomagnetic analyses of the magnetic concentrates, higher alteration temperatures are found. When heated in air and in an argon atmosphere, the increase in magnetization starts at about 190 and 230°C respectively. The characteristics of the alteration are compared with the $\gamma$-transition in hexagonal pyrrhotite. The influence of oxygen on the diffusion of vacancies in the sulphide crystal is suggested as an explanation for the variable transition temperatures. Inhomogeneous sulphide grains or grains with compositions between hexagonal and monoclinic pyrrhotite are proposed as main magnetic sulphide phases. So far as the coercivities are concerned, greigite is also a possible remanence carrier, but the thermal behaviour observed in the Vrica marls is as yet never reported for greigite.

**Photo 1.** The carbonate-rich marls of the Early Plioceen Trubi formation near Eraclea Minoa (Sicily)

**Photo 2.** Sampling site in the Late Pliocene to Pleistocene marine marls of the Vrica section near Crotone (Calabria).

# 1 Introduction

The permanent or remanent magnetization in rocks resides in iron oxides or sulphides which occur in trace amounts in virtually all rock types. The primary component of the natural remanent magnetization (NRM) is locked into the rock during or shortly after its formation. Components that are acquired later in the geologic history of the rock are referred to as secondary NRM components. The nucleus of paleomagnetic research involves the isolation and characterization of the primary NRM component.

Well-known acquisition mechanisms of a primary NRM are the acquisition of a thermoremanent magnetization (TRM) in volcanic rocks and the acquisition of a depositional remanent magnetization (DRM) in sedimentary rocks. Lava flows acquire a TRM when cooling through the blocking temperatures of the magnetic minerals. When sediment is accumulating, detrital magnetic particles settle down with a small preference for the ambient geomagnetic field direction. This direction is imprinted during deposition (DRM) or shortly after deposition when the magnetic grains are immobilized by compaction at a certain depth in the sediment, the so-called lock-in depth. The latter magnetization is called a post-depositional remanent magnetization (p-DRM). Although the intensity of the geomagnetic field is weak, approximately 50 $\mu$T, depending on the geographic latitude, usually a well-detectable NRM signal is recorded in the rock. Generally, sediments have weaker NRMs than volcanic rocks. This is not problematic, however, because sensitive spinner and cryogenic magnetometers enable reliable measurement of the NRM of virtually every sediment. Even white limestones, containing very little magnetic material, yield a well measurable signal in quite a number of cases.

To isolate the primary NRM component, undesired secondary overprints have to be removed. The method routinely used in paleomagnetism is progressive stepwise demagnetization. A rock sample or specimen is subjected to increasingly higher alternating fields (alternating field demagnetization) or to increasingly higher temperatures (thermal demagnetization) in order to selectively remove part of the NRM. Between successive demagnetization steps the residual NRM is measured. Analysis of the behaviour of the NRM vector during the demagnetization procedure allows the extraction of the primary NRM component.

Sediments are an extremely valuable source of information for the paleomagnetic record. By their very nature, sediments provide a continuous record of the ancient geomagnetic field, in contrast to a pile of lava flows which represents a series of spot readings of the ancient geomagnetic field with varying and usually poorly defined time intervals between successive flows. Marine sediments in

particular, may provide continuous records of considerable length. Successive periods of normal and reversed polarity in a sedimentary sequence can be correlated to the Geomagnetic Polarity Time Scale (GPTS), which is based on the pattern of marine magnetic anomalies on each side of mid-ocean ridges. Magnetostratigraphy offers a precise dating tool for establishing detailed chronology of biostratigraphic datum levels. Correlations can be made globally and a possible diachronic development can be established. Tectonic phases (deformation, block rotation) can be dated with the GPTS as well.

Sedimentary records also are an attractive source for the study of the behaviour of the geodynamo itself. Long records of the (relative) paleointensity of the geomagnetic field and detailed records of the behaviour of this field during geomagnetic reversals are becoming more and more available from various sediments. The true geomagnetic information of such records is currently debated, mainly because processes which may occur during and after sedimentation are still insufficiently understood. Rapid geomagnetic fluctuations will be smoothed to some extent, because the recording of the geomagnetic field is not instantaneous. Authigenic formation of magnetic minerals may produce delays and repetitions in remanence acquisition.

The simplest model of a sedimentary NRM is a composite remanence where a DRM represents the primary NRM component on which a secondary NRM component is superimposed which can be of viscous origin or created by recent weathering. DRM and p-DRM often show an inclination smaller than expected for the latitude, referred to as inclination error. Apart from the inclination error, DRM and p-DRM are thought to faithfully record changes in the magnetic field. The detrital magnetic minerals that carry this remanence originate from the source area of the sedimentary basin or from atmospheric dust, in which case the source area is not so well defined. Carriers of a detrital remanence will be mainly iron oxides, like magnetite and hematite.

Sediments are not a closed system, however. Physico-chemical conditions will change as a function of depth below the sediment-water interface. Usually sediments become suboxic or even anoxic at a certain depth, while they are oxic directly below the sediment-water interface. In rare cases, conditions are already anoxic at the sediment-water interface (e.g. the present Black Sea). After burial oxic sediments will become increasingly more reduced and a zonation can be recognized with the change from oxidizing to reducing conditions. After oxygen has been depleted, nitrate, manganese oxides, iron hydroxides and sulphate will successively be reduced. Each zone is typified by diagenetic reactions which may involve dissolution of existing magnetic minerals or authigenic growth of new magnetic minerals. In the authigenically formed magnetic minerals the geomagnetic field direction is recorded at the moment they grow through their blocking volume, thereby acquiring a chemical remanent magnetization (CRM). The concept of blocking volume is analogous to that of blocking temperature, the process through which a TRM is imprinted on a rock.

In the topmost layer of the sediment authigenic magnetite may be produced through the action of magnetotactic bacteria. These magnetotactic bacteria are restricted to the rather specific living conditions just above the iron reduction zone. Although the resulting NRM is strictly speaking not a depositional NRM, it can be regarded as primary as long as it is concurrent with the initial stage of sediment formation.

In particular sulphides are formed through authigenic growth. Sulphate reduction occurs in any sediment under sufficiently reducing conditions. The end product in the sulphate reduction chain is pyrite, but initially amorphous FeS, mackinawite and greigite are formed. In this respect, the observation of pyrrhotite in sediments is enigmatic. Possibly certain magnetotactic bacteria have pyrrhotite as magnetosomes rather than magnetite. In marine sediments characterized by the omnipresence of sulphate, one expects the intermediate monosulphides, i.e. greigite and pyrrhotite, not to be preserved. Under specific conditions, however, preservation may occur. The iron needed for the precipitation of pyrite and intermediate monosulphides partly originates from iron(oxyhydr)oxides.

Which magnetic minerals will finally contribute to the NRM depends on the conditions during deposition. A higher sediment accumulation rate and the presence of metabolizable organic material will favour sulphate reduction and sulphide formation. The primary NRM may be removed through dissolution of its carriers or new magnetic minerals may be formed in a later stage. Moreover, changing conditions may produce artefacts in the geomagnetic record due to dissolution and reprecipitation. A detailed characterization of the magnetic mineralogy is necessary to understand the process and the timing of the acquisition of the various NRM components. The reliability of the NRM recorded in the sediment depends on these processes.

For the analysis of the NRM in the laboratory, the behaviour of the magnetic minerals during demagnetization has to be studied. Separation of the primary NRM component with stepwise alternating field demagnetization may be hindered by the resistance of the secondary overprint against demagnetization. During stepwise thermal demagnetization alteration of magnetic minerals may disturb the analysis. Sulphides in particular, become unstable at the relatively high temperatures applied. Oxidation of sulphides will produce new highly magnetic minerals that can cause spurious magnetizations. At the same time, NRM components may be lost with the decomposition of magnetic sulphides.

The present rock magnetic study investigates the magnetic minerals in two Pliocene and Pleistocene marine marl formations in southern Italy. The early Pliocene Trubi formation consists of pelagic marls with a high carbonate content (60-80%) and a low sedimentation rate (4-5 cm/ky). Because of these conditions, pyrite formation during sedimentation was not very important in these marls. The primary NRM component is carried by magnetite, which may be detrital or authigenic. This component doesn't seem to be very much affected by dissolution accompanying sulphate reduction and has a relatively high intensity (10-20 mA/m).

The Pliocene and Pleistocene marine marls from the Vrica section are an example of a sulphide-dominated magnetomineralogy. The low carbonate content (15-25%) and higher sedimentation rate (25-50 cm/ky) in these marls, which is related to the shallower sedimentation depth, have promoted sulphate reduction and sulphide formation. The much weaker NRM in these marls (0.1-2 mA/m) is mainly carried by magnetic sulphides and shows a more complicated demagnetization behaviour.

The rock magnetic properties of the marls are compared with properties of well-determined grain-size fractions of magnetic minerals, that have been studied in the past decades. The behaviour of the magnetic minerals during thermal treatment is studied to obtain additional parameters for their identification and to support the interpretation of thermal demagnetization of the NRM.

# 2 Rock magnetism of the Early Pliocene Trubi formation at Eraclea Minoa (Sicily)

**Abstract**

The most important magnetic mineral in the fine-grained marls of the Early Pliocene Trubi formation near Eraclea Minoa is magnetite. Some goethite is also present. The magnetite is of high purity and of primary origin. Hysteresis and low-temperature measurements show that most magnetite grains are single-domain. The presence of superparamagnetic grains is suspected. Multi-domain grains are rare. It is shown that AF demagnetization does not yield correct NRM directions.

## 1. Introduction

The natural remanent magnetization (NRM) in sedimentary sequences provides a unique and continuous registration of the changes in the Earth's magnetic field during geological past. The NRM of sediments can be very complex, however, due to various magnetization processes that may occur in the sediment from the moment of sedimentation. Rock magnetic studies can identify the carriers of the components that make up the NRM and reconstruct the timing of the magnetization processes.

The aim of the present study is to establish the rock magnetic properties of the marine marls of the Early Pliocene Trubi formation near Eraclea Minoa on the southern coast of Sicily (Italy). The section starts at the Miocene-Pliocene boundary, which age of 4.86 Ma is based on the magnetostratigraphic results (Hilgen and Langereis, 1988). The fine-grained marls consist of carbonates (60 to 80%) and a mixture of clay minerals. Small-scale sedimentary quadruplets form a repetition of grey, white, beige and white coloured beds (Hilgen, 1987). The samples used in the present study were taken from grey and beige beds, since white beds proved to be more weathered. The samples carry various NRM components revealed by thermal demagnetization. They are investigated with emphasis on the domain state of the magnetic minerals. Techniques used for identification are IRM acquisition, low-temperature treatment and hysteresis measurements.

## 2. Demagnetization of NRM

Stepwise thermal demagnetization was used to isolate the characteristic paleomagnetic component. Its direction could be reliably determined in spite of a large secondary component (figure 1a). Three components seem to be present. A

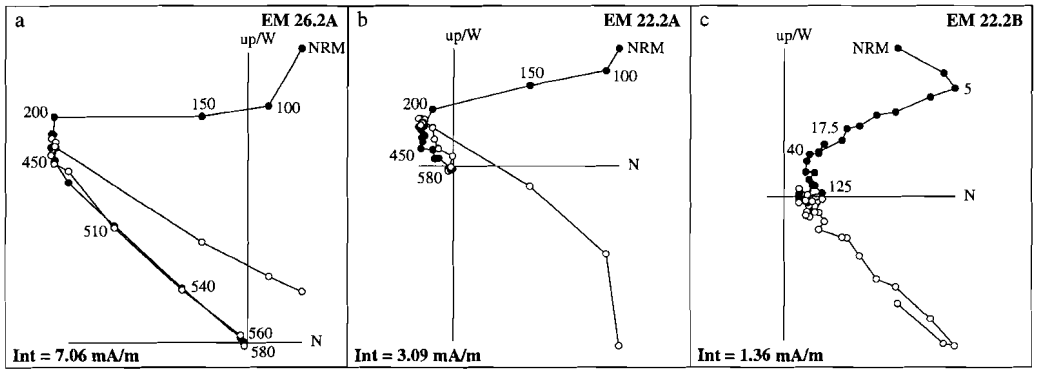


**Figure 1.** Demagnetization diagrams of progressive stepwise thermal (a and b) and alternating field (c) demagnetizations of Trubi marls, corrected for bedding tilt. Temperatures in °C, alternating fields in mT up to 300 mT. Closed circles are projections on a horizontal plane, open circles are projections on a vertical plane. Figures b and c are thermal and AF demagnetizations of specimens from one core. Int is initial NRM intensity.

small component with a random direction and therefore obviously induced in the laboratory, is removed at 100°C. A large component with a present day geomagnetic direction is consequently of recent and probably viscous origin. Because the sediment has never undergone any significant burial, it is acquired during the Brunhes normal chron at temperatures not much higher than room temperature.

Such viscous components can be almost completely removed after heating to temperatures between 200 and 250°C (Pullaiah et al., 1975). Between 200 and 450°C a very small component with an intermediate direction seems to be present. Pyrrhotite could carry such a magnetization, but it has a maximum blocking temperature of 340°C and can therefore be ruled out. Most likely this

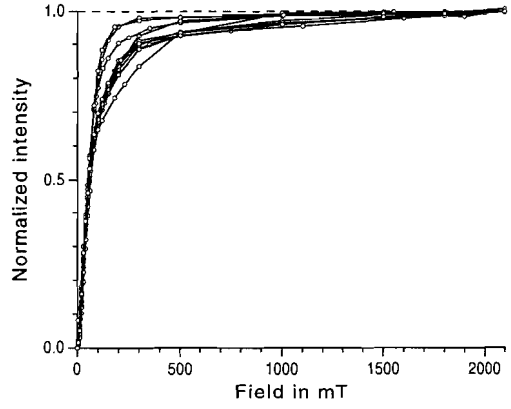


**Figure 2.** Normalized IRM acquisition curves of Trubi marls.

direction is an artefact due to an overlap between the secondary magnetization and the high-temperature component. Near 450°C a stable endpoint is reached. The third and characteristic component has maximum blocking temperatures of 560 and 580°C. Magnetite with no or very low Ti substitution must be the carrier of this characteristic magnetization. Normal and reversed directions throughout the section are almost antiparallel; they show a 35 degree clockwise rotation. It can be concluded that the magnetization carried by this magnetite is prerotational and thus most likely a primary magnetization. Considering this, the secondary component is probably also carried by magnetite, but with smaller SD grains that have lower blocking temperatures and show a long term viscous behaviour. Figure 1b and c show thermal and alternating field (AF) demagnetization diagrams of adjacent specimens of one core. The thermal demagnetization clearly reveals the reversed primary component, but a large overlap in coercivity spectra of the secondary and primary component makes it impossible to isolate this reversed primary direction by means of AF demagnetization. This is not in conflict with the suggested viscous nature of the secondary component. A low-field viscous magnetization can be resistant to AF demagnetization (e.g. Rimbert, 1959).

### 3. IRM acquisition

Isothermal remanent magnetization (IRM) acquisition curves were measured for a number of specimens up to fields of 2.15 T (figure 2). The acquisition curves are typical for magnetite. The samples are close to saturation near 0.3 T, but the IRM keeps increasing slowly in higher fields. Another mineral like goethite or hematite must be present. The presence of goethite has been detected in the $<2$ μm fraction by means of X-ray diffraction. It may have formed as a weathering product or after redistribution of iron by fluid migration. Thermal demagnetization would remove a goethite remanence at about 100°C, together with the laboratory induced component. On the other hand, such a remanence would resist the highest alternating fields. The high-coercivity mineral does contribute to the total IRM and therefore influences the measurements of the remanent coercive force ($H_{cr}$) and the high-coercivity contribution must be subtracted to determine the $H_{cr}$ for the magnetite. As a first order approximation it is assumed that the IRM acquisition of the goethite is linear in low fields up to 1 T (Dekkers, 1989a). In Table A both corrected and uncorrected values of $H_{cr}$ are listed.

The IRM is 150-300 times the sum of the NRM components and may not be a good representation of the NRM. The normalized thermal decay curves of NRM and IRM show relatively more high blocking temperatures for the NRM (figure 3a). This must be due to stable large single-domain (SD) grains. There is no indication of multi-domain (MD) grains, that contribute relatively more to IRM than to NRM, nor that different magnetic minerals contribute to NRM and IRM. NRM and IRM were AF demagnetized up to 0.3 T. In some specimens the normalized demagnetization curves were identical, while in others the NRM was more resistant to AF demagnetization than the IRM (figure 3b and 3c respectively). In general, however, the characteristics of NRM and IRM seem to match quite well.

## 4. Hysteresis

Hysteresis curves were determined using an ac field with a maximum of 0.2 T (figure 4). Test runs up to 0.3 T showed no differences. The high field susceptibility is on the order of $5.10^{-5}$ SI units. It is due to paramagnetic clay minerals and high coercivity magnetic minerals. After subtraction of this contribution the coercivity $H_C$ and the $J_{rs}/J_s$ ratio of the magnetite were determined (Table A). The relatively high $H_C$ and saturation fields indicate that the magnetite grains must be single-domain. To check this, the remanence ratio $J_{rs}/J_s$ and the coercivity ratio $H_{cr}/H_C$ may be used. For SD magnetite with some shape anisotropy, the theoretical value for $J_{rs}/J_s$ is 0.5 and the $H_{cr}/H_C$ ratio lies between 1.1 and 2.0 (Stoner and Wohlfahrt, 1948). The $J_{rs}/J_s$ ratio for the natural samples of this study (0.28-0.47) are close to experimental SD values based on the results of grown and crushed magnetites (e.g. King et al., 1983, Dunlop, 1986). $J_{rs}/J_s$ ratios plotted versus $H_{cr}/H_C$ ratios for all grain sizes of magnetite form a well defined trend with SD grains in the upper left corner and MD grains in the lower right corner (Dunlop, 1986, Day et al., 1977). Our data plot near the SD magnetites, but slightly outside the trend (figure 5). Possibly the correction of $H_{cr}$ for the high coercivity mineral was not complete, but even the largest possible correction would only slightly reduce the values of the corrected $H_{cr}$. The $J_{rs}/J_s$ values need not be corrected for high coercivity

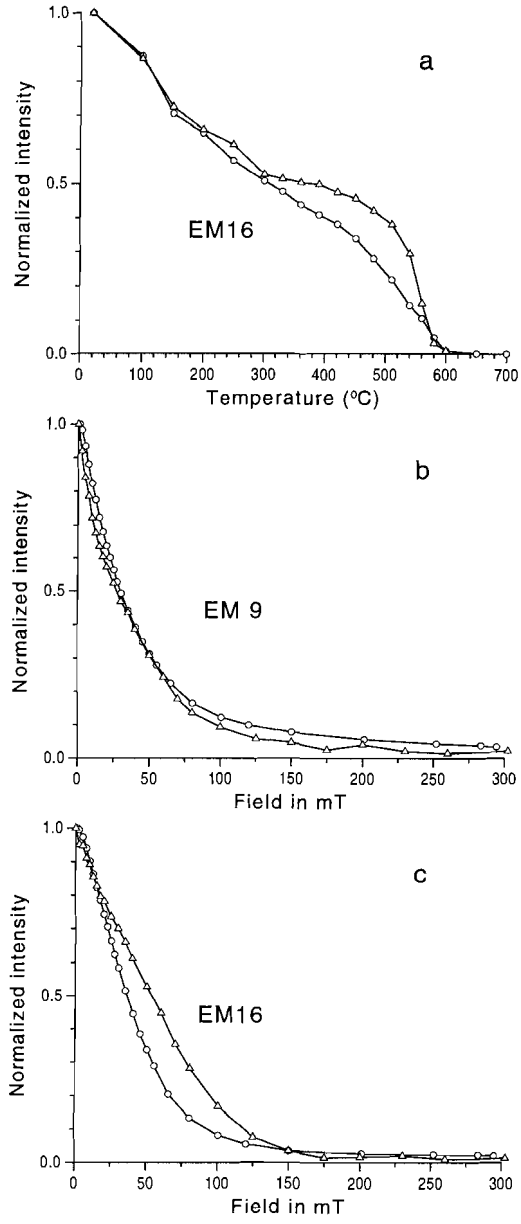


**Figure 3.** Normalized thermal (a) and AF (b and c) decay curves of the algebraic sum of NRM components (triangles) and IRM (circles) of Trubi marls. AF demagnetization in three orthogonal directions. Median destructive fields of NRM and IRM are 30 and 55 mT.

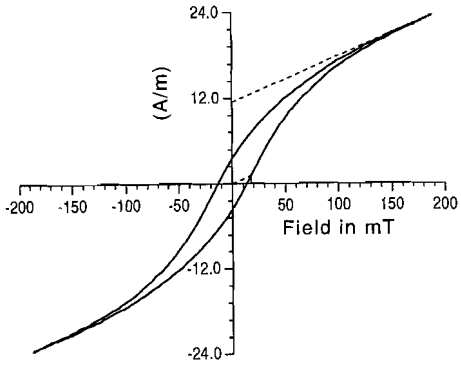


**Figure 4.** Hysteresis curve of sample EMA36.4A.

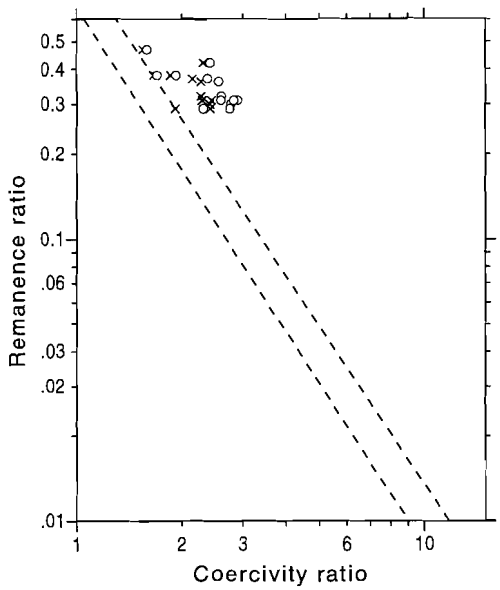


**Figure 5.** Double logarithmic plot of coercivity ratio $H_{cr}/H_c$ versus remanence ratio $J_{rs}/J_s$. Literature data for magnetite of known grain sizes fall on a single trend indicated by two dashed lines (schematic after Dunlop (1986)). Data of the Trubi marls plot near the SD magnetites, but outside this trend. Circles are uncorrected ratios. Crosses indicate the data after correction for the high-coercivity minerals.

minerals, because in the fields used for hysteresis measurements high coercivity minerals only contribute a very small amount to $J_{rs}$, while their contribution to $J_s$ is included in the correction for the high field susceptibility.

The $H_{cr}/H_c$ ratios could deviate from SD values if MD grains or superparamagnetic (SP) grains were present. However, MD grains would not produce values outside the SD-MD trend. The presence of SP grains, on the other hand, would reduce $H_c$ values considerably, because the coercive force for SP grains is almost zero. That would result in higher $H_{cr}/H_c$ ratios, like the data of this study. The $J_{rs}/J_s$ ratio would be influenced as well, since SP grains do not contribute to $J_{rs}$, but the difference would be relatively smaller. The presence of SP grains could therefore explain part of the deviation from the general trend.

## 5. Low-temperature treatment

Low-temperature treatment to liquid nitrogen temperature was performed on a room temperature IRM (2.15 T) of a number of specimens. Figure 6 shows some examples of cooling cycles. The 10 to 20% increase of magnetization during cooling and the small loss (1 to 10%) of original IRM after rewarming are remarkable. In spite of the fact that most of the magnetization is carried by magnetite, the indications for a Verwey-transition near minus 155°C are very small. Only the difference between cooling and warming curves for specimens EMA5.3A and EMA36.2A could be interpreted as a transitional effect. Titanium substitution can lower the transition temperature below liquid nitrogen temperature (Syono and Ishikawa, 1963), but the maximum

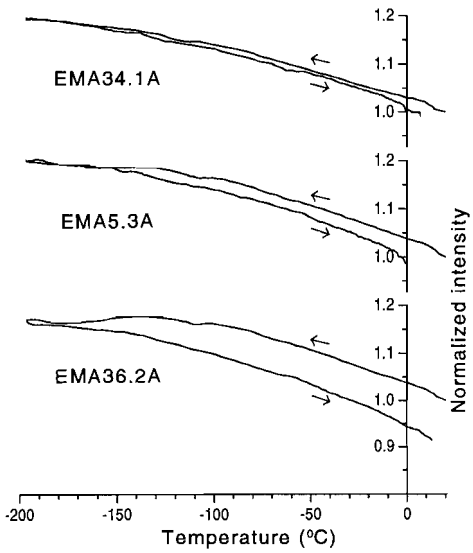


**Figure 6.** Normalized low-temperature curves of IRM. Cooling and rewarming in ca. 3 hours.

blocking temperatures show no such substitution. A better explanation is the domain state of the magnetite grains. SD magnetite does not show a transition above liquid nitrogen temperature and has a very high recovery rate (Kobayashi et al., 1965; Levi and Merrill, 1978). A degree of shape anisotropy enhances this effect. Again the conclusion must be that the IRM is almost completely carried by SD magnetite. A small amount of MD magnetite is only indicated in the last curve by the larger loss of magnetization. The reversible increase of magnetization during cooling can to a large extent be explained by the small percentage of goethite remanence. Goethite remanence increases linearly with decreasing temperature and can reach three times its room temperature value at -196°C (Dekkers, 1989b). This assumption is supported by the relation between the amount of high coercivity remanence and the low-temperature increase of IRM (Table A).

## 6. Conclusions

The most important magnetic mineral is magnetite with no or very low Ti substitution. A high coercivity mineral, most likely goethite, is of minor importance. Hysteresis parameters and low-temperature measurements show, that most of the magnetite is SD. The presence of SP grains is suspected. Only a small amount of MD grains is detected.

The primary component of NRM is carried by stable (large) SD magnetite. The secondary component is probably of viscous origin and is most likely carried by smaller SD magnetite grains. The high coercivity mineral is not explicitly seen in the demagnetization diagrams of the NRM.

Hysteresis parameters $J_{rs}/J_s$ and $H_{cr}/H_c$ and low-temperature curves provide a powerful means to determine grain sizes in samples that contain mainly magnetite.

AF demagnetization cannot be used to separate secondary and primary components of the NRM in these fine-grained marls.

| Sample | 1 IRM (A/m) | 2 % high coerc. | 3 Hcr (mT) | 4 Hcr corr. | 5 Hc (mT) | 6 Hcr/Hc | 7 Jrs/Js | 8 low-temperature %incr. | 9 %recov. |
|---|---|---|---|---|---|---|---|---|---|
| EM 5.2B | 2.9 | 9.5 | 47.9 | 41.9 | 18.4 | 2.28 | 0.32 | | |
| EMA 5.3A | 2.9 | 10.5 | 47.5 | 41.9 | 18.3 | 2.29 | 0.31 | 21 | 94 |
| EM 13.2B | 2.5 | 2.5 | 50.4 | 49.0 | 31.8 | 1.55 | 0.47 | | |
| EMA15.5B | 2.7 | 3 | 38.6 | 37.8 | 22.8 | 1.66 | 0.38 | 9 | 97.5 |
| EM 18.1B | 2.2 | 3.5 | 42.9 | 41.3 | 22.3 | 1.86 | 0.38 | | |
| EM 20.2B | 2.8 | 11 | 45.5 | 38.0 | 15.6 | 2.44 | 0.31 | | |
| EM 22.1B | 2.3 | 8.5 | 47.3 | 40.9 | 17.0 | 2.41 | 0.30 | | |
| EM 22.2B | 2.2 | 9 | 47.0 | 41.3 | 17.0 | 2.42 | 0.29 | | |
| EMA26.4A | 2.9 | 4 | 67.5 | 64.5 | 27.9 | 2.31 | 0.42 | 10 | 99 |
| EM 32.1B | 1.7 | 9.5 | 48.4 | 43.0 | 18.9 | 2.28 | 0.36 | | |
| EMA34.1A | 1.3 | 8 | 50.0 | 45.1 | 21.0 | 2.15 | 0.37 | 20 | 96.5 |
| EM 36.1B | 3.1 | 10.5 | 47.0 | 38.3 | 16.6 | 2.30 | 0.31 | | |
| EMA36.2A | 3.4 | 12.5 | 35.8 | 29.8 | 15.5 | 1.92 | 0.29 | 18 | 90 |

**Table A**. Rock magnetic properties of the Trubi marls.
Columns represent: 1. IRM(2.15 T) at room temperature. 2. Percentage of IRM contributed by high-coercivity minerals. Approximation as explained in the text. Remanent coercivity $H_{cr}$ before (3) and after (4) correction for the high-coercivity minerals. $H_c$ (5) and $J_{rs}/J_s$ (7) determined from hysteresis loops in a 200 mT ac field. $H_{cr}/H_c$ (6) with corrected $H_{cr}$ value. Low-temperature treatment of IRM: (8) increase of magnetization during cooling from room temperature to -196°C and (9) recovery of original magnetization after rewarming.

## References


Day R., Fuller M. and Schmidt V.A., Hysteresis properties of titanomagnetites: grain-size and compositional dependence. Phys. Earth Planet. Inter., 13, 260-267, 1977.

Dekkers M.J., Magnetic properties of natural goethite-I. Grain-size dependence of some low- and high-field related rockmagnetic parameters measured at room temperature. Geophys. J., 97, 323-340, 1989a.

Dekkers M.J., Magnetic properties of natural goethite-II. TRM behaviour during thermal and alternating field demagnetization and low-temperature treatment. Geophys. J., 97, 341-355, 1989b.

Dunlop D.J., Hysteresis properties of magnetite and their dependence on particle size: a test of pseudo-single-domain remanence models. J. Geophys. Res., 91, 9569-9584, 1986.

Hilgen F.J., Sedimentary rhythms and high-resolution chronostratigraphic correlations in the Mediterranean Pliocene. Newsl. Stratigr., 17, 109-127, 1987.

Hilgen. F.J. and Langereis C.G., The age of the Miocene-Pliocene boundary in the Capo Rossello area (Sicily). Earth Planet. Sci. Lett., 91, 214-222, 1988.

King J.W., Banerjee S.K. and Marvin J., A new rock-magnetic approach to selecting sediments for geomagnetic paleointensity studies: application to paleointensity for the last 4000 years. J. Geophys. Res., 88, 5911-5921, 1983.

Kobayashi K., Campbell M.F. and Moorehead J.B., Size dependence of low-temperature change in remanent magnetization of $Fe_3O_4$, in Ann. Proc. of the Rock Magnetism Research Group, pp. 33-50. Tokyo, Japan, 1965.

Levi S. and Merrill R.T., Properties of single-domain, pseudo-single-domain, and multi-domain magnetite. J. Geoph. Res., 83, 1978.

Pullaiah G.E., Irving E., Buchan K.L., Dunlop D.J., Magnetization changes caused by burial and uplift. Earth Planet. Sci. Lett., 28, 133-143, 1975.

Rimbert F., Sur l'action de champs alternatifs sur des roches portant une aimantation remanente isotherme de viscosité. C. R. Acad. Sci., 242, 2536-2538, 1959.

Stoner E.C. and Wohlfahrt E.P., A mechanism of magnetic hysteresis in heterogeneous alloys. Philos. Trans. R. Soc., London, Ser. A 240, 599-642, 1984.

Syono Y. and Ishikawa Y., Magnetocrystalline anisotropy of $xFe_2TiO_4(1-x)Fe_3O_4$. J. Phys. Soc. Japan, 18, 1230-1231, 1963.

# 3 A method to study alterations of magnetic minerals during thermal demagnetization applied to a fine-grained marine marl (Trubi formation, Sicily)


## Abstract

The method presented is based on monitoring changes in the coercivity spectrum of an isothermal remanent magnetization (IRM) during stepwise thermal demagnetization. The procedure allows one to determine alteration temperatures and the coercivities and blocking temperatures of the magnetic minerals involved in the alterations. It distinguishes between thermal decay due to unblocking of the remanence and demagnetization due to alterations of magnetic minerals. As a result the initial magnetic mineralogy can also be determined.

The method is demonstrated with samples of fine-grained marine marls from the Pliocene Trubi formation in Sicily (Italy). Single domain (SD) magnetite is the dominant remanence carrier in this sediment. A first alteration during heating to only 145°C is accompanied by a considerable reduction of coercivities higher than 0.1 T. This alteration is thought to be due to the reduction of stress in superficially maghemitized SD magnetite grains.

Between 390 and 480°C grains with magnetite-like properties are produced, most likely by oxidation of pyrite in the sediment. At about 560°C the breakdown of iron-bearing silicates also produces magnetic grains. The magnetic grains formed during both alteration processes have low blocking temperatures.

Demagnetization above 510°C is not only due to unblocking of the IRM. Alteration of magnetite to hematite proves to be an important demagnetization mechanism.


## 1. Introduction

In many rocks, especially sedimentary rocks, thermal demagnetization is most successful in separating the various components of the natural remanent magnetization (NRM). The blocking temperature (BT) spectrum of the NRM yields valuable additional information for the identification of the magnetic minerals. The main disadvantage of thermal demagnetization is, however, that heating may induce alterations in the magnetic mineralogy, even at fairly low temperatures. Alterations occur in magnetic minerals as well as in non-magnetic matrix minerals. Both types of alterations can interfere with the demagnetization process. Magnetic grains may be altered before their actual BT is reached and before primary and secondary NRM directions are separated. The formation of new magnetic minerals from

matrix minerals, on the other hand, may produce interfering (e.g. viscous) remanences.

To monitor alterations involving magnetic minerals initial susceptibility ($\chi_o$) can be measured between the heating steps of a progressive thermal demagnetization, but from $\chi_o$ alone, the nature of the alterations cannot be deduced. Not only remanence carriers contribute to $\chi_o$, paramagnetic minerals and superparamagnetic grains contribute to $\chi_o$ as well.

Isothermal remanent magnetization (IRM) is a more suitable parameter to monitor changes in magnetic minerals. Its diagnostic value can be enhanced if the coercivity spectrum of the IRM is also measured after each heating step. Dunlop (1972) determined changes in the coercivity spectrum of IRM acquisition to study several hematite dominated sedimentary rock types before and after heating to high temperatures (>520°C). The low-, intermediate- and high-coercivity remanence fractions were attributed to magnetite, specularite and hematite pigment respectively. Heller (1978) used essentially the same technique to study alterations of magnetic minerals in goethite dominated limestones. He measured coercivity spectra of IRM acquisition during stepwise thermal demagnetization in combination with continuous thermal demagnetization after every heating step. An analytical technique based on the thermal decay behaviour of different coercivity fractions was proposed by Lowrie (1990). Three coercivity fractions of IRM are induced in orthogonal directions and subjected to thermal demagnetization. This method is easy to use, but it cannot be applied for the study of alterations of magnetic minerals.

The procedure used in the present paper is developed to monitor alterations during stepwise thermal demagnetization and to study their influence on the demagnetization behaviour and the resulting thermal decay curve. The method is based on reintroduction of an IRM after each heating step. The AF coercivity spectrum of the reinduced IRM is measured to study changes in low- and high-coercivity fractions separately. The AF coercivity spectrum of the part of the IRM remaining after each heating step is determined as well. It can then be established whether the magnetic minerals involved in an alteration still carried a remanence in that stage of the thermal demagnetization and whether the BTs of newly formed magnetic minerals are higher or lower than the temperature of their formation.

An IRM acquisition coercivity spectrum requires a sample without any remanent magnetization. By using AF demagnetization instead of IRM acquisition to determine a coercivity spectrum, the same sample can be used after every temperature step, provided the influence of the repeated IRM acquisition is evaluated. Only for hematite and goethite dominated rocks it has the disadvantage that no distinction can be made between coercivities higher than the maximum available alternating field (0.3 T in the present study). The method will be demonstrated with samples of fine-grained marine marls in which single domain (SD) magnetite is the most important remanence carrier.

## 2. Methods and equipment

A complete measuring cycle as performed after each temperature step is represented schematically in figure 1. Before the cycle shown, a room temperature IRM was induced in a 2 T magnetic field. After heating this total IRM to a certain temperature T (150°C in figure 1) and cooling to room temperature in zero field, $\chi_o$ is measured and the part of the IRM not removed at this temperature (the remaining IRM, indicated by number 1 in figure 1). The AF coercivity spectrum of this remaining IRM is determined. The demagnetization steps 10, 40, 100 and 300 mT peak alternating fields have been selected to divide the remanence into five coercivity fractions (figure 2). The next step is a renewed IRM acquisition (total IRM, indicated by number 2 in figure 1) in the same 2 T field as the original IRM. The AF coercivity spectrum of this new total IRM is determined using the same steps as for the remaining IRM. After this AF demagnetization the total IRM(2T) is induced again. The last step of each cycle (number 3 in figure 1) is a control heating of this IRM up to the temperature of the previous heating step (100°C in the example of figure 1) to check whether alterations have occurred that may influence the results of further measurements. The susceptibility $\chi_o$ is recorded after the control heating as well. The next step, heating to the higher temperature $T_{+1}$ (200°C in the example of figure 1) is the first step of the next cycle.

IRM was induced in an electromagnet with a maximum field of 2 Tesla and measured on a digitized spinner magnetometer based on the Jelinek JR3 driver unit. The initial susceptibility $\chi_o$ was measured with a Jelinek KLY-1 susceptibility bridge.

Thermal demagnetizations were performed in air in a magnetically shielded laboratory built Schönsted type furnace. Temperatures are accurate up to ±5°C. The samples remained in the furnace for 30 to 35 minutes, enough to reach the intended temperature. Cooling to room temperature in a

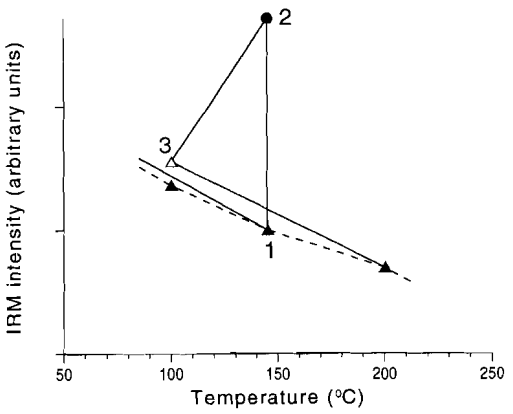


**Figure 1.** Schematic representation of one complete cycle of the measuring procedure at temperature T (145°C in the figure). A sample with a room temperature IRM(2 Tesla) is subjected to the following treatments: (1) Thermal demagnetization at temperature T. (2) Acquisition of a new IRM in the same direction and field. (3) Control heating at temperature $T_{-1}$ of the previous step (100°C in this example). After heatings 1 and 3 $\chi_o$ is measured. The IRM remaining after heating 1 and the new IRM after phase 2 are subjected to alternating field demagnetization in order to divide the IRMs in five coercivity fractions (cf. figure 2). Next the cycle is repeated at temperature $T_{+1}$ (200°C). The dashed line indicates the resulting decay curve, which generally will be influenced by the repeated IRM acquisitions (cf. figure 9).

magnetically shielded compartment took 30 minutes. Residual magnetic fields during heating and cooling were $< 20$ nT.

The maximum available peak field for AF demagnetization was 300 mT. Stationary demagnetization along three orthogonal axes was used. Zero field conditions were obtained with Helmholtz coils.

## 3. Samples

The samples of the present study are Early Pliocene fine-grained marine marls, from the Trubi formation at Eraclea Minoa in Sicily (Italy). The Trubi formation consists of a repetition of small-scale sedimentary cycles, which are expressed as a grey-white-beige-white sequence in the outcrop. On these marls magneto-stratigraphic investigations (Hilgen and Langereis, 1988) have been carried out. Although 60 to 80% of the sediment are diamagnetic carbonates, the paramagnetic clay minerals dominate the $\chi_o$ of the non-magnetic matrix. They even contribute an important part to the total $\chi_o$ of the sediment. In the grey layers, from which the present samples have been drilled, smectite, kaolinite and illite are most abundant. Minor amounts of palygorskite and chlorite occur (de Visser et al, 1989). The porosity of the dried marl samples allows access of air to some degree. Rock magnetic studies using hysteresis measurements, low-temperature cycling and IRM acquisition (van Velzen and Zijderveld, 1990) show that the remanence for the major part resides in magnetite grains in the SD grain-size range ($H_{cr}/H_c$ ratios are between 1.6 and 2.4, $J_{rs}/J_s$ ratios are between 0.5 and 0.3). The primary NRM is carried by magnetite grains. Maximum BTs were situated between 560 and 590°C. A variable amount of high-coercivity minerals carries up to 10% of the IRM acquired in a 2 T magnetic field.

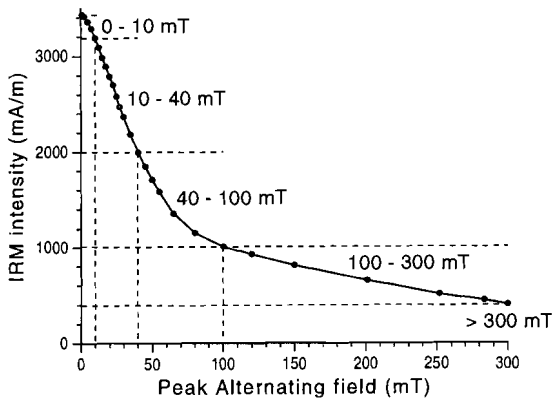


**Figure 2.** Alternating field demagnetization of IRM. During the measuring procedure the demagnetization was performed in four steps (10, 40, 100 and 300 mT). Stationary AF was performed in three orthogonal directions. The example shown is of the initial IRM of samples EM25.2B.

Two pairs of samples were used for the present study. EM14.1B and EM16.1B are similar samples, as will be illustrated with rock magnetic data, and so are EM25.2B and EM26.1B. Of each pair, one sample was subjected to the whole experimental procedure. The sister sample was only subjected to routine thermal demagnetization and served as a reference sample. During the thermal treatment it appeared that sample EM16.1B contained part of a pyrite-filled burrow. Initially the magnetic properties of this sample did not differ from

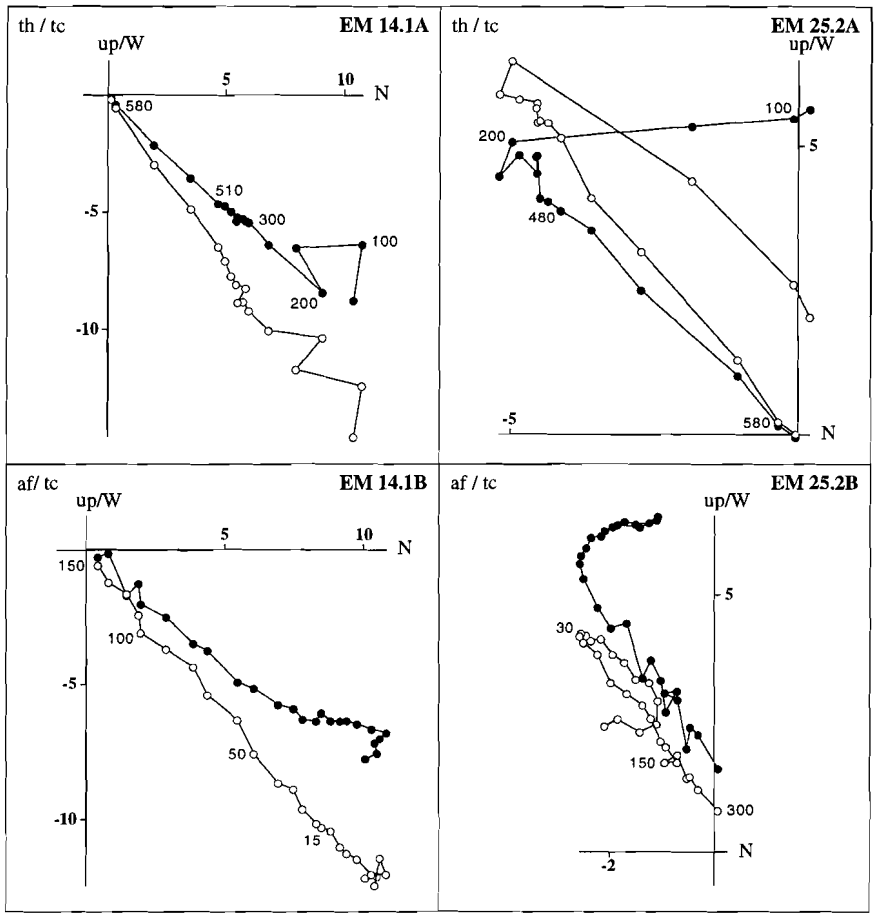


**Figure 3.** Demagnetization diagrams of thermal (th) and alternating field (af) demagnetizations of the NRM of samples from site EM14 and EM25 after tectonic correction. Closed symbols for projections in the horizontal plane, open symbols for the vertical plane. Temperatures are in degrees centigrade, peak alternating fields in mT. Units are mA/m.

Figure 3 shows thermal and AF demagnetization diagrams of the NRM of the two samples and similar samples from the same sites. The NRM consists of three components. A small laboratory component, probably of viscous origin, is removed at 100°C or 10 mT AF. A secondary component with a present-day field direction appears to be removed at temperatures below 200/250°C (figure 3, EM25.2A). The primary component mainly has BTs above 480°C. In sample EM25.2B AF field demagnetization seems to separate the primary component from the secondary component very well, but a high-coercivity mineral contributes to the NRM that is not demagnetized in the maximum available alternating field of 0.3 T.

Figures 4a and b show AF and thermal decay curves of the samples. The IRM of the first pair (EM14 and EM16) clearly has lower coercivities than that of the second pair (EM25 and EM26). This matches the difference between the coercivity spectra of the NRM of these samples (figure 4a, closed symbols). The thermal decay curves of the samples are very similar (figure 4b). The NRM has a relatively large contribution of stable grains with high BTs, when compared with the IRM.

IRM acquisition curves (figure 5, closed symbols) illustrate the difference in coercivities between the two pairs. EM14 and EM16 are close to saturation in a 0.3 T field, whereas EM25 and EM26 are not. The intensity of the 0.3 T IRM is almost equal for both pairs. Remanent coercive forces of samples EM25 and 26 are higher than those of EM14 and 16 (Table A). The grains with higher coercivities, which carry part of the remanence in samples EM25 and 26, seem to be responsible for the difference.

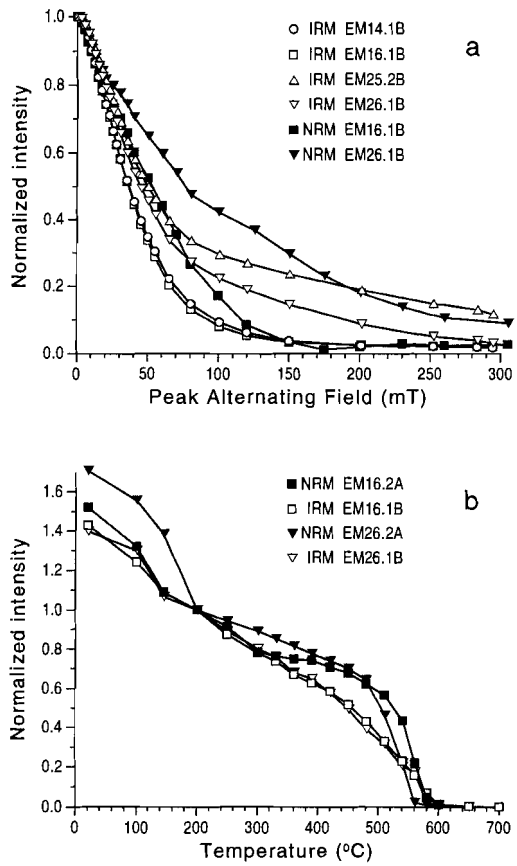


**Figure 4.** (a) Normalized AF demagnetization curves of NRM of two and IRM of all four samples used in the measurements. Stationary AF demagnetization in three orthogonal directions. (b) Thermal decay curves of NRM and IRM of samples from two sites. NB The NRM intensities are calculated as the sum of the intensities of the separate components. IRM/NRM ratios are in the order of 150.

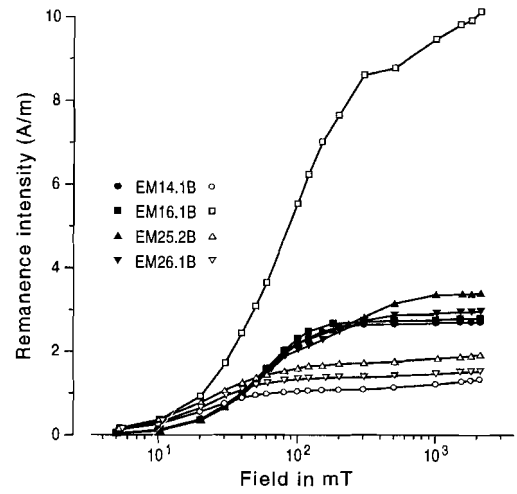


**Figure 5.** IRM acquisition curves before (closed symbols) and after (open symbols) stepwise thermal demagnetization up to 700°C. Shown is the initial part of the acquisition that was performed up to the maximum available DC field of 2 T. Before thermal treatment samples EM14.1B and EM16.1B are almost saturated in a 300 mT field, while EM25.2B and EM26.1B are not.

## 4. Results

The IRM measurements that have been performed during the complete thermal demagnetization procedure are presented in figure 6. For samples EM14.1B and EM25.2B the measurement cycle, represented schematically in figure 1, is repeated at a large number of temperatures. The same temperature steps are used as in routine thermal demagnetization of the NRM. For some of the lower temperature steps (100 and 200°C) the procedure was not executed completely. The measurements of the sister samples are given as well. Different aspects of the results will be discussed separately.

### *4.1. Initial susceptibility and total IRM*

Changes in the values for $\chi_o$ and total IRM, i.e. the IRM(2T) induced after each temperature step (figure 7), occur at 145°C and above 390°C in all samples. The parameters $\chi_o$ and IRM both seem to indicate the same alteration temperatures, but an increase of $\chi_o$ is not always accompanied by an increase of the total IRM (e.g. the changes at 145°C). The increase in $\chi_o$ above 390°C precedes the increase in total IRM. Sample EM26.1B shows similar changes of $\chi_o$ as its sister sample EM25.2B. Sample EM16.1B behaves differently during the thermal demagnetization. The increase of $\chi_o$ of this sample above 390°C is remarkably large (to 10 times the initial value). At 700°C the value of $\chi_o$ decreases again to about two times its initial value, well comparable to the other samples.

The subdivision of the total IRM induced after each temperature step in five AF coercivity fractions (figure 8a and b) reveals to which of the coercivity fractions the magnetic minerals, which are affected by the alterations, belong. At 145°C the higher-coercive part (>40 mT in EM14 and >100 mT in EM25) of the IRM decreases, while the lower-coercive part (<40 mT) increases, resulting in a small overall decrease in total IRM intensity (figure 7). The original difference between the coercivity spectra of the two samples becomes smaller after heating at 145°C. The large higher-coercivity part (>100 mT) of the IRM in EM25 no longer exists.

| Sample | NRM mA/m | IRM(2 T) mA/m | Susc. 10-5 SI | Hcr mT | MDF mT |
|---|---|---|---|---|---|
| EM 14.1B | 18 | 2490 | 22 | 48 | 36 |
| EM 16.1B | 16 | 2660 | 23 | 47 | 36 |
| EM 25.2B | 13 | 3290 | 21 | 61 | 50 |
| EM 26.1B | 11 | 2820 | 18 | 56 | 45 |

**Table A.** Rock magnetic parameters of marl samples from the Early Pliocene Trubi formation near Eraclea Minoa (Sicily). NRM intensities are the approximate sum of the intensities of the primary and secondary components. Median destructive fields (MDF) of IRM(2T) obtained with stationary AF demagnetization in three orthogonal directions.

The increase of the total IRM above 390°C is most pronounced in sample EM14. It is due to an increase in the two lower-coercivity fractions (<40 mT) which reach their highest intensity at 480°C. Between 390 and 600°C the higher-coercivity IRM (>100 mT) increases as well, but initially the change is small. Differences between EM14 and EM25 above 480°C are mainly due to differences in the <40 mT fractions. For EM14 both $\chi_o$ and the total IRM start to decrease at 510°C, mainly as a result of decreasing 10-40 mT and 40-100 mT fractions. Similar changes in EM25 seem to develop more slowly as evidenced by the temperatures corresponding with the maximum values for the 0-10 mT and 10-40 mT fractions. In sample EM25 the total IRM increases again at 580°C (figure 7). This increase, which seems to be absent in EM14, is due to an increase in the <40 mT fractions (figure 8b).

After the last heating step of 700°C the intensity of the total IRM acquired by the samples, is about half the intensity of the original IRM. The relative contributions of the individual coercivity fractions have changed considerably. This is also visible in the IRM acquisition curves of the four samples after 700°C (figure 5). The very low coercivities (<10 mT) have become relatively more important compared to the original acquisition curves. Also a high-coercivity part has developed, that is not saturated in a 2 T field. This agrees with the AF coercivity spectrum measured after this last temperature step (figure 8a,b). The IRM acquisition curve of the deviating sample EM16 shows that also in this sample a low-coercivity part has developed, but the acquisition in higher fields is much

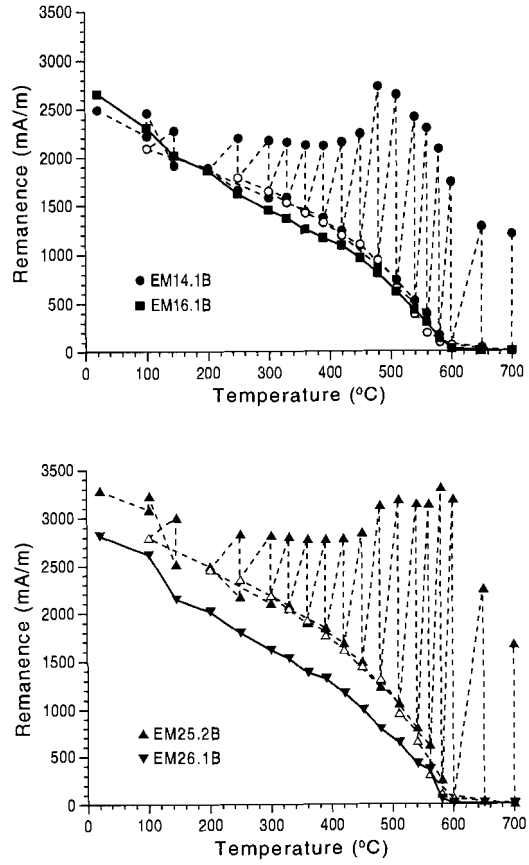


**Figure 6.** The complete set of remanence measurements that were carried out during the procedure, i.e. the repetition of the measuring cycle shown schematically in figure 1, at a large number of temperature steps. EM14.1B and EM25.2B were subjected two the whole procedure. Closed symbols depict changes in total IRM(2T) and the part of this IRM that is not demagnetized at the next temperature step. Open symbols show the results of the control heatings, performed to check for the influence of alterations on the latter. EM16.1B and EM26.1B served as reference samples and were only subjected to stepwise thermal demagnetization.

larger than in the other samples. This behaviour of EM16 is apparently related to the presence of the pyrite-filled burrow.

*4.2. Thermal decay curves of IRM*

The thermal decay curves of the two reference samples are true decay curves of an IRM induced only once. For the other two samples, that repeatedly acquired a new IRM, the IRM remaining after each heating step is likely to differ from a true thermal decay curve. Magnetic grains, newly formed at a certain temperature, will carry a remanence after the acquisition of a new IRM, part of which may not be demagnetized at the next heating step (the part with BTs higher than the next heating temperature). Apart from the control heatings (see next section), comparison of the decay curves of sister samples can detect such effects.

The decay curves of all four samples were normalized (figure 9). The two samples that acquired a new IRM at each temperature step (EM14 and EM25) have almost identical decay curves and as do the two control samples. Between sister samples, deviations occur between 145 and 200°C and between 250 and 330°C. Samples EM14 and EM25 acquire a new part of the IRM after heating to 145°C, 250°C and 300°C, although the total IRM slightly decreases in this temperature range (figure 7). This new part of the IRM is not demagnetized at 200°C, 300°C and 330°C respectively and causes the deviation from the sister samples (figure 9). Apparently, at 145°C, 250°C and 300°C magnetic grains are formed or altered, resulting in a larger IRM with BTs higher than the temperature at which they originate.

To investigate the BTs of each coercivity fraction of the IRM, the IRM remaining after each heating step was also demagnetized in alternating fields (figure 8c,d). At 145°C a similar decrease of the higher-coercivity fractions and increase of the lower-coercivity fractions occurs as in the total IRM (cf. figure 8a,b). At 300 and 330°C a slight increase in the 40-100 mT fraction occurs. These are the same temperatures at which the deviation of the thermal decay curves of these samples occurred (figure 9).

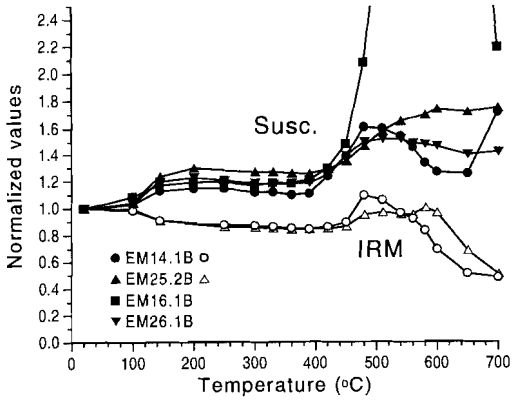


**Figure 7.** Normalized total IRM(2T), acquired after each temperature step, and initial susceptibility ($\chi_o$) during thermal demagnetization. For sample EM16.1B $\chi_o$ reaches a normalized peak value of about 5 at 650°C.

Above 390°C the coercivity fractions of the IRM remaining after thermal demagnetization behave differently than the fractions of the total IRM. The increase of the total IRM fractions with the lowest coer-

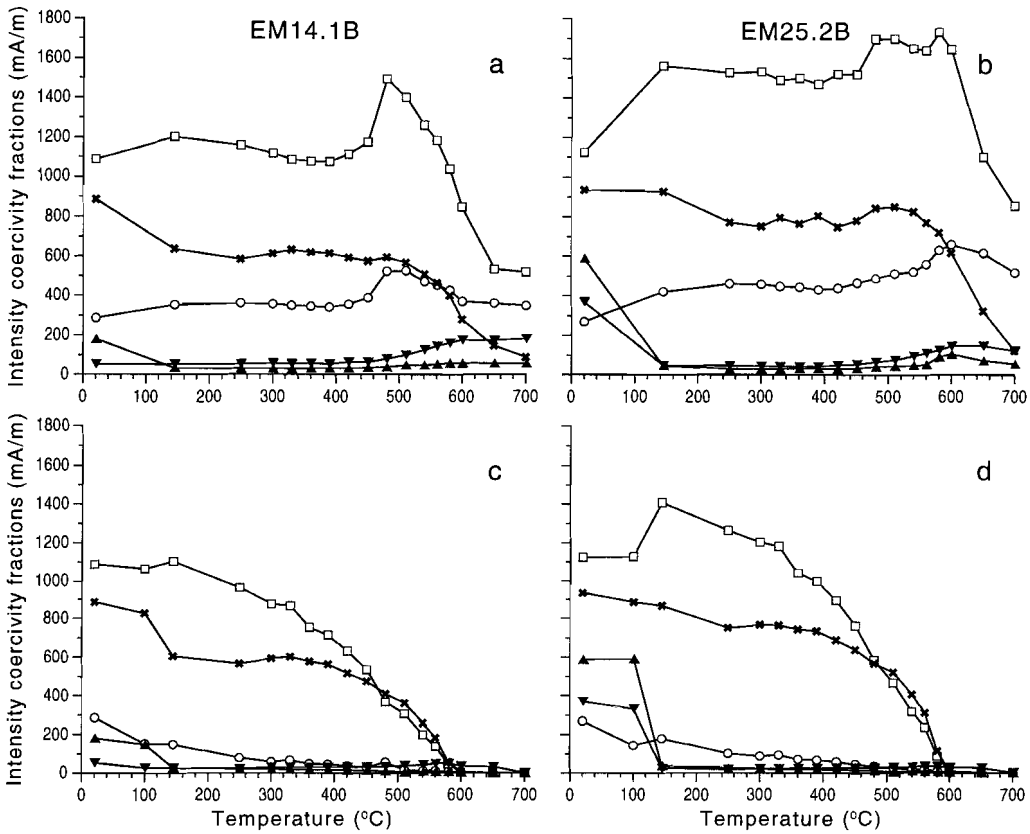


**Figure 8.** (a) and (b) Coercivity fractions of the IRM(2T) acquired after each heating step. The sum of the five fractions is the total IRM (shown normalized in figure 7).
(c) and (d) Coercivity fractions of the IRM(2T) remaining after each heating step.
0-10 mT: ○ 10-40 mT: □ 40-100 mT: x 100-300 mT: ▲ >300 mT: ▼

civities is not reflected in the same fractions of the remaining IRM. The difference between a coercivity fraction of the total and of the remaining IRM at each heating step is the part of the fraction that has BTs lower than the heating temperature. Apparently, the newly formed magnetic grains that cause the increase of total IRM have BTs lower than the temperatures of the next heating steps.

Above 390°C the coercivity fractions of the IRM remaining after thermal demagnetization behave differently than the fractions of the total IRM. The increase of the total IRM fractions with the lowest coercivities is not reflected in the same fractions of the remaining IRM. The difference between a coercivity fraction of the total and of the remaining IRM at each heating step is the part of the fraction that has BTs lower than the heating temperature. Apparently, the newly formed magnetic grains that cause the increase of total IRM have BTs lower than the temperatures of the next heating steps.

For the 40-100 mT fraction the difference between total and remaining IRM remains very small up to high temperatures, indicating high BTs. The major part of the <10 mT fraction of the total IRM, however, has very low BTs. The 10-40 mT fraction is more stable, but more than half of this fraction has BTs lower than 480°C. Furthermore, it is remarkable that part of the >300 mT fraction (presumably fine-grained hematite), that has developed at high temperatures, is demagnetized below 600°C, as comparison of the total and remaining IRM shows.

### *4.3. Influence of alterations on decay curves*

After each temperature step T the newly induced IRM is first heated to the temperature of the previous step $T_{-1}$. This is done to reveal the influence of possible alterations involving magnetic minerals with BTs higher than the highest heating temperature. In fact, the best check would be to heat the sample to the same temperature T a second time and compare the remaining IRM with the IRM remaining after the first heating at that temperature. But alterations which started during the first heating, will continue during the second heating at the same temperature. During heating to the temperature $T_{-1}$ of the previous step, however, alterations will be relatively small (which was checked by measuring $\chi_0$ after every control heating).

If no alterations have taken place, the demagnetized IRM should be equal to the remaining IRM after the sample was heated to that temperature for the first time. Alterations merely involving grains with BTs lower than $T_{-1}$ will not cause a difference between the two values either. If a difference does occur, it could be due to alterations during the heating at T, but, in case new magnetic grains were formed, alterations during the first heating at $T_{-1}$ also contribute to the difference. These altered grains may not carry a remanence directly after the heating, when the remaining IRM is measured. Only after the subsequent IRM acquisition will they contribute to the remanence and thus to the IRM measured after the control heating to $T_{-1}$, if their BTs are higher than $T_{-1}$. An exception must be made, however, for alterations at $T_{-1}$ during which grains keep their original magnetization directions. They will not contribute to the difference, because the magnetization of these grains is the

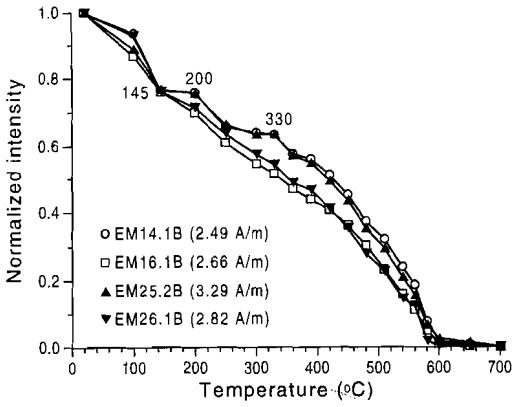


**Figure 9.** Normalized thermal decay curves of IRM for the data of figure 6. Samples EM14 and EM25 have acquired a new IRM after each temperature step causing deviations from the decay curves of the other two samples. The initial IRM(2T) is given between brackets.

same in both measurements.

In figure 10 the difference between the values of the IRM remaining after the first and second (control) heating to temperature $T_{-1}$ is shown (open symbols). Alterations in grains with BTs lower than $T_{-1}$ do not contribute to the difference. Since changes in total IRM reflect alterations in all remanence-carrying minerals, these are shown for comparison (closed symbols). The changes are calculated over the two temperature steps $T_{-1}$ and T, because the control measurements in most cases reflect changes during both steps as well.

The sign of the changes in the total IRM and the sign of the changes due to alterations involving magnetic grains with BTs higher than $T_{-1}$ is not necessarily the same. At 300°C the IRM carried by grains with BTs higher than this temperature increases, while the total IRM decreases slightly (see figure 7). From 420 to 480°C the reverse is true. The total IRM increases considerably, but IRM carried by grains with BTs higher than the temperature at which the alterations take place, decreases or increases much less.

Above 510°C, at each temperature, an alteration causes a decrease of the IRM with BTs higher than the previous temperature step. This trend is the same in both samples, even though sample EM25 shows an increase in total IRM at 580 and 600°C. Apparently, this increase involves grains with BTs lower than 560 and 580°C respectively. The decrease is also reflected in the total IRM of EM14. In EM25 the increase of total IRM at 580 and 600°C masks the decrease caused by the alteration. The results of the control heatings imply that in the alteration grains are involved that carry the remaining remanence unless all of the grains affected at T fall in the BT range $T_{-1}$-T, which is very unlikely. During heating steps from 540 to 600°C, the decrease in this high BT remanence constitutes even a considerable part of the total decay of the remaining IRM between $T_{-1}$ and T (see figure 6). This raises the question whether demagnetization at these temperatures close to the Curie temperature of magnetite is a matter of unblocking or alteration of magnetic grains.

## 5. Discussion

The changes observed in the rock magnetic parameters measured during thermal demagnetization indicate a number of different alterations involving magnetic minerals. The data obtained allow a detailed study of the nature of these alterations as well as their influence on the thermal demagnetization results. Successively, the changes in magnetic properties occurring at 145°C, 250-330°C, 390-510°C and 510-700°C and their consequences will be discussed.

### *5.1. Alterations at 145°C*

The first substantial change in magnetic properties occurs at temperatures as low as 145°C. The total IRM decreases and $\chi_0$ increases (figure 7). The AF coercivity spectra of the total IRM (figure 8a and b) show a decrease of the high-

coercivity fractions (40-100 mT and 100-300 mT for EM14, 100-300 mT and >300 mT for EM25) and an increase of the 0-10 mT and 10-40 mT fractions. At 100°C no AF demagnetization of the total IRM was performed. It is unlikely, however, that part of the changes occurred at 100°C since the changes in $\chi_o$ and total IRM are very small (figure 7).

The changes in the coercivity spectra of the decay curves (i.e. of the thermally demagnetized IRM, figures 8c and d) are similar to those in the total IRM. The results of the 100°C step show that the decrease of the high-coercivity fractions, in fact, did occur at 145°C. The absence of an increase of the total IRM at 100°C shows that the increase of the low-coercivity fractions occurred at 145°C as well. The magnitude of the decrease of the high-coercivity fractions in the two samples is proportional to the increase of the low-coercivity fractions. Both changes must be the result of the same alteration.

These observations have important implications concerning the nature of the alteration responsible for the observed changes in magnetic properties. The fact that the *increase* of the intensity of the low-coercivity fractions, as a result of an alteration process at 145°C, becomes visible in the coercivity spectrum of the decay curve *before* induction of a new IRM (figures 8c and d), shows that the alteration reduces the coercivity of the grains, but does not affect the magnetization directions of at least part of the grains. This limits the possible alterations to those with positive magnetic interaction between the remanence of original and altered grain.

Magnetostatic interaction could be positive in the case of closely packed magnetic grains, but in the marl specimens interaction between grains is not likely. Since rock magnetic parameters are close to those of SD magnetite grains the following explanation for the

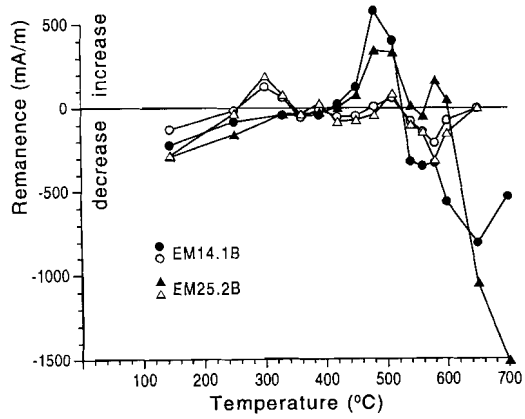


**Figure 10.** Results of the control heatings. Following each new IRM acquisition after heating step T a control heating was performed at temperature $T_{-1}$. The difference between the IRM remaining after the control heating and the IRM remaining after the first heating to $T_{-1}$ is a measure for the influence of alterations on the subsequent steps of the measuring procedure (open symbols). Only alterations of grains with BTs higher than $T_{-1}$ contribute to the difference. At temperature T (at that moment the highest heating step) the result of the control heating at $T_{-1}$ is plotted, because with the control heating the effects of alterations during heating steps $T_{-1}$ and T are measured. Only alterations during heating step $T_{-1}$ that do not affect the remanence direction of the altered grains do not contribute to the difference. For comparison the change in the total IRM during the last two heatings (T and $T_{-1}$) is plotted (closed symbols). This second curve includes all alterations, not only those involving grains with BTs higher than $T_{-1}$.

observed changes is proposed. The magnetite grains that carry the remanence in the sediment, might be partly oxidized. Oxidation is limited to a surface layer and has produced a partially maghemitized shell. Due to the similarity of the lattices, the exchange coupling remains intact over the transition zone between the partly oxidized surface layer and the unoxidized magnetite core. The change in lattice parameters does, however, produce stresses between the surface and the core of the grains, causing high coercivities and low susceptibilities. Moderate heating, as applied here, reduces the stresses, which cause the effects observed, while the exchange coupling preserves the magnetization direction of the grains. The observed decrease of the total IRM (figure 7) could either mean that the bulk magnetization of the altered grains decreases or that some of the transformed grains become superparamagnetic in size.

Only part of the grains keeps its original magnetization direction. Another part of the magnetization is randomized and remagnetized with acquisition of a new IRM after the 145°C heating step. This part appears in the decay curve at the next heating step of 200°C (figure 9), as far as the grains have BTs higher than 200°C. It causes the apparent decay curves of the two samples, that acquire a new IRM, to deviate from those of their sister samples at 200°C.

### *5.2. Alterations between 250 and 330°C*

The changes in rock magnetic properties between 250 and 330°C are less conspicuous. The only indication for a change comes from the deviation from the thermal decay curves of the sister samples (figure 9). This relative increase indicates the formation of magnetic grains at 250 and 300°C with BTs higher than the formation temperatures. In the coercivity spectra only a small decrease of the 10-40 mT and a small increase of the 40 -100 mT fraction can be noticed (most evident in EM14, figure 8a). This increase seems to be related to the observed deviation of the decay curves. Figure 10 also shows that at these temperatures the IRM with higher BTs slightly increases whereas the total IRM slightly decreases. The new magnetic grains seem to have very high BTs, because the difference between the decay curves (figure 9) persists up to temperatures close to the maximum BTs of the remanence.

### *5.3. Alterations between 390 and 510°C*

After the 390°C step the susceptibility $\chi_0$ in all four samples starts to increase (figure 7). It is a first indication of an alteration that influences all magnetic parameters. The total IRM starts to increase at 420°C in EM14 and at 450°C in EM25. The coercivity spectra of the total IRM (figures 8a and b) show, that the increase is due to an increase in the low-coercivity fractions ($<40$ mT in EM14 and $<100$ mT in EM25). In EM25 the increase is less pronounced and starts at higher temperatures. There is no trace of this increase in the coercivity fractions of the decay curves (figures 8c and d). Also the thermal decay curves of a sample

and its sister sample show the same decay of magnetization in spite of the repeated IRM acquisition of one of them (figure 9). Apparently, magnetic particles are formed with BTs lower than the heating temperature. This agrees with the results of the control heating after each new IRM introduction. The total IRM increases moderately during these temperature steps (figures 7 and 10, closed symbols), but the IRM fraction with BTs higher than the temperature of the control heating shows a slight increase only after the 510°C heating step (figure 10, open symbols). Only at that temperature a number of grains are formed with BTs higher than the temperature of the control heating (here 480°C).

So the alteration first leads to an increase in $\chi_o$ followed by an increase of the low-coercivity fractions of the IRM at higher temperatures. It was also noticed that samples became increasingly viscous starting at 390°C. These features can be explained by the growth of magnetic particles from initial SP size through the SP/SD boundary to SD size. This new phase is highly magnetic and has low coercivities, strongly pointing to magnetite. Possible precursors are iron sulphides and goethite (Dekkers 1990a and b). Clay minerals like chlorite are stable up to higher temperatures (e.g. Brindley and Lemaitre, 1987). The most likely source for the growth of magnetite starting at 390°C is the decomposition of pyrite. Interesting in this context is the behaviour of sample EM16 with a pyrite rich burrow. It shows an enormous increase of $\chi_o$ at these temperatures (figure 7), whereas the decay curve of this sample is not different from the others (figure 9). In the other samples the magnetite production may be attributed to dispersed pyrite which is present throughout the sediment, but in low concentrations. Pyrite was detected with XRD in the magnetic concentrates of the sediment.

### *5.4. Alterations between 510 and 700°C*

#### 5.4.1. Magnetite to hematite transformation

At 510°C the IRM and $\chi_o$ of EM14 start to decrease (figure 7). A strong decrease of the low-coercivity fractions of the total IRM is accompanied by a smaller increase of the >0.3 T fraction (figure 8a). The >0.3 T coercivity fraction of the decay curve shows a slight increase as well (figure 8c), indicating that part of the alteration product has BTs higher than the alteration temperature. The alteration from a strongly magnetic low-coercivity mineral to a less magnetic high-coercivity mineral that starts at 510°C (or earlier) must be the oxidation of magnetite to hematite. This includes the magnetite-like grains that have been newly formed between 390 and 510°C. The alteration is more pronounced in EM14 than in EM25, but a gradual change of colour to bright orange due to pigmentary hematite, shows that the transformation occurs in both. The slower rate at which reactions seem to proceed in EM25 is responsible for the difference. Possibly EM25 is less porous and therefore the supply of oxygen in the sample is less.

The >0.3 T fraction of the total IRM increases much more than the same fraction of the decay curves (compare figures 8a and b with 8c and d). This is

because the first hematite grains that are formed are very small and consequently have low BTs. Gradually larger grains are formed with coercivities higher than 0.3 T, but not many have BTs higher than 600°C.

After 700°C the high-coercivity fraction (>0.3 T) forms a considerable part of the total IRM. Nevertheless, also low-coercivity grains remain. When comparing the IRM acquisition after heating to 700°C with the acquisition before the heating (figure 5), it is clear that the low-coercivity fraction of the samples has changed. The initial increase of magnetization has shifted to lower coercivities (0-10 mT). The contribution of the intermediate coercivities (40-100 mT) has almost disappeared. The same observations can be made from the AF-coercivity spectra (figures 8a and b, crosses).

These changes can be explained by the following model. It can be assumed that the oxidation proceeds from the outside to the inside of the magnetite grains, slowly reducing the size of the magnetite core of the grains and producing an hematite shell of increasing thickness. It is likely that the magnetite will become cation deficient during this process (Heider and Dunlop, 1987). Since, in the case of a magnetite/hematite transformation, evidence accumulates against exchange interaction between parent and daughter phase (Özdemir and Dunlop, 1989), the ferromagnetic interaction between core and shell is expected to be minimal and the oxidation process will cause a decrease of coercivities and BTs of the magnetite part of the grains. The originally large SD magnetite grains that may become partly maghemitized themselves, reduce in size and move towards the SP-SD size boundary. The decrease of the BTs can be shown with a second complete stepwise thermal demagnetization of the samples after they have been heated to 700°C (figure 11). The IRM in samples that were heated up to 700°C (open symbols) shows a rapid decay up to 300°C, pointing to extremely fine-grained magnetite, and an almost linear decrease to BTs above 600°C, attributed to hematite. Other specimens of the same cores had only been heated up to 600°C (closed symbols). They show a much more gradual decay to temperatures just above 500°C, indicating that the magnetite cores of the grains are still larger. The process can also explain the unexpected increase of susceptibilities at 700°C (figure 7), since many of the magnetite cores must have decreased to SP size after this heating. The higher BTs of the EM16 samples are due to the large amount of magnetite that was formed during the first series.

### 5.4.2. Magnetite production from clay minerals

Another alteration can be related to the changes observed in the weight of the samples during the thermal demagnetization procedure. After an initial weight decrease caused by the loss of adsorbed water, the sample mass is stable until about 480°C. Then it starts to decrease more and more rapidly (at 700°C about 85% of the initial weight remains). Since carbonates are stable up to higher temperatures, this decrease must be due to the breakdown of clay minerals (e.g. illite and smectite, Brindley and Lemaitre, 1987) in the matrix. EM25 shows a

renewed (small) increase of low-coercivity fractions (0-10 mT and 10-40 mT) above 540°C. It is superimposed on the other changes. In EM14 this increase may also occur, but it is probably much smaller than the overall decrease in that temperature range (figures 7 and 8a). Apparently, iron coming from the clay minerals forms new magnetic grains with low coercivities.

### 5.4.3. Demagnetization by magnetite alteration

The question arises whether at temperatures between 540 and 600°C the IRM decay curves truly reflect the BT spectrum of the magnetic grains. Transformation of magnetite to hematite seems to be an important factor. The total IRM is reduced considerably during these heating steps. The results of the control heatings show that a considerable portion of the total IRM carried by grains with BTs higher than $T_{-1}$ has disappeared after the heating to temperature T (figures 6 and 10). After the heating at 580°C, for example, the control heating at 560°C shows, that about 300 mA/m of the capability of the samples to carry an IRM with BTs higher than 560°C is lost (cf. open symbols at 580°C in figure 10). This amount is almost equal to the total loss of remanence between 560 and 580°C (figure 6). For EM25 this happens in spite of an increase in the total IRM. Between 540 and 600°C in all cases, the part of the total IRM remaining after the control heating is much less than after the first heating at the same temperature. It is therefore likely that only a small part of the decay between 540 and 600°C reflects a true BT spectrum. Transformation of magnetite to hematite turns out to be an important demagnetizing mechanism.

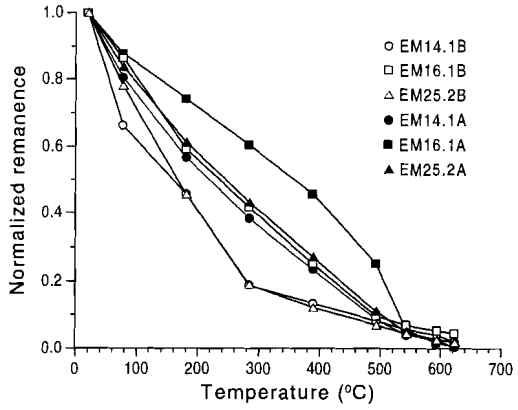


**Figure 11.** Second stepwise thermal demagnetization of IRM(2T) acquired by the samples after thermal treatment. The samples of this paper (open symbols) had been subjected to temperatures up to 700°C. The A-samples (closed symbols) are samples from the same cores. They had only been heated up to 600°C.

This has consequences for the interpretation of the decay curves as a BT spectrum. Formerly (van Velzen and Zijderveld, 1990) it was concluded that pure magnetite was the most important remanence carrier. This was also based on the large decay that occurs between 510 and 590°C. Now it seems possible that the actual maximum BTs are higher and that the carriers of the thermally most stable remanence are not pure magnetite grains, although the other magnetic properties still plead for magnetite. A slight oxidation of the grains could explain the observed phenomena. Oxidation would increase the Curie point of the grains (Readman and O'Reilly, 1972;

Nishitani and Kono, 1983), but at the same time it would make them more susceptible to further oxidation at high temperatures.

### *5.5. Consequences for NRM demagnetization*

The results are obtained for IRM(2T) and one should be cautious to apply them directly to the NRM. Like in most rocks, in these marine sediments the NRM intensity is only a fraction of the IRM intensity: the IRM/NRM ratio is in the order of 150. However, the carriers of the NRM components seem to be well represented in the IRM. Differences between the IRM and the NRM in the decay curves are due to an overrepresentation of grains with BTs between 250 and 480°C in the IRM (figure 4b) and a relatively small contribution of the 40-100 mT fraction to the AF coercivity spectrum of the IRM (figure 4a). The secondary NRM component is demagnetized between 100 and 200/250°C (figure 3). The primary component is mainly carried by grains with BTs higher than 480°C. In some instances the secondary NRM component cannot be completely demagnetized in 0.3 T alternating fields. The low BTs and high coercivities of the secondary component seem to point to goethite. However, goethite does not alter below some 300°C (Dekkers, 1990b), whereas the >0.3 T fraction of the IRM is reduced considerably after heating to 145°C. Although goethite may contribute to the NRM, its contribution can only a minor one.

The secondary component usually has a recent geomagnetic direction. It was attributed to viscous behaviour (van Velzen and Zijderveld, 1990), implying that it might be completely removed at low temperatures. However, part of the carriers of the secondary component have high coercivities and may well belong to the magnetic grains that are subject to alteration at 145°C. Since this alteration occurs with partial preservation of magnetization directions, the altered grains may have acquired high BTs, possibly even in the range used to determine the characteristic directions (510 to 580°C). Investigations are in progress to assess the extent of the influence of this alteration.

The alteration of magnetite to hematite above 540°C will only have effects on the shape of the BT spectrum. The apparent maximum BTs may not really represent the maximum BTs of the magnetic grains. The characteristic directions determined by thermal demagnetization, however, will not be influenced by the actual demagnetization mechanism: unblocking or alteration of the magnetic carriers.

The examples shown illustrate the potential of the measuring procedure. The division in coercivity fractions of the total IRM and the part of the IRM remaining after thermal demagnetization is proven to be very successful. The changes in the coercivity spectrum during the stepwise thermal demagnetization procedure reveal valuable information about the alterations involving magnetic minerals. The control measurements and measurements on sister samples are also an important part of the procedure. Apart from providing a check for the influence of repeated IRM acquisition on the remaining measurements, they also yield extra data. The

method is quite laborious. Nevertheless in many cases it may prove worthwhile to subject a number of carefully selected samples to the procedure. The marine sediment that was used as an example in this paper did not seem to pose problems during thermal demagnetization. In spite of that, the described measuring procedure revealed a number of alterations of magnetic minerals, one of which may influence the measured characteristic directions.

## 6. Conclusions

Alterations of magnetic minerals during stepwise thermal demagnetization can be studied in detail with the measuring procedure described in this paper. By monitoring changes in the AF coercivity spectrum of an IRM and the part of this IRM that remains after each heating step, the effect of alterations can be studied for each coercivity fraction of the IRM separately. The method is also a useful tool to check the validity of decay curves as true blocking temperature (BT) spectra. It can be established whether a rapid decay during thermal demagnetization is due to true unblocking of grains related to their Curie temperatures, or whether it is caused by alterations.

In samples of the Early Pliocene Trubi marls an alteration was detected after heating at a relatively low temperature: 145°C. This alteration was attributed to relaxation of stress in superficially maghemitized magnetite grains. Coercivities were reduced and $\chi_o$s were enhanced during the alteration. Part of the IRM carried by the affected grains was preserved during alteration. The alteration can be recognized by a rapid decrease in the thermal decay curve of IRM between 100 and 150°C, caused by the loss of remanence of another part of the affected grains. The alteration has paleomagnetic importance, because the NRM component that is removed in the temperature range between 100 and 200°C usually has a recent geomagnetic direction. The primary direction may be biased, if part of the secondary component becomes stable during the alteration at 145°C.

Increasing $\chi_o$ and total IRM at temperatures $>390$°C are due to the formation of magnetic grains with magnetite-like properties. They are most likely formed by the alteration of pyrite. The BTs of the newly formed grains are practically all below the temperature of formation, minimizing the possibility of acquisition of spurious magnetizations during formation in the furnace. The new grains do, however, cause the samples to become viscous.

Above 480°C the alteration of magnetite grains to hematite becomes increasingly important. Not only are the newly formed grains altered but the more stable, original grains are also affected. Above 540°C a small amount of new magnetic minerals is formed, probably due to the breakdown of iron-bearing clay minerals.

The rapid decay of magnetization above 510°C had formerly been interpreted to represent the demagnetization of magnetite grains close to their Curie temperature. (van Velzen and Zijderveld, 1990). Apparent maximum BTs were believed to be between 560°C and 590°C. However, the demagnetization process might for an important part be the result of the progressive oxidation of

magnetite grains. Data are interpreted to show that grains are formed with a (possibly cation-deficient) magnetite core and an increasingly thick hematite shell.

The alterations at 145°C and above 510°C suggest that the magnetite grains in the sediment are slightly oxidized, possibly due to recent weathering. As a result part of the grains has higher coercivities than expected for magnetite. Alterations like these may occur in many rocks, since many rocks have suffered some degree of oxidation.

**References**


Brindley G.W. and Lemaitre J., Chemistry of clays and clay minerals, ed. ACD Newman, Mineralogical Society Monograph no. 6, Langman, 1987.

Dekkers M.J., Magnetic monitoring of pyrrhotite alteration during thermal demagnetization. Geophys. Res. Lett. 17, 779-782, 1990a.

Dekkers M.J., Magnetic properties of natural goethite--III. Magnetic behaviour and properties of minerals originating from goethite dehydration during thermal demagnetization. Geophys. J. Int. 103, 233-250, 1990b.

de Visser J.P., Ebbing J.H.J., Gudjonsson L., Hilgen F.J., Jorissen F.J., Verhallen P.J.J.M. and Zevenboom D., The origin of rhythmic bedding in the Pliocene Trubi formation of Sicily, Southern Italy. Palaeogeography, Palaeoclimatology, Palaeoecology 69, 45 - 66, 1989.

Dunlop D.J., Magnetic mineralogy of unheated and heated red sediments by coercivity spectrum analysis. Geophys. J. R. Astr. Soc. 27, 37-55, 1972.

Heider F. and Dunlop D.J., Two types of chemical remanent magnetization during the oxidation of magnetite. Phys. Earth Planet. Int. 46, 24-45, 1987.

Heller F., Rockmagnetic studies of Upper Jurassic limestones from Southern Germany. J. Geophys. 44, 525-543, 1978.

Hilgen F.J. and Langereis C.G., The age of the Miocene-Pliocene boundary in the Capo Rossello area (Sicily). Earth Planet. Sci. Lett. 91, 214-222, 1988.

Lowrie W., Identification of ferromagnetic minerals in a rock by coercivity and unblocking temperature properties. Geophys. Res. Lett. 17, 159-162, 1990.

Nishitani T. and Kono M., Curie temperature and lattice constant of oxidized titanomagnetite. Geoph. J.R. Astron. Soc. 74, 585-600, 1983.

Özdemir Ö. and Dunlop D.J., Chemico-viscous remanent magnetization in the $Fe_3O_4$-$\gamma Fe_2O_3$ system. Science 243, 1043-1047, 1989.

Readman P.W. and O'Reilly W., Magnetic properties of oxidized (cation-deficient) titanomagnetites (Fe, Ti, $0)_3O_4$. J. Geomagn. Geoelectr. 24, 69-90, 1972.

van Velzen A.J. and Zijderveld J.D.A., Rock magnetism of the Early Pliocene Trubi formation at Eraclea Minoa (Sicily). Geophys. Res. Lett. 17, 791-794, 1990.

# 4 Effects of weathering on single domain magnetite in Early Pliocene marine marls


## Abstract

Rock magnetic parameters are often used to recognize variations in the original magnetic mineralogy and for normalizing purposes in paleointensity studies. Incipient weathering, however, is shown to have profound but reversible influence on the rock magnetic properties of the marls of the Early Pliocene Trubi formation in southern Sicily (Italy). The remanence in the marls resides in single domain (SD) magnetite grains, but the remanent coercive force ($H_{cr}$) shows a strong variation and most values observed are anomalously high ($H_{cr}$ range 36-188 mT).

The enhanced coercivities are attributed to stress in the magnetite grains induced by surface oxidation at low temperature. Upon heating to 150°C a reduction of coercivities occurs that can be explained by a stress reduction as a result of a higher $Fe^{+2}$ diffusion rate at higher temperature. After heating to 150°C coercivities are quite uniform throughout the outcrop and the values are characteristic of SD magnetite ($H_{cr}$ range 30-38 mT). Other parameters are also influenced by heating at 150°C. The bulk susceptibility increases 4-24%, and the isothermal remanent magnetization (IRM) decreases 5-11%. The increase in anhysteretic remanent magnetization (ARM) is large: 20-242%. The magnitude of the changes seems to be related to the degree of weathering.

Another effect of heating the marl samples to 150°C is a substantial reduction of the coercivities of the secondary overprint in the natural remanent magnetization. After heating, separation of the secondary and primary components by alternating field demagnetization is more efficient. The usual difficulties of thermal demagnetization above 300°C can thus be avoided by a combination of moderate heating to 150°C and subsequent alternating field demagnetization.


## 1. Introduction

Between the acquisition of the primary component of the natural remanent magnetization (NRM) and the sampling for paleomagnetic purposes the magnetic mineralogy of rocks can be subject to alterations. These are a major concern for paleomagnetists, because each change may influence the stability of the primary component or introduce a new remanence component.

In this chapter the effects of weathering on the NRM and the magnetic properties of samples from outcrops of Early Pliocene marine marls of the Trubi formation at Eraclea Minoa (Sicily, Italy) are reported. The marls of the Trubi

formation are exposed in a series of cliffs along the south coast of Sicily. The fine-grained marls have a high carbonate content (60 to 80%). Repeating small-scale sedimentary cycles, related to variations in the precession of the earth, are expressed as grey-white-beige-white sequences in the outcrop (Hilgen, 1987). These are the colours of the weathered sediment. Only after removing this weathered surface layer the colours start to change to the blue-grey typical of fresh marls. The weathered surface varies in thickness depending on the position in the outcrop. It can be over a meter thick but, in other places, fresh sediment is covered by no more than ten centimetres of weathered sediment.

Most samples for the present study were collected for a magnetostratigraphic study (Langereis and Hilgen, 1991) at Eraclea Minoa. Samples were taken from grey and beige levels, because they appeared to be less weathered. For magnetostratigraphic purposes a uniform sampling interval is required and it was not always feasible to remove the weathered layer completely. This did not present a problem, however, since the normal or reversed polarity of the primary component could be easily established with routine stepwise thermal demagnetization, despite the presence of a secondary component of varying magnitude (figure 1). Heating to 100°C removes a viscous laboratory component. The major part of a secondary component, having a near present-day geomagnetic field direction, is demagnetized between 100 and 200°C. It is not clear at which temperature this secondary overprint is completely removed. The secondary component varies in magnitude and sometimes has a considerable overlap with the primary component (figure 1c). Samples taken from fresh-looking sediment generally have a secondary remanence which is completely removed at about 200°C (figure 1b). The secondary component is absent in truly fresh samples (figure 1a).

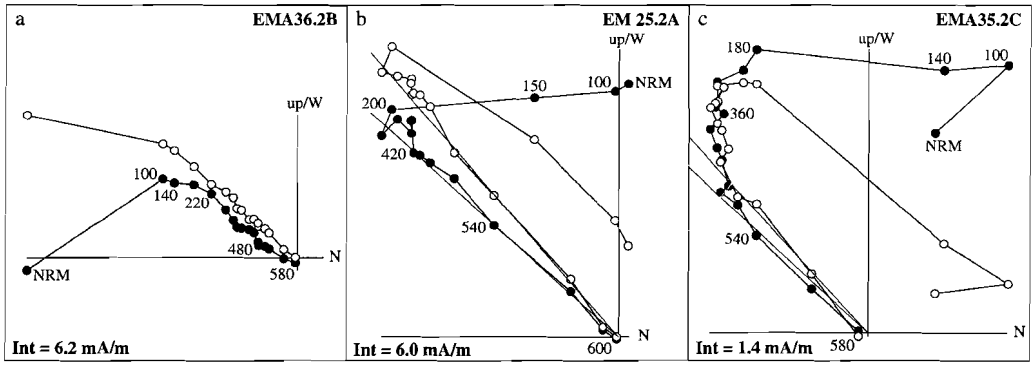


**Figure 1.** Thermal demagnetization diagrams of Trubi samples with a reversed primary component and a secondary component with a near present-day field direction (corrected for a 14° bedding tilt). A laboratory component is removed by heating to 100°C. (a) Fresh sample without secondary component. (b) Typical sample with secondary component (c) Weathered sample with a large overlap of primary and secondary components. Temperatures in °C. Int is the initial NRM intensity.

As indicated by the maximum unblocking temperatures, the primary remanence of the marls resides in magnetite. Rock magnetic experiments demonstrated that the remanence resides in large single domain (SD) magnetite (van Velzen and Zijderveld, 1990). At that time the influence of weathering on the magnetic properties of the magnetite was not evident. The effects of weathering were revealed by a subsequent study of alteration of magnetic minerals during routine stepwise thermal demagnetization (van Velzen and Zijderveld, 1992). Apart from alterations at higher temperatures (>350°C), changes in rock magnetic properties were observed after heating the samples to 145°C.

The temperature needed to accomplish the changes may be lower than 145°C. In the previous study samples the heating steps were 100°C and 145°C and samples were about ten minutes at these temperatures. At 100°C no changes in rock magnetic properties were observed. After the 145°C step the alteration was completed. For the present study a heating temperature of 150°C was chosen to ensure that rock magnetic changes occur in the samples.

## 2. Characteristics of the alteration at 150°C

The effects of alteration at about 150°C (van Velzen and Zijderveld, 1992) can be summarized as follows (see figure 2). The alteration is accompanied by an increase in initial susceptibility ($\chi_o$). The Isothermal Remanent Magnetization (IRM) that is acquired in a 2 T magnetic field after the 150°C heating step is less than after the 100°C step (figure 2a). The thermal decay curve of an IRM(2T) shows a relatively large remanence loss at 150°C (figure 2b).

More important, however, is a significant change in the coercivities of remanence carrying minerals. The alternating field (AF) coercivity spectrum of the total IRM(2T), induced after heating to 100°C, shows a considerable contribution of the >100 mT fractions (figure 2c). These relatively high-coercivity fractions almost disappear in the coercivity spectrum of the part of this IRM remaining after heating to 150°C.

It is tempting to attribute this change to the demagnetization of goethite, a typical product of weathering with high coercivities and a Néel temperature of the well-crystalline form between 120 and 130°C (e.g. Strangway et al., 1968; Hedley, 1971; Dekkers, 1989a). However, goethite is stable up to much higher temperatures (the conversion of goethite to hematite starts at about 250°C; Dekkers, 1990) and its typical hard remanence should reappear when after heating at 150°C a new IRM is induced in the sample. This is not the case. The >100 mT fractions contribute only a few per cent to this new IRM (figure 2c) proving that the high-coercivity remanence carrier no longer exists, excluding goethite as a possible explanation. For the same reason hematite cannot be responsible for the changes in the coercivity spectrum.

The coercivity spectra in figure 2c contain more information about the nature of the alteration and the magnetic mineral involved. While the >100 mT fractions decrease during heating to 150°C, the 10-100 mT fractions increase. Part of this

increase occurs during heating, as seen when comparing the 10-40 mT fraction of the IRM induced after heating to 100°C and the 10-40 mT fraction remaining after heating to 145°C. The increase of this fraction indicates a transfer of part of the >100 mT remanence to lower-coercivity fractions. This can only be interpreted as representing the reduction of coercivities of remanence carrying grains.

### 3. High-coercivity magnetite

To identify the mineral responsible for the high coercivities and the changes observed during heating to 145°C, thermal demagnetization of the high-coercivity part of the IRM was performed. After acquiring a 2 T IRM, five samples from the

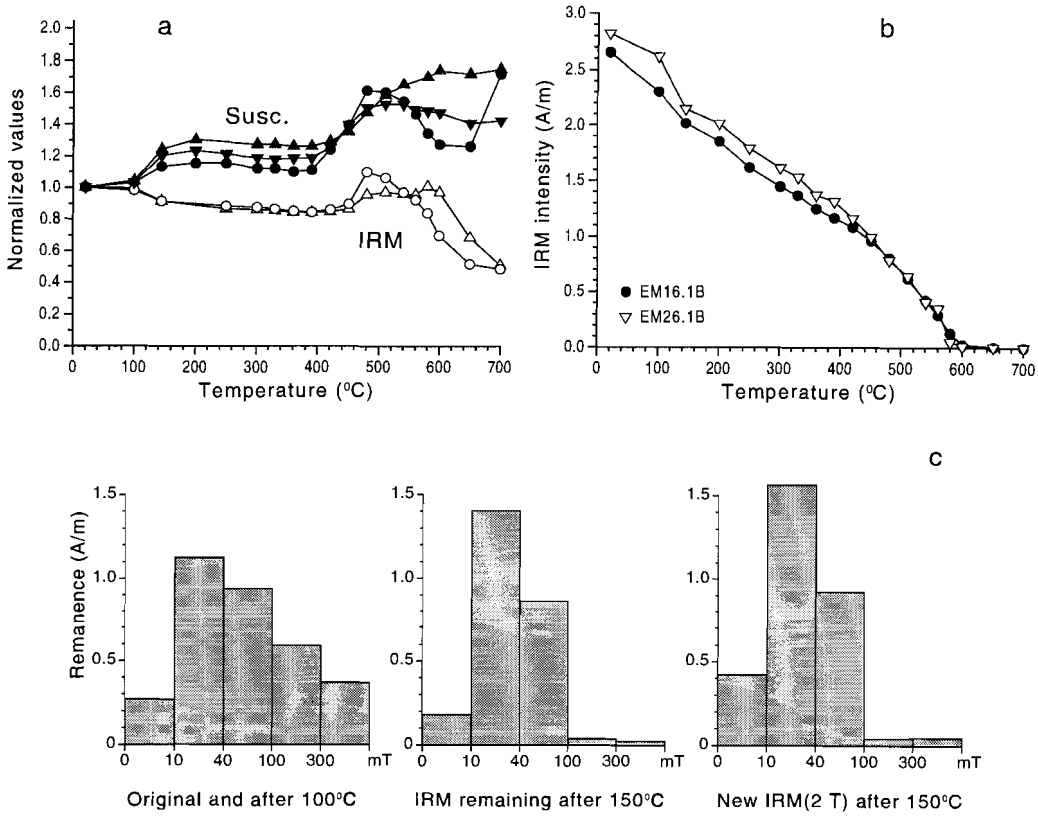


**Figure 2.** Changes in rock magnetic parameters during heating to 150°C. The magnitude of these changes is related to the degree of weathering. (a) Bulk susceptibility (Susc.) and the total IRM(2T) induced in the samples after each temperature step. (b) Routine thermal decay curves of IRM(2T), induced only once. (c) Coercivity spectrum of the original IRM and the IRM induced after heating to 100°C, spectrum of the same IRM after heating to 150°C (before inducing a new IRM) and spectrum of a new IRM induced after heating to 150°C (see van Velzen and Zijderveld (1992) for a complete description of the thermal alterations).

outcrop at Eraclea Minoa were demagnetized in alternating fields of 80 mT and five in alternating fields of 300 mT (stationary AF demagnetization in three orthogonal directions). The theoretical maximum coercivity for (very elongated) SD domain magnetite grains is 300 mT (e.g. Stacey and Banerjee, 1974). In practice even coercivities over 100 mT are rare. After demagnetization in alternating fields of 80 mT still a considerable part of the IRM remains (13 to 25%; see figure 3a). After partial AF demagnetization, the samples were subjected to normal stepwise thermal demagnetization without the repeated IRM acquisition (figure 3a). The four samples with more than 20% of the original IRM remaining show a large decay at 150°C and a final decay of a considerable part of the remanence between 560 and 600°C, close to the Curie temperature of pure magnetite. Apparently, the >80 mT IRM is mainly carried by magnetite grains, but magnetite with rather high coercivities. The small part of the IRM demagnetized above 600°C indicates a hematite contribution.

All magnetite remanence should be removed after demagnetized with 300 mT alternating fields. The >300 mT remanence in the other five samples is therefore expected to be carried by goethite and hematite, which were shown to carry a small part (about 5%) of the IRM (van Velzen and Zijderveld, 1990). The thermal decay curves of three of the samples indeed show a large decay at 100°C (figure 3b), indicating the presence of goethite, which generally has unblocking temperatures substantially lower than the Néel temperature of 120°C for well-crystalline goethite (Lowrie and Heller, 1982; Dekkers, 1989b). In these three samples, a monotonous decrease of the remanence between 200 and 650°C is due to the contribution of different grain sizes of hematite. The >300 mT remanence of these samples is only about 7% of the total IRM. The other two samples have a larger contribution of the >300 mT IRM (11 and 23%, respec-

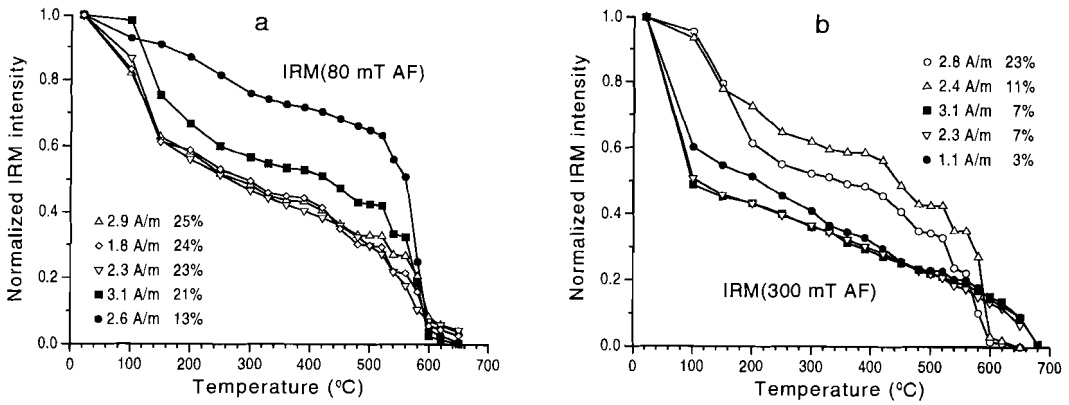


**Figure 3.** Normalized thermal decay curves of the high-coercivity part of the IRM. (a) IRM after 80 mT AF. (b) IRM after 300 mT AF. For each sample the total IRM(2T) and the percentage of this IRM remaining after AF treatment is tabulated in the figure. Samples with the highest percentage of remaining IRM show a relatively large decay of remanence at 150°C, attributed to the presence of magnetite with enhanced coercivities (see text).

tively) and a different demagnetization behaviour. They show a relatively large remanence decay after the 150 and 200°C steps and also a distinct decay close to the Curie temperature of magnetite. Apparently, in these two samples even a large part of the >300 mT IRM is carried by magnetite grains, but magnetite with unusually high coercivities.

An explanation for the high coercivities can be the presence of stress. During heating at 150°C the stress is reduced and part of the remanence is randomized. This causes the relatively large decay near 150°C, by which the alteration can be recognized (figures 2b and 3). Apparently, another part of the affected grains preserves the remanence during alteration and this remaining remanence is stable until over 560°C (figure 3). The high unblocking temperatures indicate that the magnetite grains that preserve their remanence are probably of SD or pseudo single domain (PSD) grain size and the maximum unblocking temperatures some 20°C above the Curie temperature of stoichiometric magnetite may point to some oxidation of the grains (Nishitani and Kono, 1983).

## 4. The 150°C alteration versus weathering

Although it is difficult to judge the exact degree of weathering of a sample from its appearance, it is clear that the lowest remanent coercivities are found in samples taken from fresh-looking, blue-grey sediment. The highest remanent coercivities measured are five times as high as the lowest ones (188 mT compared to 36 mT; see table A). The high coercivities are reduced by heating to 150°C. Thus there appears to be a strong relationship between these high coercivities and the 150°C alteration. This can be illustrated with an example of a large number of samples that were collected for a study of a polarity transition in the Trubi formation at Punta di Maiata (van Hoof et al., 1993).

In spite of considerable effort the weathered sediment could be removed to expose truly fresh sediment only at the lower most 10 cm of the 1 m stratigraphic sampling interval. The samples from this lower level are significantly different from the more weathered samples. They do not have a secondary overprint in the NRM. Their remanent coercivities are considerably lower than those of the more weathered samples (46 mT and about 70 mT, respectively). Also they do not show the large decay of IRM after heating to 150°C (figure 4). In the more weathered samples this decay indicates the presence of the 150°C alteration, during which the high coercivities were shown to decrease, minimizing the initial differences between relatively fresh and weathered samples. At the Eraclea Minoa section, the freshest samples show the same characteristics as the samples from the lowest level.

The magnitude of the changes that occur during heating to 150°C are considerable. Some rock magnetic properties of samples with different weathering degrees were measured before and after heating (Table A). The $\chi_o$ increase of the samples (4-24%) is significant, especially when considering that up to 50% of $\chi_o$ is due to paramagnetic matrix minerals. The decrease of the total IRM(1.5 T) is

relatively smaller (5-11%). The changes hardly affect the large variation in IRM intensities found in the Trubi marls. Both IRM and $\chi_o$ remain representative of lithological variations, despite of the influence of weathering. This is not the case for the remanent coercive force ($H_{cr}$). After heating to 150°C, the $H_{cr}$ values are quite uniform (30-38 mT). The small remaining variation may be partly due to the varying contribution of goethite and hematite to the IRM (roughly between 3-7%). Clearly, the initial $H_{cr}$ values (36-188 mT) can largely be attributed to the degree of weathering rather than varying primary magnetic mineralogy. From the wide range of the initial $H_{cr}$ values it is clear that the effect of low-temperature oxidation can be enormous.

Anhysteretic remanent magnetization (ARM) is a parameter that is often used for normalization purposes in relative paleointensity studies (e.g. King et al., 1983; Tauxe, 1993). ARM is very sensitive to the distribution of coercivities of the magnetic minerals, because the inducing alternating fields are usually not higher than 100 mT. In this study, ARM was induced before and after heating, using slowly decreasing alternating fields with a maximum of 100 and 200 mT and an inducing steady field of 0.03 mT (Table A). As a consequence of the reduction of high coercivities to values below 100 mT and 200 mT, respectively, the ARM intensities increase considerably during heating. For the ARM(100 mT) the smallest increase was 20%, but in samples with initially high coercivities increases of more than 200% were measured.

Because the degree of weathering usually varies within an outcrop, the coercivities of the unheated samples will mainly reflect the degree of weathering. After heating to 150°C they will give a better representation of the original magnetic mineralogy. In paleointensity and polarity reversal studies ARM is often used as a normalization parameter to separate lithological effects from the effects of paleofield variations. Weathering can seriously interfere with this method. It is therefore recommended to check for weathering induced changes of magnetic properties.

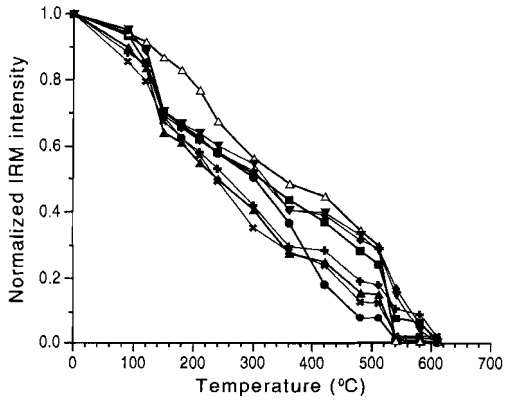


**Figure 4**. Thermal demagnetization of IRM(2T) in closely spaced samples taken at Punta di Maiata for a polarity transition study (van Hoof et al., 1993). Samples were drilled from a vertical surface prepared by removing a thick surface layer of weathered sediment. The rapid decay at 150°C indicates that most samples are nevertheless affected by weathering (closed symbols). Only a sample from the lowest level, where the sediment was visibly fresher, does not show that decay (open symbols).

| sample | Susceptibility in E-06 SI | | | IRM(1.5 T) in mA/m | | | Hcr(1.5 T) in mT | | | ARM(100 mT) in mA/m | | | ARM(200 mT) in mA/m | | |
|---|---|---|---|---|---|---|---|---|---|---|---|---|---|---|---|
| | original | after 150°C | | original | after 150°C | | original | after 150°C | | original | after 150°C | | original | after 150°C | |
| EM 4.2B | 58 | 67 | +16% | 1049 | 960 | -8% | 54.4 | 37.6 | -31% | 49.0 | 79.3 | +62% | 56.3 | 81 | +44% |
| EM 7.1B | 92 | 99 | +8% | 1309 | 1233 | -6% | 36.9 | 29.8 | -19% | 69.3 | 90.6 | +31% | 73.7 | 90.9 | +23% |
| EM11.2B | 96 | 101 | +5% | 1284 | 1215 | -5% | 35.9 | 30.1 | -16% | 77.1 | 92.6 | +20% | 81.3 | 92.9 | +14% |
| EM15.2B | 167 | 185 | +11% | 2855 | 2673 | -6% | 54.5 | 34.8 | -36% | 156.9 | 236.9 | +51% | 174.3 | 240.8 | +38% |
| EM51.1B | 78 | 97 | +24% | 1725 | 1536 | -11% | 187.6 | 35.6 | -81% | 43.1 | 147.6 | +242% | 47.9 | 149.2 | +211% |
| EM53.3A | 91 | 112 | +23% | 1832 | 1634 | -11% | 123.1 | 33.3 | -73% | 45.6 | 145.6 | +219% | 52.5 | 146.4 | +179% |
| EM54.1B | 224 | 249 | +11% | 3425 | 3080 | -10% | 47.7 | 32.8 | -31% | 76.9 | 157.4 | +105% | 79.1 | 158.4 | +100% |
| EM58.3 | 206 | 215 | +4% | 2912 | 2696 | -7% | 37.4 | 32.3 | -14% | 108.0 | 130.5 | +21% | 118.7 | 131.3 | +11% |

**Table A**. The effects of heating at 150°C on samples with different degrees of weathering. ARM was induced in AC coils in a DC field of 0.03 mT and peak alternating fields of 100 and 200 mT respectively.

## 5. A re-evaluation of magnetite grain size

Magnetite is the major remanence carrier the Trubi marls. The conclusion that the magnetite is of SD grain size (van Velzen and Zijderveld, 1990) was mainly based on three rock magnetic results: (1) the hysteresis properties are close to those of SD grain size fractions of magnetite and theoretical values for SD magnetite, (2) a large part of the remanences (both NRM and IRM) is unblocked close to the Curie temperature of magnetite, and (3) the absence of a Verwey-transition when cycling to liquid nitrogen temperature through the isotropic point at -153°C. However, these properties can all be influenced by weathering. A re-evaluation is therefore necessary, using the fact that the original magnetic properties seem to be largely restored after heating to 150°C.

The remanence ratio $J_{rs}/J_s$ and the coercivity ratio $H_{cr}/H_c$ are indicative of grain size and domain structure (Day et al.,1977). For magnetite grains of different sizes all experimental values seem to follow a single trend (Dunlop, 1986). For the Trubi samples the ratios are close to the values for large SD grains, but both ratios tend plot above this trend (van Velzen and Zijderveld, 1990). Considering the high coercivities of the oxidized magnetite grains, however, all magnetite can not have been saturated in the alternating fields applied during the hysteresis measurements (a maximum field of 200 mT was available). An additional aspect is the presence of stress. These hysteresis parameters are less reliable as grain size indicators when stress is present (Gapeev and Tselmovich, 1992). With increasing stress the remanence and coercivity ratios change, but they change in such a way that even crushed grains do not seem to digress from the observed trend (Dunlop, 1986). The ratios are merely moved to values that are characteristic of larger grain sizes. Because heating to about 150°C seems to reduce the stress and change the properties of the grains to those normal for magnetite, the hysteresis parameters of some samples were measured before and after heating to 150°C (Table B). After heating, the hysteresis parameters will be closer to the true values, because

| Sample | Total IRM mA/m | IRM after heating | Hcr(1.5 T) (mT) | Hc (mT) | Hcr/Hc | Jrs/Js | LT recov. % | LT incr. % |
|---|---|---|---|---|---|---|---|---|
| EM 25.1B | 3411 | 2222 | 56.5 | 30.4 | 1.86 | 0.48 | 100 | 10 |
| 150°C | 2790 | | 34.7 | 22.5 | 1.54 | 0.48 | 100 | 10 |
| EMA 35.8A | 978 | 598 | 134 | 26.6 | 5.04 | 0.48 | 100 | 15 |
| 150°C | 834 | | 33.7 | 21.1 | 1.6 | 0.42 | 100 (100) | 15 (9) |

**Table B.** Comparison of rock magnetic properties before and after heating to 150°C. The columns show, from left to right: the total IRM acquired in a 1.5 T field; the part of this IRM remaining after the heating; the $H_{cr}$ after acquisition of the IRM(1.5 T); $H_c$ from hysteresis measurements in a maximum field of 0.2 T; coercivity ratio $H_{cr}/H_c$; remanence ratio $J_{rs}/J_s$; recovery of the IRM after cycling to -196°C; increase of IRM at -196°C compared to room temperature (values between brackets for the IRM remaining after heating to 150°C).

the samples are closer to saturation. The ratios are still close to those of large SD grains (Day et al., 1977) and the data points are closer to the generally observed trend (Dunlop, 1986).

In these samples unblocking of remanence is not the only demagnetization mechanism. Near 580°C the conversion of magnetite to hematite is, at least partly, responsible for demagnetization (van Velzen and Zijderveld, 1992). After the 150°C alteration, the magnetite grains likely remain in a partly oxidized state, which would raise the Curie temperature (e.g. Nishitani and Kono, 1983). Possibly, the alteration to hematite is facilitated by the partial oxidation of the grains. The thermal decay curves therefore also indicate that the remanence carrier is SD magnetite, probably with some degree of oxidation.

The behaviour of magnetite grains during low-temperature cycling may also be influenced by stress. The absence of the Verwey transition and a high recovery of magnetization are generally regarded characteristic of SD grains (Kobayashi et al., 1965; Levi and Merrill, 1978; Dunlop and Argyle, 1991; Heider and Dunlop; 1992). There are two factors that should be considered, however. Stress in multi-domain (MD) magnetite grains cancels the effect of near zero anisotropy constants at the isotropic point (-143°C), since magnetostriction rather than magneto-crystalline or shape anisotropy controls coercive force at low temperatures (Hodych, 1991). The recovery of magnetization during heating through the crystallographic Verwey transition (-153°C) is usually low in MD grains, but it will be enhanced by the presence of stress-induced anisotropies (Heider et al., 1992). The large recovery could be misinterpreted to be due to a SD grain size of the magnetite. Moreover, the absence of the Verwey transition in SD grains is attributed to oxidation (Özdemir et al., 1993). Minor surface oxidation can induce sufficient stress to suppress the transition. In the present samples, the absence of

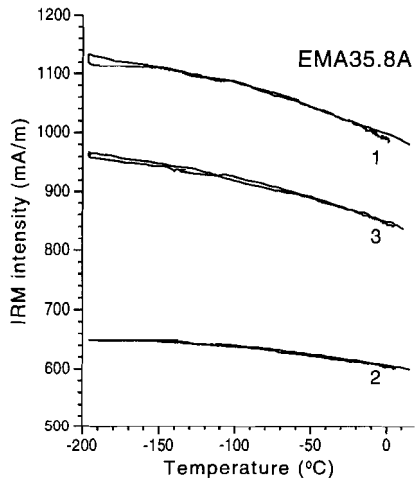


**Figure 5.** Low-temperature cycling of IRM for sample EMA35.8A: (1) before thermal treatment; (2) the part of the IRM remaining after heating to 150°C and (3) the newly induced IRM. The absence of a Verwey transition near -153°C indicates oxidation of the SD magnetite (Özdemir et al., 1993). Additional proof that some goethite contributes to the IRM and is responsible for part of the increase in magnetization towards lower temperatures comes from the low-temperature cycling of the part of the IRM remaining after heating at 150°C (cf. Table B). Goethite remanence increases almost linearly with decreasing temperature (Heller, 1978; Dekkers, 1989b; Rochette and Fillion, 1990). The IRM in (1) and (3) increased by 125 mA/m at -196°C, but the IRM remaining after heating at 150°C (i.e. above the Néel temperature of goethite) increases only 25 mA/m (2).

the Verwey transition should therefore be regarded as a confirmation of the presence of surface oxidation rather than an argument for the SD size of the magnetite. After heating at 150°C, the recovery of the original magnetization is complete (figure 5, Table A). Apparently, some stress is still present after heating.

The former conclusion that the magnetite is large SD (van Velzen and Zijderveld, 1990) can be maintained. It must be added that the properties of the grains are modified by surface oxidation. These modifications seem to be largely undone by heating to 150°C.

## 6. Effects on NRM

The low-temperature oxidation of the magnetite grains and heating at 150°C cause appreciable changes in rock magnetic properties that will also influence the behaviour of the NRM. Heating seems to remove the effects of weathering to a large degree, but this does not necessarily mean that the NRM is restored to its original form.

Weathering has more influence on the efficiency of AF demagnetization than on the efficiency of thermal demagnetization (cf. figure 1). Initially samples show a large variation in AF demagnetization behaviour. In truly fresh samples, the NRM can be completely demagnetized with 100 mT fields (figure 6a). For other, more weathered samples, fields of 300 mT are needed (figure 6b) or even not sufficient to accomplish complete demagnetization (figure 6c).

To investigate the influence of heating at 150°C on the NRM a combination of AF and thermal demagnetization was used. Samples with reversed primary components were selected, in which the influence of weathering was clearly present. First, stepwise AF demagnetization was performed in fields up to 150 mT (figure 7). In all samples the NRM was only partly demagnetized at these fields. Subsequently the samples were heated and almost no changes are evident at 100°C. This confirms that none of the remaining NRM is carried by goethite. The effect of heating at 150°C on the NRM is remarkable, albeit less surprising with the IRM results in hand. A large NRM component is demagnetized with a direction close to that of the secondary component, i.e. the present-day field direction. However, while preserving their original magnetization direction, the carriers of the remaining NRM have been altered. This is revealed when starting a new stepwise AF demagnetization. Now low alternating fields remove the formerly high-coercivity (>150 mT) remanence, starting with the remaining part of the secondary component: fields of 100 mT suffice to remove the remanence completely (cf. figure 7). These fields are comparable to those needed in unheated samples that are truly fresh. The same reduction of coercivities that was found for the IRM apparently affects the carriers of the NRM.

During the AF-Thermal-AF demagnetization sequence, and after removal of the laboratory component, the NRM vectors for all samples are close to a single plane through the origin. Apparently, the NRM consists only of two components throughout the demagnetization procedure, in spite of the low-temperature

oxidation due to weathering and the 150°C alteration. It is therefore possible to separate the behaviour of the primary and secondary component during demagnetization. The calculated decay curves will, however, depend on the choice of directions of the two remanence components. In the following a reasoning similar to the remagnetization circles analysis is used (McFadden, 1977), but in reversed order, starting with a choice of most likely directions and adjusting this choice for each individual sample. For the secondary component the local geocentric axial dipole direction (360°, 57°) is a logical choice, since this component likely has a viscous origin (see below). The reversed primary component has an average clockwise tectonic rotation of about 35° after correction for dip of the strata (Langereis and Hilgen, 1991; Scheepers and Langereis, 1993). The average inclination is about 46°, which is somewhat shallower than that of the present geomagnetic field (Scheepers and Langereis, 1993).

To find the best fitting plane for each sample, the perpendicular projection of every remanence vector to the plane was determined. The sum of the distances between original and projected vector endpoints (after removing the laboratory component) was minimized by slightly adjusting the primary direction in order to allow for small differences in inclination and possibly declination. The resulting planes were close to the standard best-fit planes (Kirschvink, 1980) obtained using no *a priori* directional information. The angular difference between the poles of the calculated and the best-fit planes (0.5° to 4.5°) was generally well within the maximum angular deviation of the best-fit planes (3° to 8°).

An extra check for a possible erroneous choice of directions is provided by the changes in the distance between every measured remanence vector and its projection during demagnetization. After demagnetization of the laboratory component (with 10 mT AF), these distances remain consistently close to zero throughout the total demagnetization sequence (figure 7). Taking the foregoing into account, it is therefore likely that the chosen primary and secondary directions are close to the true directions of the two components in each sample. It should be kept in mind, however, that a slightly different choice of the two NRM directions the calculated plane results in different decay curves.

The decay curves confirm that both the primary and secondary NRM components have increased coercivities (>150 mT) due to oxidation (figure 7). After the first AF series both components are only partly demagnetized. It is now possible to separate the effect of the 150°C heating on stable SD grains that carry the remaining primary NRM and the effect on the less stable grains that carry the remaining secondary NRM. While, as expected, the secondary remanence diminishes during heating, the primary remanence increases in all samples. The second AF demagnetization shows that, after heating, the carriers of the secondary component generally have lower coercivities than those of the primary component.

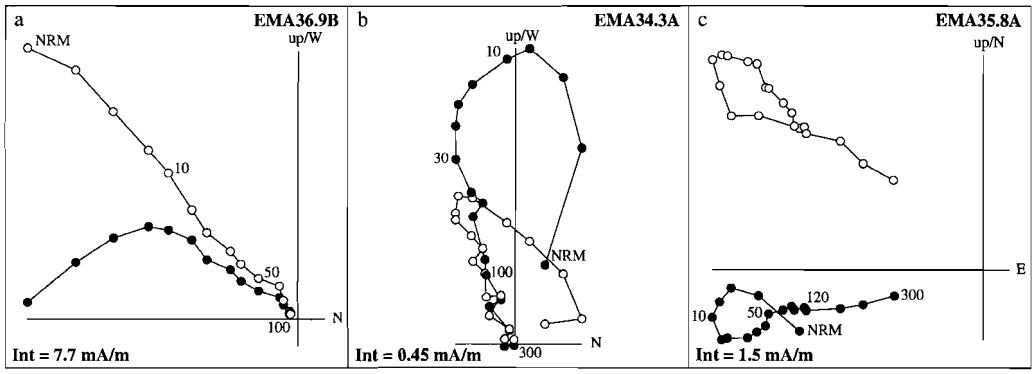


**Figure 6.** AF demagnetizations of NRM (corrected for bedding tilt) for (a) a fresh sample; the NRM is completely demagnetized at 100 mT, (b) a typical sample; large overlap between primary and secondary components and (c) a relatively weathered sample; the NRM cannot be completely demagnetized at 300 mT. Alternating fields indicated in mT. Int is initial NRM intensity.

## 7. Origin of the secondary remanence

The secondary component has a near present-day geomagnetic field direction before tilt correction, which indicates an age of less than 780 ka, but the lack of a secondary component in the freshest samples restricts its age to the period over which weathering affects the sediment. It is unlikely that the secondary remanence is a chemical remanence due to low-temperature oxidation. Even during the oxidation of SD titanomagnetite and magnetite up to very high oxidation degrees in an ambient magnetic field, the direction of the parent remanence is preserved (Özdemir and Dunlop, 1985; Heider and Dunlop, 1987). The exchange coupling between mother and daughter phases is very strong. Moreover, the magnetite grains in the sediment are only in a first stage of maghemitization and the enhanced coercivities would make it even more difficult for the magnetization of the grains to switch to the present-day field direction.

The presence of a secondary component with a present-day field direction in more weathered samples can be argued to be due to the stabilizing effect of the low-temperature oxidation. In the freshest samples this component is absent (cf. figure 1 and 6). Before weathering, small SD grains and superparamagnetic (SP) grains have a magnetic moment directed along the local geomagnetic field in the outcrop. Weathering results in an increase of coercivities and relaxation times of these magnetite grains, creating a stable secondary component. Because the component is stabilized through alteration, it becomes by definition a chemical remanent magnetization (CRM). The initial viscous nature of the secondary remanence is confirmed by the results of the combined AF-Thermal-AF demagnetization of the NRM (figure 7). During heating at 150°C, the anomalously high coercivities of the magnetite grains are reduced and the blocking

temperatures are reduced correspondingly. A large part of the secondary component is demagnetized after heating at 150°C, indicating that the blocking temperatures of this remanence become lower than 150°C after the stabilizing effects of the weathering have been largely removed. The secondary NRM may reside in small SD and SP, that are stabilized by the increased coercivities. At room temperature the viscous behaviour of small SD grains is only small due to their long relaxation times, that correspond to their blocking temperatures, but over a period of 780 ky they can acquire a significant viscous remanence. SP grains are viscous by definition, but the increase of coercivities accompanying oxidation will also have a stabilizing effect on those grains, so that both small SD grains and grains that were originally SP may contribute to secondary component.

The changes with respect to the IRM can be explained in a similar fashion. After heating to 150°C less IRM can be induced in the samples (figure 2a, Table A), because the grains that were temporarily stabilized by the oxidation become superparamagnetic again. The relatively large decay of remanence during thermal demagnetization of the IRM at 150°C (figures 2b and 3) is due to the reduction of blocking temperatures of the small SD grains to values below 150°C.

There are two possible explanations for the differences between fresh and weathered samples. The first explanation assumes the same grain-size distribution for all samples. The grains that carry the secondary NRM in weathered samples, have relatively short relaxation time in fresh samples and consequently carry the laboratory component. The second explanation is that in weathered samples other chemical processes have been active before the stabilizing oxidation. In the presence of formation water, iron can be leached from more stable SD grains, reducing their size and bringing them nearer the SP-SD grain size (very effective in small grains). The leaching facilitates oxidation, since $Fe^{2+}$ is preferentially removed from iron oxide crystals (Stumm and Sulzberger, 1992). During the low-temperature oxidation the reduction of size may continue, because in an aqueous environment removal of iron rather than addition of oxygen is the most likely process by which maghemitization proceeds (Akimoto et al., 1984; Brown and O'Reilly, 1987). This new grain-size fraction will have viscous properties, but it

---

**Figure 7.** Combined AF-Thermal-AF demagnetizations of NRM, demagnetization diagrams and remanence decay curves. The demagnetization diagrams are corrected for bedding tilt and values are in mT unless indicated otherwise. AF demagnetization up to 150 mT, followed by thermal demagnetization at 100 and 150°C. After heating to 150°C, a new AF demagnetization up to 100 mT completely demagnetizes the remaining NRM. The decay curves of primary (open circles) and secondary (open squares) components (see text), after demagnetization of the laboratory component, show a large overlap between the two components and an increase of primary NRM after heating at 150°C. Closed circles show the sum of primary and secondary intensities. Stars denote the perpendicular distances between measured remanence vectors and the plane through the primary and secondary remanence vectors. All values are normalized to the maximum of the sum of the intensities (after demagnetization of the laboratory component with approximately 10 mT).

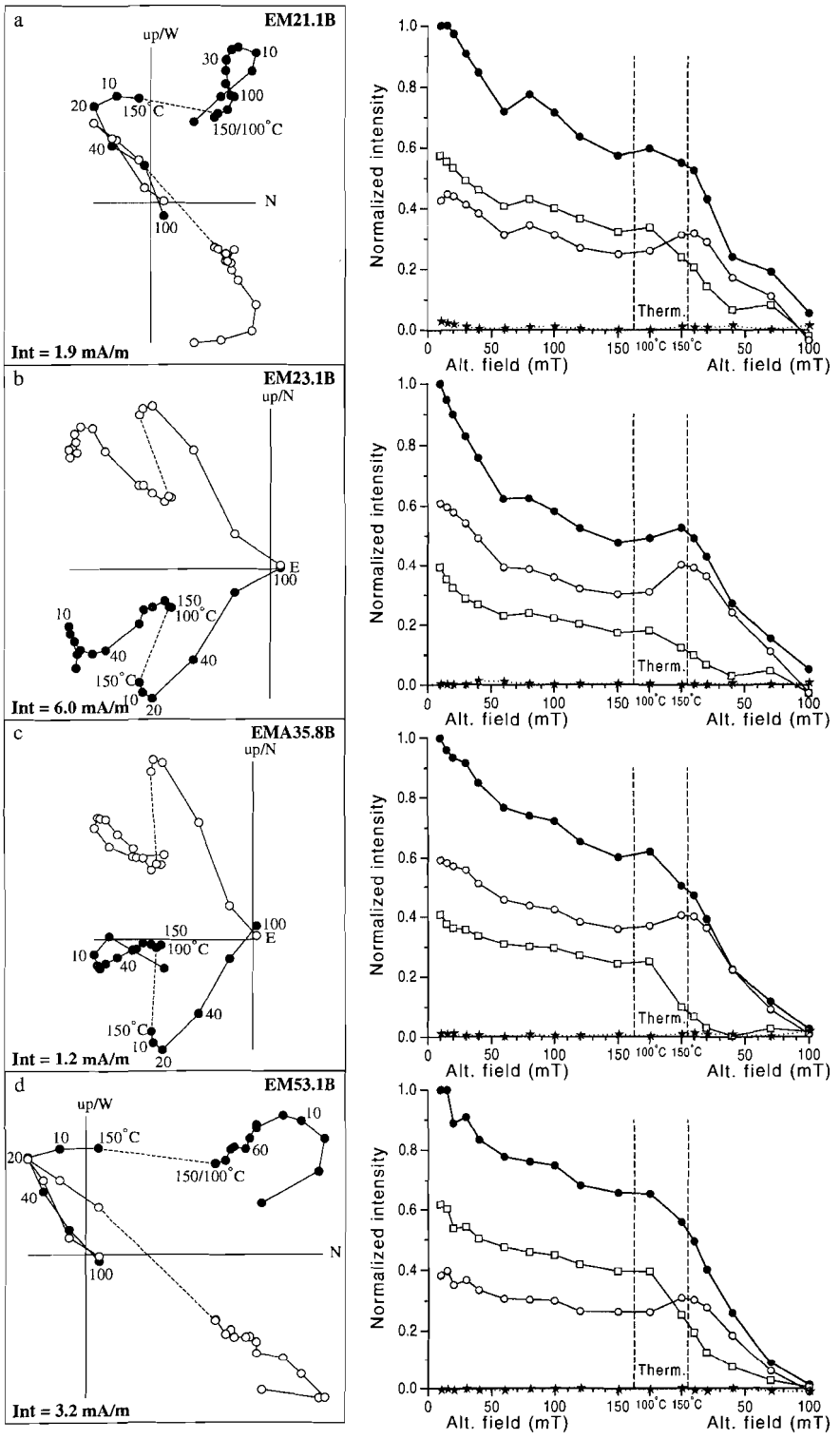
a
EM21.1B
up/W
30
10
10
20
150°C
100
150/100°C
40
N
100
Int = 1.9 mA/m
b
EM23.1B
up/N
E
100
150
100°C
10
40
40
150°C
10
20
Int = 6.0 mA/m
c
EMA35.8B
up/N
150
100
E
100°C
10
40
40
150°C
10
20
Int = 1.2 mA/m
d
EM53.1B
up/W
10
10
150°C
20
60
150/100°C
40
N
100
Int = 3.2 mA/m
Normalized intensity
Therm.
Alt. field (mT)
100°C 150°C

may carry the secondary component in the weathered samples, because viscous behaviour is prevented. The increase of coercivities prolongs the relaxation time and hence stabilizes the remanence.

### 8. Surface oxidation and stress

During low-temperature maghemitization of titanomagnetites in ocean floor basalts, changes in coercivities are observed that are comparable to the changes in the Trubi marls. This is not surprising, since weathering induced oxidation may be seen as the initial stage of low-temperature maghemitization. Models for maghemitization in ocean floor basalts assume that during oxidation the titanomagnetite grains consist of an oxidized shell around a non- (or less-) oxidized core (Knowles, 1981; Petersen and Vali, 1987; Housden and O'Reilly, 1990). In the partly oxidized shell the lattice constants decrease, so that the shell is stretched over the core and stresses occur in the grains. For larger grains ($>5$ μm) the stress leads to shrinkage cracks (Petersen and Vali, 1987). In SD grains the stress causes an increase in coercivity and a decrease in remanent magnetization in the initial stages of oxidation (e.g. Knowles, 1981; Beske-Diehl and Soroka, 1984; Appel, 1987; Smith, 1987; Housden and O'Reilly, 1990).

The cause of the higher coercivities is an increased contribution of magnetostriction to the magnetic energy state of the magnetite grains. Average stress values can easily be large enough to make the magnetostriction contribution larger than either magnetocrystalline anisotropy or shape anisotropy (Appel, 1987). In a spherical grain, for reasons of symmetry, the surface oxidation model predicts no anisotropy due to stress. In an ellipsoidal grain the stress anisotropy depends on the degree of eccentricity of the ellipsoid. With increasing anisotropy, the energy barrier between two energetically favourable states becomes higher and consequently the coercive force needed to switch between states becomes larger. Housden and O'Reilly (1990) show that for ellipsoidal titanomagnetite grains the variation in median destructive field (MDF) with oxidation grade in ocean floor basalts can be explained by a model in which a stressed maghemitized shell encloses an unaltered titanomagnetite core. In this model the six-fold increase in MDF of ocean floor basalts with increasing oxidation degree (Petersen and Vali, 1987) can be attained in grains with only small ellipsoidal eccentricity.

Another aspect is the change in microstructure that is likely to occur due to stresses. This can, for example, be observed in large (MD) titanomagnetite grains that are affected by low-temperature oxidation. The domain pattern in these grains becomes chaotic near the edge, where the oxidation degree is expected to be highest (Appel, 1987). In SD grains the preferential direction of magnetization may be turned away on a local scale in a similar way, causing a decrease of net magnetization. In SD grains with a higher degree of oxidation an incoherent spin structure with a circular spin in the oxidized mantle may even become energetically more favourable (Housden and O'Reilly, 1990).

Of these partial oxidation effects, only the increase in coercivity is observed in

samples from the Trubi formation. The different degrees of oxidation are reflected in the variation in coercivity. The factor of five between the highest and lowest $H_{cr}$ values observed (Table A) may correspond to the six-fold increase in MDF in ocean floor basalts. A possible remanence decrease cannot be observed directly in the Trubi marls, because comparison with unaffected samples is not possible due to the natural variation of the quantity of magnetic minerals with lithology.

## 9. Reduction of stress model

In light of the above explanation for the observed high coercivities, a reduction of stress model can explain the 150°C alteration. Apparently, the most severe effect of oxidation is removed by heating: the stress-induced high coercivities are reduced to values that are normal for magnetite. The stresses originate in the difference in lattice constants of the shell and the core. The more oxidized shell shrinks because it contains more $Fe^{3+}$ and vacancies and less $Fe^{2+}$ than the less oxidized core. The oxidation proceeds through diffusion of $Fe^{2+}$ from the core to the shell. For each $Fe^{2+}$-ion diffusing out of the core, one vacancy is produced and two $Fe^{2+}$-ions are converted to $Fe^{3+}$. The total rate of oxidation is limited by the concentration of $Fe^{2+}$ near the grain surface. Because diffusion rates are highly temperature dependent, a large oxidation gradient will occur when the oxidation takes place at low temperatures (near room temperature in this case). The stresses in the grains are proportional to this gradient. An increase in temperature to 150°C accelerates the diffusion and the oxidation gradient will be considerably reduced. Consequently, the stresses in the grains will decrease.

The reduction of stress will also influence the microstructure within the magnetite grains. The deviations from the preferred spin direction that likely exists in the stressed grains (see section 8), will become less. Consequently the net magnetization per grain may increase. This would explain the increase of the primary NRM component after heating to 150°C in the AF-Thermal-AF demagnetization (figure 7). By observing the effects of stress reduction, the otherwise invisible effects of oxidation-induced stress on the microstructure of the magnetite grains might indirectly be inferred.

## 10. Conclusions

The SD magnetite grains in the Early Pliocene marine marls of the Trubi formation are affected by low-temperature oxidation due to recent weathering. The most conspicuous effect of the oxidation is increased coercivities. Remanent coercivities originally vary between 36 and 188 mT, depending on the degree of weathering. Heating the samples to 150°C has the opposite effect of weathering: the high remanent coercivities are reduced to uniform values between 30 and 38 mT, which are normal for SD magnetite.

The increased coercivities, due to weathering, are similar to the increased coercivities that occur during the first stages of low-temperature maghemitization

of titanomagnetites in ocean floor basalts. A similar model was therefore adopted to explain the effects of weathering on the Trubi samples. Stresses in magnetite grains are induced by a large gradient in the oxidation degree from the shell to the core of the grains. The more oxidized shell shrinks and is stretched over the less oxidized core. In an aqueous environment the oxidation proceeds through the superficial removal of $Fe^{2+}$. It is suggested that for stress to occur the oxidation must take place at low temperatures. At room temperature the diffusion rate of $Fe^{2+}$, from the magnetite core to the shell, is low and a large oxidation gradient arises, resulting in stress and the related increase in coercivity. When the samples are heated to 150°C, the stresses are reduced due to the considerably higher diffusion rate of $Fe^{2+}$ at that temperature. The large oxidation gradient is removed, as is the cause of the stress and the enhanced coercivities.

The changes in rock magnetic parameters observed after heating to 150°C, are all related to the reduction in coercivity. The total IRM(1.5 T) decreases (5-11%) and $\chi_o$ increases (4-24%) after heating to 150°C. The decrease in IRM is attributed to the increased number of grains with superparamagnetic behaviour, which owed their stability before heating only to their enhanced coercivities due to an oxidized shell. The same phenomenon causes a relatively large decay of IRM that is observed at the 150°C step of a normal stepwise thermal demagnetization in weathered samples. Despite these changes, IRM and $\chi_o$ give a good representation of the lithological variations before as well as after heating at 150°C.

The initial variation of the coercivities and ARM in the unheated sediment, however, is a reflection of the variation of oxidation degree and not of magnetic mineralogy. Due to the reduction of coercivities after the heating the ARM(0.03 mT; 100 mT) was between 20 and 240% higher.

The effect of thermal treatment at 150°C is demonstrated by NRM demagnetization in which a combination of AF and thermal demagnetization is used. Both the secondary and primary NRM components are affected by weathering. Regular AF demagnetization does not succeed in separating the two components and, in more weathered samples, 300 mT alternating fields are not high enough to demagnetized the NRM completely. After thermal treatment at 150°C, the AF demagnetization becomes much more effective. The secondary remanence can be demagnetized at 20 mT alternating fields and the hardness of the primary component is reduced as well. With 100 mT alternating fields the remaining NRM can be completely demagnetized. The same reduction of coercivities as found in the IRM is observed for the NRM.

Low-temperature oxidation is a common process. The surface oxidation of (titano-) magnetites and the related stress reduction after heat treatment described here may well be widespread, but they can only be recognized after dedicated experiments. The relatively large decay of remanence between 140°C (i.e. higher than maximum blocking temperatures of goethite) and 200°C and an increase of $\chi_o$ may help recognition of the presence of oxidation-induced stress. Due to the influence of weathering, variations of some rock magnetic parameters (especially

coercivities and ARM) may be misinterpreted. It is therefore advisable to measure the rock magnetic parameters before and after heating to 150°C, when influence of low-temperature oxidation is suspected.

**References**

Akimoto T., Kinoshita H. and Furuta T., Electron probe microanalysis study on processes of low-temperature oxidation of titanomagnetite. Earth Planet. Sci. Lett. 71, 263-1278, 1984.

Appel E., Stress anisotropy in Ti-rich titanomagnetites. Phys. Earth Planet. Inter. 46, 233-240, 1987.

Beske-Diehl S.J. and Soroka W.L., Magnetic properties of variably oxidized pillow basalt. Geophys. Res. Lett. 11, 225-228, 1984.

Brown K. and O'Reilly W., Aqueous maghemitization of titanomagnetite. J. Geophys. 61, 82-89, 1987.

Day R., Fuller M. and Schmidt V.A., Hysteresis properties of titanomagnetites: grain-size and compositional dependence. Phys. Earth Planet. Inter. 13, 260-267, 1977.

Dekkers M.J., Magnetic properties of natural goethite-I. Grain-size dependence of some low- and high-field related rockmagnetic parameters measured at room temperature. Geophys. J. Int. 97, 323-340, 1989a.

Dekkers M.J., Magnetic properties of natural goethite-II. TRM behaviour during thermal and alternating field demagnetization and low-temperature treatment. Geophys. J. Int. 97, 341-355, 1989b.

Dekkers M.J., Magnetic properties of natural goethite-III. Magnetic behaviour and properties of minerals originating from goethite dehydration during thermal demagnetization. Geophys. J. Int. 103, 233-250, 1990.

Dunlop D.J., Hysteresis properties of magnetite and their dependence on particle size. J. Geophys. Res. 91, 9569-9584, 1986.

Dunlop D.J. and Argyle K.S., Separating multidomain and single-domain-like remanences in pseudo-single-domain magnetites (215-540 nm) by low-temperature demagnetization. J. Geophys. Res. 96, 2007-2017, 1991.

Gapeev A.K. and Tselmovich V.A., The microstructure and domain structure of multiphase oxidized titanomagnetites. Phys. Earth Planet. Inter., 70, 243-247, 1992.

Hedley I.G., The weak ferromagnetism of goethite (α-FeOOH). Z. Geophys. 37, 409-420, 1971.

Heider F. and Dunlop D.J., Two types of chemical remanent magnetization during the oxidation of magnetite. Phys. Earth Planet. Inter. 46, 24-45, 1987.

Heider F., Dunlop D.J. and Soffel H.C., Low-temperature and alternating field demagnetization of saturation remanence and thermoremanence in magnetite grains (0.037 μm to 5 mm). J. Geophys. Res. 97, 9371-9381, 1992.

Heller F., Rock magnetic studies of Upper Jurassic limestones from Southern Germany. J. Geophys. 44, 525-543, 1978.

Hilgen F.J., Sedimentary rhythms and high-resolution chronostratigraphic correlations in the Mediterranean Pliocene. Newslett. Stratigr. 17, 109-127, 1987.

Hodych J.P., Low-temperature demagnetization of saturation remanence in rocks bearing multidomain magnetite. Phys. Earth Planet. Inter. 66, 144-152, 1991.

van Hoof A.A.M, van Os B.J.H., Rademakers J.G., Langereis C.G. and de Lange G.J., A paleomagnetic and geochemical record of the upper Cochiti reversal and two subsequent precessional cycles from Southern Sicily (Italy). Earth Planet. Sci. Lett. 117, 235-250, 1993.

Housden J. and O'Reilly W., On the intensity and stability of the natural remanent magnetization of ocean floor basalts. Phys. Earth Planet. Inter. 64, 261-278, 1990.

King J.W., Banerjee S.K. and Marvin J., A new rock-magnetic approach to selecting sediments for geomagnetic paleointensity studies: application to paleointensity for the last 4000 years. J. Geophys. Res. 88, 5911-5921, 1983.

Kirschvink J.L., The least squares line and plane and the analysis of paleomagnetic data. Geophys. J. R. Astron. Soc. 62, 699-718, 1980.

Knowles J.E., The properties of acicular particles of $(\gamma\text{-}Fe_2O_3)_x(Fe_3O_4)_{1-x}$, J. Magn. Magn. Materials 22, 263-266, 1981.

Kobayashi K., Campbell M.F. and Moorehead J.B., Size dependence of low-temperature change in remanent magnetization of $Fe_3O_4$, in Ann. Proc. of the Rock Magnetism Research Group, pp. 33-50, Tokyo, Japan, 1965.

Langereis C.G. and Hilgen F.J., The Rossello composite: a Mediterranean and global reference section for the Early to early Late Pliocene. Earth Planet. Sci. Lett. 104, 211-225, 1991.

Levi S. and Merrill R.T., Properties of single-domain, pseudo-single-domain, and multi-domain magnetite. J. Geoph. Res. 83, 309-323, 1978.

Lowrie W. and Heller F., Magnetic properties of marine limestones. Rev. Geophys. 20, 171-192, 1982.

McFadden P.L., Comments on "A least-squares method to find a remanence direction from converging remagnetization circles" by H. C. Halls. Geophys. J. R. Astron. Soc. 48, 540-550, 1977.

Nishitani T. and Kono M., Curie temperature and lattice constant of oxidized titanomagnetite. Geophys. J. R. Astron. Soc. 74, 585-600, 1983.

Özdemir Ö. and Dunlop D.J., An experimental study of chemical remanent magnetizations of synthetic monodomain titanomaghemites with initial thermoremanent magnetizations. J. Geophys. Res. 90, 11513-11523, 1985.

Özdemir Ö., Dunlop D.J. and Moskowitz B.M., The effect of oxidation on the Verwey transition in magnetite. Geoph. Res. Lett. 20, 1671-1674, 1993.

Petersen N. and Vali H., Observation of shrinkage cracks in ocean floor titanomagnetites. Phys. Earth Planet. Inter. 46, 197-205, 1987.

Rochette P. and Fillion G., Field and temperature behavior of remanence in synthetic goethite: paleomagnetic implications. Geophys. Res. Lett. 16, 851-854, 1990.

Scheepers P.J.J. and Langereis C.G., Analysis of NRM directions from the Rossello composite: implications for tectonic rotations of the Caltanisetta basin (Sicily). Phys. Earth Planet. Inter. 119, 243-258, 1993.

Smith B.M., Consequences of the maghemitization on the magnetic properties of submarine basalts: synthesis of previous works and results concerning basement rocks from mainly D.S.D.P. Legs 51 and 52. Phys. Earth Planet. Inter. 46, 206-226, 1987.

Stacey F.D. and Banerjee S.K., The Physical Principles of Rock Magnetism, Elsevier, Amsterdam, 195 pp., 1974.

Strangway D.W., Honea R.M., McMahon B.E. and Larson E.E., The magnetic properties of naturally occuring goethite. Geophys. J. R. Astron. Soc. 15, 345-359, 1968.

Stumm W. and Sulzberger B., The cycling of iron in natural environments: Considerations based on laboratory studies of heterogeneous redox processes. Geochim. Cosmochim. Acta 56, 3233-3257, 1992.

Tauxe L., Sedimentary records of relative paleointensity of the geomagnetic field: Theory and practice. Rev. Geophys. 31, 319-354, 1993.

van Velzen A.J. and Zijderveld J.D.A., Rock magnetism of the Early Pliocene Trubi formation at Eraclea Minoa (Sicily). Geophys. Res. Lett. 17, 791-794, 1990.

van Velzen A.J. and Zijderveld J.D.A., A method to study alterations of magnetic minerals during thermal demagnetization applied to a fine-grained marine marl (Trubi formation, Sicily). Geophys. J. Inter. 110, 79-90, 1992.

# 5 Magnetic iron-nickel sulphides in the Pliocene and Pleistocene marine marls from the Vrica section (Calabria, Italy)


## Abstract

The rock magnetic properties of the late Pliocene and early Pleistocene open-marine marls from the Vrica section in Calabria (Italy) point to magnetic sulphide as the main magnetic mineral and remanence carrier. The maximum blocking temperatures, however, are between 340 and 360°C, which is too high for stoichiometric monoclinic pyrrhotite. Magnetic concentrates of the sediment are rich in iron sulphide grains and iron-nickel sulphide grains. Microprobe observations show that most of the grains are of the order of 1 μm in size and attached to iron-bearing clay flakes.

Microprobe analyses of the sulphides yield a large range of compositions, ranging from pyrite through greigite-pyrrhotite to sulphur-deficient monosulphides, and with Ni contents varying from zero to a few atom percent in the pyrite grains and from zero to as much as 35 atm% in the monosulphides. The high Ni content of many of the grains is extraordinary and has not been reported before in marine sediments. Most of the compositions cannot be directly connected with a known mineral phase. The marine depositional environment of the marls imposes an authigenic origin for the sulphides, and this is supported by several observations.

The great number of sulphide grains in the magnetic concentrates suggests that at least one of the sulphide compositions must have a ferrimagnetic structure, possibly the sulphides with a metal to sulphur ratio close to that of monoclinic pyrrhotite, and between 25 and 35% of the Fe replaced by Ni. The Ni substitution could possibly be the cause of the high blocking temperatures.


## 1. Introduction

The Vrica section (Crotone-Spartivento basin of northern Calabria, Italy) consists of open-marine marls dating from ca. 2.1 Ma to 1.55 Ma. The section has been formally designated as the Pliocene-Pleistocene boundary stratotype (Aguirre and Pasini, 1985) and has consequently been intensively studied (e.g. Pasini et al., 1975; Selli et al., 1977; Obradovitch et al., 1982; Backman et al., 1983; Tauxe et al., 1983; Hilgen, 1990). Most recent paleomagnetic results from the Vrica section contributed to a detailed magnetostratigraphy for the late Pliocene to early Pleistocene and the absolute age for the P/P boundary (Zijderveld et al., 1991). The groups of sapropelitic layers that are found throughout the section in the otherwise homogeneous marls are interpreted as interference patterns related to

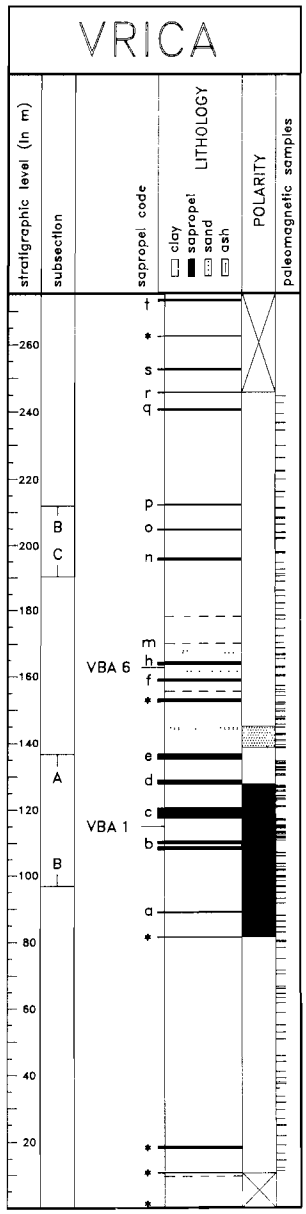


**Figure 1**. Vrica composite section. Samples VBA 1 and VBA 6 were taken from subsection Vrica B at stratigraphic levels 114 m and 162 m, respectively. Magnetostratigraphic results in Zijderveld et al. (1991). Normal polarities are indicated in black, reversed polarities in white.

the Earth's orbital cycles (Hilgen, 1987; 1991) and provide an astronomically calibrated polarity time scale for the time interval represented by the section.

During the recent magnetostratigraphic study (Zijderveld et al., 1991) much attention was paid to the interpretation of the thermal demagnetization diagrams. For the present study rock magnetic measurements were performed and magnetic concentrates were made in order to improve our understanding of the demagnetization process. This paper reports the results of microprobe analyses of magnetic concentrates.

## 2. Sampling sites

Concentrates were made of two samples (VBA 1 and VBA 6) taken from subsection Vrica B, 2.5 m below sapropel *c* and 0.5 m below sapropel *h* respectively (sapropel labelling by Selli et al. (1977), see Figure 1). The average accumulation rate of subsection Vrica B is 30 cm per thousand years (Zijderveld et al., 1991). Between sapropels *b* and *c* and between *f* and *h* the sedimentation rate is 48 and 23 cm/ky respectively on the basis of the astronomical age of the individual sapropels (Hilgen, 1991). The sedimentation depth was about 500 m. Conditions were oxygen-poor or anoxic during deposition of the sapropelitic layers but oxygenated otherwise.

The carbonate content of the marls ranges from 13% (in the sapropels) to 25% (Thunell, 1986; van der Weijden, 1993). In the non-sapropel sediment the organic carbon content is between 0.4 and 0.8% (van der Weijden, 1993). The clay minerals in the Vrica section are mainly smectite (ca. 55%), illite (20%), chlorite (15%) and kaolinite (10%) (van der Weijden, 1993; Combourieu-Nebout, 1987).

### 3. Natural remanent magnetization

The intensities of the natural remanent magnetization (NRM) in the Vrica section vary considerably (Zijderveld et al., 1991). In the lower part of subsection Vrica B up to sapropel c relatively high intensities are found (0.5-3 mA/m). Progressive thermal demagnetization removes a characteristic component with a normal polarity between 200 and 300°C, after demagnetizing a viscous laboratory component at 100°C and a small secondary component with a slightly different direction at about 200°C (figure 2a). The upper limit of the demagnetization temperatures remains obscure, however, due to the spurious behaviour of the remanence starting around 340°C. The increase of the bulk susceptibility of the samples, which starts at the same temperature, indicates the formation of new magnetic minerals in this temperature range (figure 2c).

Above sapropel *c* NRM intensities drop to 0.1-0.2 mA/m. Due to the low intensities and consequently relatively large secondary remanences it is often more difficult to determine characteristic directions in this interval (Fig 2b). Half way between sapropels *e* and *f* NRM intensities start to increase again to values between 0.1 and 0.5 mA/m. Thermal demagnetization diagrams are similar to those in the lower part of the subsection, only here the characteristic component removed between 200 and 300 or 340°C has a reversed polarity. Above 340°C again the formation of new magnetic minerals prevents further interpretation of the demagnetization results. Alternating field demagnetization would avoid thermal alterations, but alternating fields higher than 40 mT create new remanences that

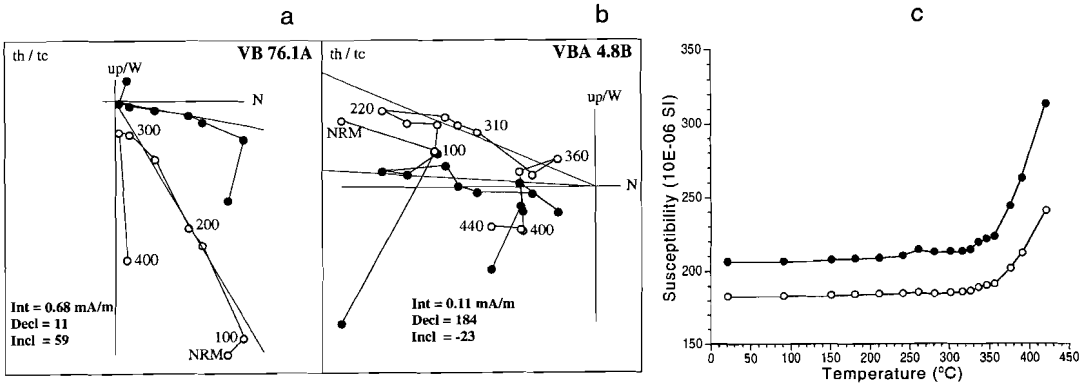


**Figure 2.** (a) Stepwise thermal demagnetization of a sample with a relatively high NRM intensity from the lower part of subsection Vrica B. Closed symbols and open symbols are horizontal and vertical projection respectively. Temperatures in degrees centigrade. *Int* is NRM intensity at 200°C. *Decl* and *Incl* are calculated as the best fit for the vector removed between ca. 200 and 300°C. (b) The same for a sample from the part of the section characterized by lower NRM intensities. (c) Changes in initial susceptibility occurring during the thermal demagnetization. High-intensity sample shown by closed symbols; low-intensity sample shown by open symbols.

disturb the demagnetization process.

The overall trend in the NRM intensities of the section is distinct, but on a small scale the sediment is quite inhomogeneous with respect to the magnetic properties. Samples taken next to each other can have very different NRM intensities and demagnetization behaviour.

## 4. Rock magnetic properties of the sediment

The rock magnetic properties of the sediment indicate that the dominant magnetic mineral might be an iron sulphide. Isothermal remanent magnetization (IRM) acquired in fields up to 2 T varies between 0.1 and 0.8 A/m. Coercivities are generally lower than 0.3 T and this is confirmed by the alternating field demagnetization of the IRM (figure 3a and b). Remanent coercivities ($H_{cr}$) are between 45 mT for the low-intensity samples and 80 mT for the high-intensity samples. Sites VBA 1 and VBA 6 both have relatively high intensities (Table A). Their coercivities are substantially higher than typical magnetite coercivities (e.g. Dunlop, 1986) and compare well with coercivities of pyrrhotite grains in the pseudo-single domain size range (Clark, 1984; Dekkers, 1988). Thermal demagnetization of IRM (figure 3c) shows that a large part of the remanence has maximum demagnetization temperatures lower than 360°C, comparable to those of the NRM. A smaller part of the remanence has maximum demagnetization temperatures well above 500°C. The linear decay of the latter remanence points to very fine magnetite grains in the size range between superparamagnetic and stable single domain grain sizes (cf. van Velzen and Zijderveld, 1992). It is not possible to establish whether a small part of the NRM also has these high blocking temperatures. The NRM intensities are only 0.1% of the IRM intensities and the NRM demagnetizations are disturbed by the thermal alterations above 340°C.

The coercivities and the maximum demagnetization temperatures are close to those of monoclinic pyrrhotite, except that the maximum demagnetization temperatures are some 20-40°C higher than the Curie temperature of monoclinic pyrrhotite which is generally reported as being between 305 and 325°C (e.g.

**Table A.** Rock magnetic properties at the sampling sites

| | VBA 1 | VBA 6 |
|---|---|---|
| Stratigraphic level | 114 m | 162 m |
| Polarity | normal | reversed |
| NRM intensities | 0.15-2.5 mA/m | 0.05-0.37 mA/m |
| Average | 0.5 mA/m | 0.2 mA/m |
| IRM(2T) | 380-680 mA/m | 460-760 mA/m |
| Hcr | 80-81 mT | 73-78 mT |
| MDF of IRM(2T)* | 62 mT | |

* Median destructive fields of stationary alternating field demagnetization in three orthogonal directions

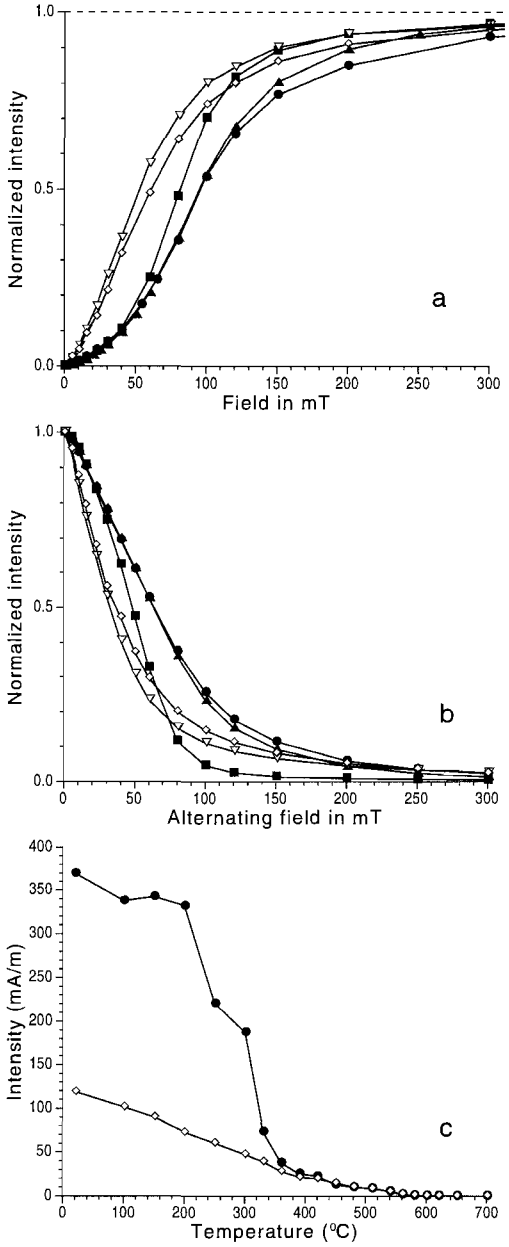


Schwarz and Vaughan, 1972; Schwarz, 1975; Vaughan and Craig, 1978; Dekkers, 1989). However, higher maximum blocking temperatures (up to 350°C) were found in fine-grained pyrrhotites by Rochette et al. (1990). The spurious magnetizations that occur during AF demagnetization of the NRM are also similar to the behaviour found in pyrrhotites (Schwarz, 1966; Thomson, 1990).

Greigite ($Fe_3S_4$) is also known to be a strongly magnetic mineral occurring in reducing sedimentary environments (e.g. Snowball, 1991; Hoffman, 1992; Diaz et al., 1992; and references therein). The mineral becomes thermally unstable at about 300°C, however, which is not compatible with the high maximum blocking temperatures observed in the marls in this study. Moreover, coercivities reported for greigite are generally lower than those of pyrrhotite. Like pyrrhotite, greigite exhibits spurious behaviour during AF demagnetization (Krs et al., 1990).

Pyrrhotite and greigite cannot explain the combination of high blocking temperatures and high coercivities. However, the observed rock magnetic properties do not exclude these two pure iron sulphides as contributors to the remanence.

**Figure 3.** (a) IRM acquisition of samples with high-intensity NRM (closed symbols) and low-intensity NRM (open symbols). Normalized at 2 T. The IRM of the high-intensity samples is about four times the IRM of the weak samples. (b) Alternating field demagnetization of the normalized IRM(2T) of the same samples. Demagnetization was stationary in three orthogonal directions. Rock magnetic data for samples VBA 1 and VBA 6 in Table A. (c) Stepwise thermal demagnetization of IRM(2T).

## 5. Magnetic concentrates

For further study of the magnetic minerals in the sediment magnetic separation was performed. A suspension of 400 g of sediment in 2 l of demineralized water was slowly passed through a glass tube between the poles of a Frantz isodynamic separator operating at a high current (1.5 A). Some ascorbic acid was added to the suspension in order to create slightly reducing conditions and prevent possible oxidation of mineral phases. Every few hours the circulation was stopped and the mineral grains attracted by the magnet were washed from the tube. They were stored under reducing conditions in demineralized water with some ascorbic acid. This first magnetic concentrate still consisted mainly of clay minerals. It was subjected to a second concentration step to separate the strongly magnetic fraction from the less magnetic part. The suspension was again passed between the poles of the isodynamic separator, first operating at a low current (0.25 A), to obtain only highly magnetic minerals (yield ca. 0.03 g), and then at a high current to extract the remaining magnetic minerals (yield ca. 3 g). The two concentrate fractions still contained a considerable amount of clay minerals.

Polished thin sections of the concentrates were prepared for microprobe analysis (EDA) and electron microscope observation to determine the composition and the appearance of magnetic particles.

## 6. Microprobe observations

Back scatter images of the polished thin sections confirm that all concentrates still contain a large number of clay flakes. In low-field concentrates of VBA 6 many of the clay flakes have small grains attached to them; these are the bright areas in the images (figure 4). These bright grains are sulphides of various compositions. As expected, sulphur and iron form the main constituents of these grains, although many of them also contain a large amount of nickel. Microprobe analysis of the clay flakes on which sulphide grains were observed reveals that these clay flakes contain iron (Table B). Apart from the clay minerals and sulphides, some few grains containing iron and titanium were found in sizes from 1 to 50 μms. These grains often have sharp edges and Fe:Ti ratios close to unity, indicating that they are grains of ilmenite, which is paramagnetic at room temperature (e.g. Stacey and Banerjee., 1974). Fe-Ti grains with other ratios were seldom found. In the VBA 6 low-field concentrates grains with Fe and Cr are also present. These grains usually contain as least twice as much Fe as Cr, and in some instances they also contained considerable amounts of Ni and traces of other metals (Table B). These grains are supposedly paramagnetic too.

The abundance of the sulphides and the absence of other magnetic minerals in the magnetic concentrates indicates that these sulphide grains contribute to an important part of the remanent magnetic signal in the marls. Attention was therefore focused on these iron-nickel sulphides. Most sulphide grains are attached to clay flakes and have a uniform appearance. The majority of the grains are smaller

| | Si | Al | Mg | Fe | K | Ca | Other elements | |
|---|---|---|---|---|---|---|---|---|
| Clay flakes with sulphides | 1 | 1.07 | 0.49 | 0.99 | 0.02 | 0.00 | | VBA 1 low field |
| | 1 | 0.75 | 0.81 | 0.51 | 0.02 | 0.01 | Na, Ti, S | VBA 1 high field |
| | 1 | 0.63 | 0.34 | 0.49 | 0.21 | 0.01 | Na, Ti, S | VBA 6 low field |
| | 1 | 0.60 | 0.21 | 0.35 | 0.13 | 0.06 | Na, Ti, S | VBA 6 high field |
| | Fe | Cr | Ni | Mn | Mg | | | |
| Fe-Cr oxides | 1 | 0.25 | 0.12 | 0.02 | | | Si, Al | |
| | 1 | 0.16 | | 0.02 | | | Ni, Mg, Ti, Si, Al | |
| | 1 | 0.21 | | 0.01 | 0.03 | | Ti, Zn, Si, Al | |
| | Fe | Ti | | Mn | Mg | | | |
| Fe-Ti oxides | 1 | 1.02 | | 0.02 | .07 | | Si | |
| | 1 | 1.13 | | 0.08 | .01 | | Si | |
| | 1 | 0.5 | | 0.01 | .05 | | Al | |

**Table B.** Some representative microprobe analyses of clay minerals that have sulphide grains attached to them, of some Fe-Cr oxides, and of some Fe-Ti oxides. The values are given as atom percentages normalized to Si (for the clay flakes with sulphides) and Fe (for the Fe-Cr and Fe-Ti oxides). The clay flakes come from magnetic concentrates that were separated with low and with high magnetic fields. The Fe-Cr oxides come from the low-field concentrate of VBA 6.

than 1.5 μm and seem to be spherical (although for the smallest grains it is difficult to assess the exact shape, because they are close to the detection limit of the microprobe).

The measurement of the exact composition of the sulphide grains with the microprobe was complicated by the small size of most of the grains (<1.5 μm, a size that is comparable to the spot size of the electron beam (ca. 1 μm)). In addition, the sulphide grains are possibly thin, so that part of the background (generally a clay flake) may be analyzed together with the sulphide grain. These conditions result in biased compositions for the sulphides, especially with respect to Fe. Therefore, the clay flake background was measured separately and the composition of the sulphide grains was corrected for iron from the background, assuming that all Si and Al measured is actually derived from the background. After correction the atom percentages are considered to be fairly accurate. Depending on the magnitude and the estimated accuracy of the correction the results are divided in well-determined (with estimated errors less than 2 atm% sulphur and 2% Ni) and somewhat less well-determined (errors <4%) compositions. Most microprobe analyses were performed on sulphide grains in the low- and high-field concentrates of VBA 6 and on some in the concentrates of VBA 1. Some of the very dispersed sulphides in polished thin sections of the original sediment were also analyzed. The sulphur percentage in the grains varies over a large range (figure 5), from compositions close to pyrite via pyrrhotite to sulphur contents close to that of pentlandite. The percentage of nickel replacing the iron in

the sulphides is not restricted to a few percent only. Nickel concentrations of up to 35% are measured.

The sulphide compositions can be roughly divided into four groups: (1) a pyrite group with 60-70% S and occasionally a few percent Ni, (2) a greigite-pyrrhotite group with 52-60% S and generally high Ni content (20-35% of the total metal content), (3) a large group with S content between 43 and 52% and Ni percentages from zero to 32, and (4) a highly sulphur deficient group with less than 43% S and Ni between 5 and 15% of the total metal content.

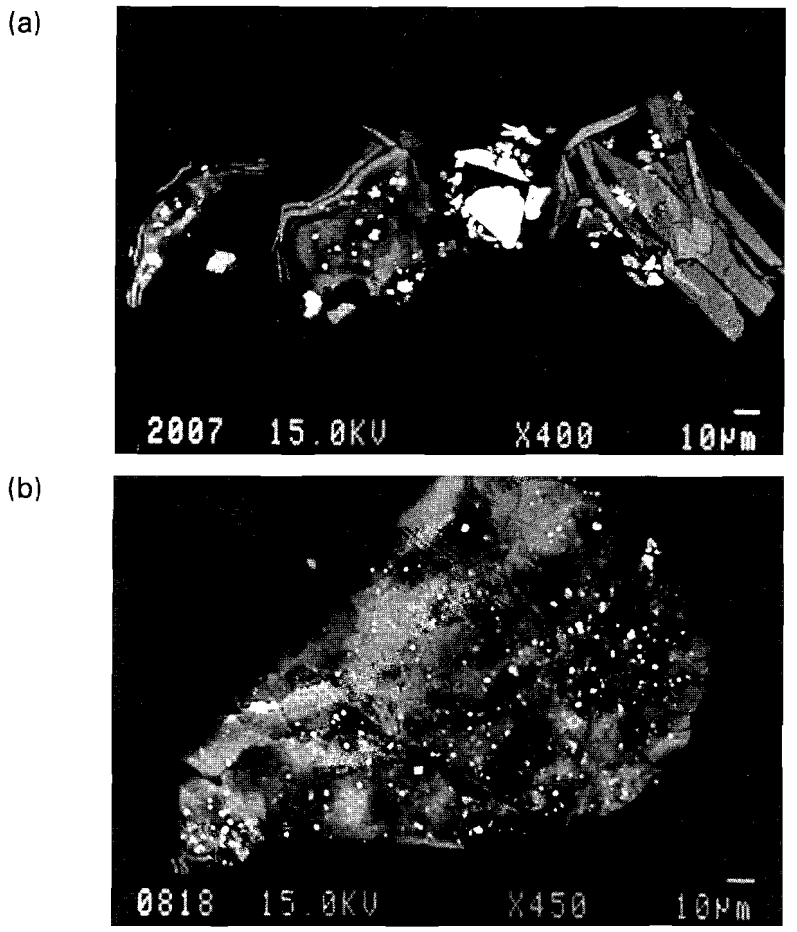


**Figure 4.** Microprobe back scatter images of grains separated in low magnetic fields (VBA 6). Sulphide grains appear bright in the image. (a) A collection of different clay flakes, iron-titanium oxides (large white pieces) and iron-nickel sulphides (the small white grains on and between the flakes) with ca. 15 atm% Ni. (b) Many small sulphide grains on an iron-bearing clay flake: mainly pyrite grains, sometimes with a trace of Ni (0.2 atm%) and some monosulphide grains with ca. 45 atm% S and 4-6 atm% Ni.

The compositions of sulphide grains on a single clay flake are not always the same. Iron sulphides with and without Ni occur on the same flake. Also, pyrite-like compositions and monosulphide compositions may occur together on the same flake.

In one case, on the inside of a carbonate shell (figure 4d), zinc was found to be a major constituent of the iron-nickel sulphides. The sulphur content of separate grains varies only between 46.2 and 50.7 atm%, placing them in the third group of sulphide compositions. The metal content, however, varies considerably. On the

(c)

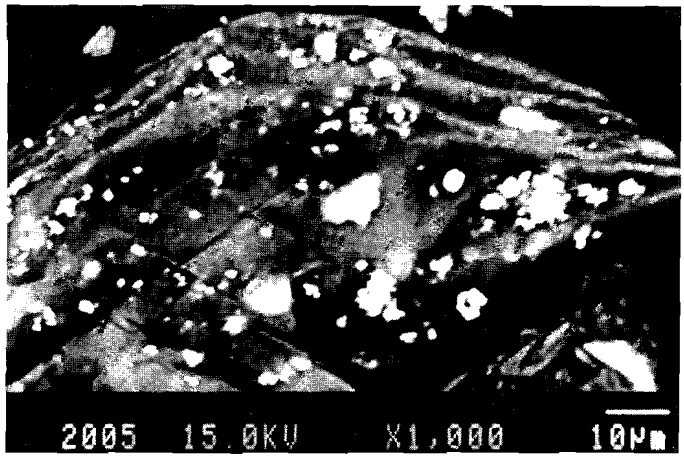


(d)

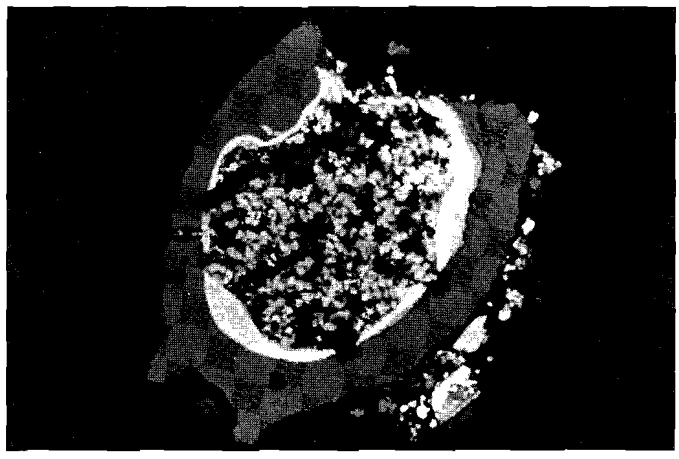

**Figure 4.** (c) Iron-bearing clay flake with sulphide grains: pyrite (without Ni) and monosulphide grains (42 atm% < S < 47 atm%) with between 4.5 and 17 atm% Ni.
(d) Carbonate shell with sulphides that approximate monosulphides, containing Fe, Ni and Zn. The Zn content of the sulphide increases towards the middle of the cavity (see Table C). The width of the shell is ca. 140 mm (magnification 350×).

| Position | atm% S | atm% Fe | atm% Ni | atm% Zn |
|---|---|---|---|---|
| In carbonate | 44.7 | 55.0 | 0.2 | 1.0 |
| Edge of carbonate | 49.6 | 49.4 | 0.9 | 0.6 |
| Edge of carbonate | 50.7 | 43.7 | 4.8 | 0.6 |
| In middle | 48.1 | 11.3 | 0.1 | 40.4 |
| In middle | 46.2 | 17.2 | 0.1 | 36.4 |

**Table C.** Microprobe analyses of sulphides inside carbonate shell. The microprobe was calibrated for Fe, Ni and Zn with standards of pure Fe, Ni and Zn and for S with pyrite.

inside edge of the shell the sulphides contain a variable amount of Ni (0.2-4.8%, see Table C), and Zn. Zinc becomes more important nearer the middle of the cavity, where it is a major constituent (up to 40 atm% of the sulphide). This increase in Zn content towards the middle of the cavity may reflect time-dependent availability of the metal ions (Huerta-Diaz and Morse, 1992). This is a typical example of authigenic sulphide formation related with the presence of organic material (cf. Krs et al., 1992; Pruysers et al., 1991). Black spots found throughout the sediment probably represent similar concentrations of sulphides, some of which may be magnetic. This would explain why the sediment is very inhomogeneous with respect to the remanent intensities (cf. Table A).

## 7. Comparison with known sulphides

The wide range of sulphide compositions makes it difficult to determine which sulphide or sulphides are the remanence carriers. Most of the sulphide compositions of the grains found in the sediment are not compatible with any known mineral. In particular, the high Ni content of many of the grains is very distinctive compared to any natural sulphide reported hitherto. Most sulphides of the first group (60-70% S) have compositions close to pyrite ($FeS_2$), with occasionally some Ni (up to 2%). The grains containing Ni could be a member of the bravoite $(Fe,Ni)S_2$ solid solution series. Bravoite has a highly variable Ni content and has been synthesized at low temperatures (Shimazaki, 1971). Unlike the sulphides in the sediment, bravoite is metastable. It is difficult to imagine that the observed low Ni content will change the diamagnetic properties of the pyrite.

In the second group a number of grains have sulphur contents between greigite (57.1 atm% S) and pyrrhotite (53.3 atm% S) and very high Ni contents (20-35%). Smythite, with a composition of $(Fe,Ni)_9S_{11}$, is also in this range (55 atm% S). This mineral is often observed in combination with pyrrhotite (Jover et al., 1989) and greigite mineralizations (Krs et al., 1992). Smythite is magnetic (Vaughan and Craig, 1978; Jover et al., 1989), but it has a very limited thermal stability (<75°C; Taylor, 1970), and it would therefore not survive our thermal demagnetization at higher temperatures. Also, the smythites reported have only a very low Ni content.

The third group is sulphur deficient, with Ni ranging from 0 to 32%. The

sulphur content is close to that of pentlandite ($(Fe,Ni)_9S_8$, 47.4 atm% S), but the Ni content is lower than in naturally occurring pentlandites (35-66%; Vaughan and Craig, 1978). The measured chemical composition is not consistent with any known mineral. However, a synthetic iron sulphide ($Fe_9S_8$) with the cubic pentlandite structure has been prepared by the flash-evaporation technique of vacuum deposition (Nakazawa et al., 1973). No properties of this $Fe_9S_8$ are known. One could speculate on having found the natural analog of this synthetic mineral, an extension of the pentlandite compositional range to more Ni poor and even Ni-free, compositions. Since both $Fe_9S_8$ and pentlandite have the same cubic pentlandite structure, it is not unlikely that all compositions ranging from 0 to 30% Ni have the same cubic structure. The ordering of the Ni-ions in the lattice could then determine whether the sulphide has ferrimagnetic properties.

Pentlandite itself is paramagnetic and is associated with magmatic ore deposits, in which it often occurs intergrown with pyrrhotite. Pentlandite/-pyrrhotite intergrowths are formed through exsolution from the (Fe,Ni)S solid

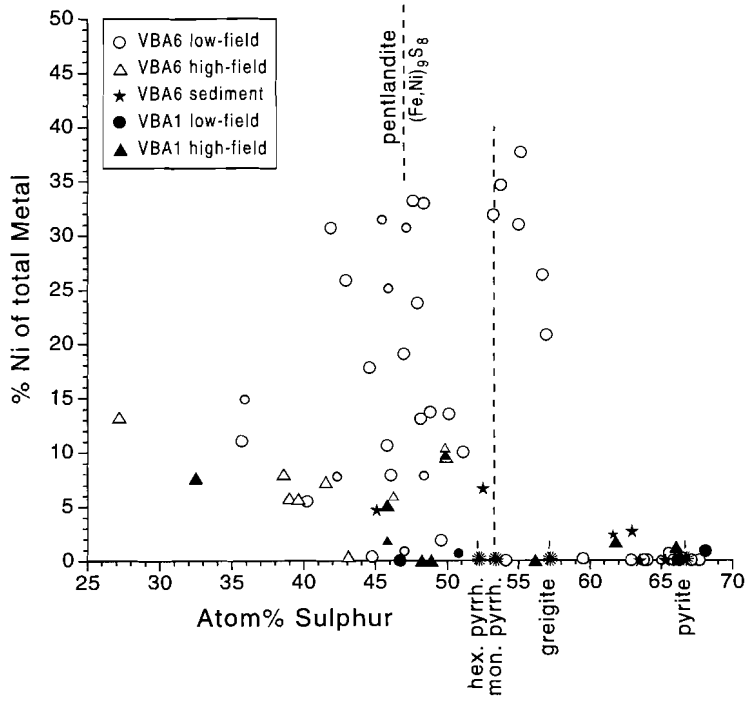


**Figure 5.** Microprobe analyses (EDA) of sulphide grains from VBA 6 (low- and high-field magnetic concentrates and a sediment thin section) and VBA 1 (magnetic concentrates). Larger symbols for the most accurate measurements (see text). The microprobe was calibrated for Fe, Ni and S with standards of pure iron, pure nickel and pyrite. Asterisks denote the position of four iron sulphides in the diagram. The Ni content in natural pentlandites varies between 35 and 66% of the total metal.

solution series, the series being complete at high temperatures. This mode of occurrence does not imply that the present Ni-poor 'pentlandite' observed in our marls is detrital: apart from the fact that pentlandite weathers easily, the deviating Ni content of the sulphide grains also argues against a detrital origin.

Many sulphides of this third group also have a sulphur content close to that of mackinawite ($Fe_{1+x}S$, with $0.04<x<0.07$, i.e. 48.3-49.0 atm% S) or troilite (FeS). Mackinawite is a metastable low-temperature mineral that can incorporate a large amount of Ni (and Co) in its structure. Vaughan (1969) found up to 18.7 wt% Ni in mackinawite in basic rocks and Clark (1969) up to 8% Ni. Mössbauer studies have yielded conflicting results on whether mackinawite possesses a magnetic structure (Morice et al., 1969; Vaughan and Ridout, 1971). Troilite (FeS) is antiferromagnetic, but terrestrial troilite is extremely rare; it occurs only in meteorites. Possible Ni substitution is not known.

The fourth group of grains is even more sulphur deficient than the third. Grains from this fourth group have a limited but not unimportant Ni content. A mineral with a similar metal to sulphur ratio is heazlewoodite ($Ni_3S_2$), which is paramagnetic (Vaughan and Craig, 1978).

Although the microprobe analyses are accurate, there are two complicating factors that must be taken into consideration. One is the possibility that the sulphide grains actually consist of two (or more) intimately intergrown phases. Because the grain sizes are of the order of 1 μm, intergrowths would not be visible under the microprobe. The analyses would then yield average values for sulphur, iron and nickel, between the true compositions of the two distinct phases. No indications exist for such intergrowths, however, and the high Ni content of the sulphides would still remain unexplained. Another complicating factor might be a possible oxidation of the sulphides during concentration and preparation for the microprobe. The concentration procedure was performed under reducing conditions, so oxidation should be inhibited, but the sulphides nevertheless remain vulnerable. Indeed, one thin section of a concentrate was visibly oxidized after polishing and had to be prepared a second time. Thus, a slight degree of oxidation cannot be ruled out. Supposing the Ni/Fe ratio were not affected by superficial oxidation, the analyses would yield a slightly diminished S content. The real S percentage would be slightly higher. It is therefore possible that the four analyses with a very low S content are due to more severe oxidation. In general, however, considering the consistency of the analyses between concentrates, discrepancies are not expected to be very large.

## 8. Origin of the iron-nickel sulphides

Iron sulphides are very common in marine sediments. Authigenic pyrite formation through bacterially mediated sulphate reduction occurs wherever reducing conditions are established and iron and sulphate are available. Pyrite is the final product in a chain of reactions starting with the formation of so-called amorphous FeS. Subsequent to this FeS phase, mackinawite, greigite and finally

pyrite are formed. Amorphous FeS, mackinawite and greigite are usually referred to as Fe-monosulphides. These intermediate monosulphides are in principle metastable (e.g. Berner, 1981; 1984; Mossmann et al., 1991), but they may be preserved in the sediment when sulphate from the pore water is depleted and reducing conditions continue to exist. Mossmann et al. (1991) conclude that polysulphides are necessary for the reaction of monosulphides to pyrite. Hence, monosulphides may be preserved if formation of polysulphides is inhibited. The observation of pyrrhotite in sediments is, however, rather enigmatic from the sulphate reduction point of view, and only Sweeny and Kaplan (1973) mention hexagonal pyrrhotite as part of the sulphate reduction reaction chain.

In contrast to the omnipresence of iron sulphides, the presence of nickel-bearing sulphides in marine sediments is rarely reported. Luther et al. (1980) found up to 4 wt% of Ni in pyrite framboids in recent estuarine sediments in Newark Bay, New Jersey. They also found Zn and Mn sulphides in the sediment. Authigenic greigite-smythite mineralizations with on average 0.2 wt% Ni have been reported from Middle Miocene claystones in Bohemia (Krs et al., 1990; 1992; Hoffmann, 1992). Whenever iron-nickel sulphides in a sedimentary environment are reported, the contribution of Ni is restricted to a few percent. It is therefore remarkable that the Ni content of sulphide grains in the Plio-Pleistocene marine sediments from the Vrica section is much higher, even more so because the abundant presence of sulphide grains in the magnetic concentrates demonstrates that at least one, and possibly several, of the sulphide compositions is strongly magnetic.

The iron and iron-nickel sulphides in the Vrica sediment have an authigenic origin. Detrital sulphides are very unlikely to occur in a marine environment. Sulphides such as pyrite, and especially pyrrhotite and greigite, are readily oxidized under the oxic conditions to which they are subjected during transport (e.g. Snowball and Thompson, 1990). An iron-nickel sulphide such as pentlandite also weathers under atmospheric conditions.

The relatively high sedimentation rate and input of organic material created a reducing environment once the sediment was sealed of from oxygenated bottom waters (e.g. Berner, 1984) setting the stage for sulphate reduction. Nickel can apparently participate in these reactions. If Ni is available, it may partly substitute for iron during authigenic sulphide formation (Luther et al., 1980). In high-temperature assemblages Ni substitution is very common. A small percentage of Ni in pyrrhotite, for example, is not unusual in sulphide deposits (Page, 1972; Misra and Fleet, 1973). In the latter case the Ni substitutes for Fe and the pyrrhotite vacancy distribution remains unchanged (Shishkin et al., 1974).

### 9. Sources of iron and nickel

The iron for the sulphides in the sulphate reduction reactions is usually derived from poorly crystalline Fe oxides like goethite and ferrihydrite (Goldhaber and Kaplan, 1974), which occur as coatings on silicate grains. The fact that almost all

sulphide grains are attached to iron-bearing clay flakes suggests that the clay flakes may also have been a source of iron during the sulphide formation. Depending on the availability of Fe and S, ferrous ions in fine-grained chlorite can serve as a source for Fe for the formation of sulphides (Manning et al., 1979; Suttill et al., 1982). The source for nickel is more puzzling. The sampling sites are not close to sapropels and consequently the Ni in the sulphides does not seem to be connected with the enrichment of Ni encountered in sapropels (Calvert, 1983; Pruysers et al., 1991; van der Weijden, 1993). The Ni might be derived from Fe-Cr oxides which were found to contain varying amounts of Ni (Table B). It is possible that very local factors determine the Ni availability.

### 10. Influence of Ni on magnetic properties

The presence of Ni in the iron sulphides will of course influence their magnetic properties. Substitution of a few per cent Ni in pyrrhotite does not change the vacancy distribution (Shishkin et al., 1974), although the Curie temperature of pyrrhotite with just 1% Ni is slightly lower than that of normal pyrrhotite (Vaughan et al., 1971). If the monoclinic pyrrhotite structure is also preserved with the high Ni contents observed here, these sulphides are likely to be ferrimagnetic as well. In the latter case the lower number of Bohr magnetons of Ni in comparison with ferrous Fe (2 and 4 $\mu_B$, respectively) will undoubtedly have major implications for the magnetic properties.

Greigite also is a strongly ferrimagnetic mineral, but its magnetic properties are poorly understood and the influence of possible nickel substitution can only be guessed at. The chemical composition of none of the other sulphides matches that of any known mineral and their mineralogical structure could not be determined. The question of their possibly ferrimagnetic nature must be addressed by laboratory studies of synthetic equivalents.

### 11. Timing of natural remanent magnetization

Seeing as magnetic sulphides turn out to be the dominant remanence carriers, the authigenesis of the sulphides possibly resulted in non-instantaneous NRM acquisition. Such authigenesis may have obscured the position of boundaries between normal and reversed intervals in the sediment. However, in general a fast rate of sulphate reduction and formation of sulphides is restricted to a small interval in the sediment column. The reactions virtually cease as soon as sulphate from the pore water is depleted or the readily metabolizable organic matter is completely oxidized (Goldhaber and Kaplan, 1974). Sulphate reduction continues at a much lower rate dictated by sulphate diffusion in the sediment or the slower oxidation of the remaining organic compounds. The magnetostratigraphic results show that the polarity intervals observed in the Vrica sediment compare well with the geomagnetic polarity time scale for the time interval in question (Zijderveld et al., 1991). The results thus suggest that the majority of the magnetic sulphides

must have formed in a relatively short period not long after sedimentation. Small-scale variations in magnetic properties and consequent differences in demagnetization behaviour of some samples may indicate that very locally magnetic sulphides can have formed over a longer period of time. This could be due to the local occurrence of less accessible organic material (e.g. within the carbonate shell of figure 4d).

## 12. Conclusions

The rock magnetic parameters of the Plio-Pleistocene open-marine marls of the Vrica section point to magnetic iron sulphide as remanence carrier, although the blocking temperatures of NRM and IRM are too high for stoichiometric monoclinic pyrrhotite (340-360°C).

Magnetic concentrates of the sediment were prepared for microprobe analysis. However, in spite of two upgrading steps abundant iron-bearing clay flakes still remained in the concentrates. Attached to the clay flakes are numerous small spherical sulphide grains, most of which are smaller than 1.5 μm. Microprobe analysis reveals that these grains are iron-nickel sulphides with nickel contents of as much as 35% of the total metal content. Apart from pyrite many monosulphide compositions are present, and these normally comprise an intermediate stage in authigenic pyrite formation. This and other observations indicate that the sulphides are of authigenic origin.

Four major compositional groups can be distinguished: (1) pyrite with a few percent Ni, (2) greigite-pyrrhotite compositions with usually between 20 and 35% Ni, (3) sulphur-deficient pentlandite-like compositions with between 0 and 32% Ni, and (4) even more sulphur deficient compositions with between 5 and 15% Ni. The compositions of group (2), (3) and (4) do not match those of any known mineral. The high Ni contents in particular are different from any natural sulphides hitherto reported. (A mineralogical characterization of the mineral phases by X-ray diffraction was not successful due to the high clay content of the magnetic concentrates, which resulted in the sulphides being below the detection limit.)

It is not possible to determine which of the sulphides is magnetic. The only phase that can be inferred to be ferrimagnetic has a composition close to that of monoclinic pyrrhotite, but with Ni replacing 20-35% of the Fe. The influence of the high Ni substitution on the properties of pyrrhotite is not known. The fact that the pentlandite-like sulphides form the largest group of sulphide compositions in the magnetic concentrates suggests that they are ferrimagnetic too. Further studies to characterize the mineral phases and their possible ferrimagnetic structure are in progress.

## References


Aguirre E. and Pasini G., The Plio-Pleistocene boundary. Episodes 8, 116-120, 1985.

Backman J., Shackleton N.J. and Tauxe L., Quantitative nannofossil correlation to open ocean deep-sea sections from Plio-Pleistocene boundary at Vrica, Italy. Nature 304, 156-158, 1983.

Berner R.A., Authigenic mineral formation resulting from organic matter decomposition in modern sediments. Fortschr. Miner. 59, 117-135, 1981.

Berner R.A., Sedimentary pyrite formation: An update, Geochim. Cosmochim. Acta 48, 605-615, 1984.

Calvert S.E., Geochemistry of Pleistocene sapropels and associated sediments from the Eastern Mediterranean. Oceanolog. Acta 6, 255-267, 1983.

Clark A.H., Preliminary observations on chromian mackinawite and associated native iron, Mina do Abessedo, Vinhais, Portugal. Jahrb. Mineral Monatsh. 6, 282-288, 1969.

Clark D.A., Hysteresis properties of sized dispersed monoclinic pyrrhotite grains. Geophys. Res. Lett. 11, 173-176, 1984.

Combourieu-Nebout N., Les premiers cycles glaciaires-interglaciaires en région Méditerranéenne d'après l'analyse palynologique de série Plio-Pleistocène de Crotone (Italie Méridionale). Thèse, 161 pp, l'Université des Sciences et Techniques du Languedoc, 1987.

Diaz Ricci J.C. and Kirschvink J.L., Magnetic domain state and coercivity predictions for biogenic greigite ($Fe_3S_4$): a comparison of theory with magnetosome observations. J. Geophys. Res. 97, 17,309-17,315, 1992.

Dekkers M.J., Magnetic properties of natural pyrrhotite Part I: Behaviour of initial susceptibility and saturation-magnetization-related rock-magnetic parameters in a grain-size dependent framework. Phys. Earth Planet. Int. 52, 376-393, 1988.

Dekkers M.J., Magnetic properties of natural pyrrhotite Part II. High- and low-temperature behaviour of $J_{rs}$ and TRM as function of grain size. Phys. Earth Planet. Int. 57, 266-283, 1989.

Dunlop D.J., Hysteresis properties of magnetite and their dependence on particle size: a test of pseudo-single-domain remanence models. J. Geophys. Res. 91, 9569-9584, 1986.

Goldhaber M.B. and Kaplan I.R., The sulfur cycle, in: The Sea, vol. 5, Marine chemistry, E.D. Goldberg, ed., pp. 569-655, John Wiley and Sons, Inc., 1974.

Hilgen F.J., Sedimentary rhythms and high-resolution chronostratigraphic correlations in the Mediterranean Pliocene. Newslett. Stratigr. 17, 109-127, 1987.

Hilgen F.J., Closing the gap in the Plio-Pleistocene boundary stratotype sequence of Crotone (southern Italy). Newslett. Stratigr. 22, 43-51, 1990.

Hilgen F.J., Astronomical calibration of Gauss to Matuyama sapropels in the Mediterranean and implication for the Geomagnetic Polarity Time Scale. Earth Planet. Sci. Lett. 104, 226-244, 1991.

Hoffmann V., Greigite ($Fe_3S_4$): magnetic properties and first domain observations. Phys. Earth Planet. Int. 70, 288-301, 1992.

Huerta-Diaz M.A. and Morse J.W., Pyritization of trace metals in anoxic marine sediments. Geochim. Cosmochim. Acta 56, 2681-2702, 1992.

Jover O., Rochette P., Lorand J.P., Maeder M. and Bouchez J.L., Magnetic mineralogy of some granites from the French Massif Central: origin of their low-field susceptibility. Phys. Earth Planet. Int. 55, 79-92, 1989.

Krs M., Krsová M., Pruner P., Zeman A., Novák F. and Jansa J., A petromagnetic study of Miocene rocks bearing micro-organic material and the magnetic mineral greigite (Sokolov and Cheb basins, Czechoslovakia). Phys. Earth Planet. Int. 63, 98-112, 1990.

Krs M., Novák F., Krsová M., Pruner P., Kouklíková L. and Jansa J., Magnetic properties and metastability of greigite-smythite mineralization in brown-coal basins of the Krusné hory Piedmont, Bohemia. Phys. Earth Planet. Int. 70, 273-287, 1992.

Luther III G.W., Meyerson A.L., Krajewski J.J. and Hires R., Metal sulfides in estuarine sediments. J. Sediment. Petrol. 50, 1117-1120, 1980.

Manning P.G.,. Williams J.D.H, Charlton M.N., Ash L.A. and Birchall T., Mössbauer spectral studies of the diagenesis of iron in a sulphide-rich sediment core. Nature 280, 134-136, 1979.

Misra K.C. and Fleet M.E., The chemical compositions of synthetic and natural pentlandite assemblages. Econ. Geol. 68, 518-539, 1973.

Morice J.A., Rees L.V.C. and Rickard D.T., Mössbauer studies of iron sulphides. J. Inorg. Nucl. Chem. 31, 3797-3802, 1969.

Mossmann J.-R., Aplin A.C., Curtis C.D. and Coleman M.L., Geochemistry of inorganic and organic sulphur in organic-rich sediments from the Peru Margin. Geochim. Cosmochim. Acta 55, 3581-3595, 1991.

Nakazawa H., Osaka T. and Sakaguchi K., A new cubic iron sulphide prepared by vacuum deposition. Nature Phys. Sci. 242, 13-14, 1973.

Obradovitch J.D., Naeser C.W., Izett G.A., Pasini G. and Bigazzi G., Age constraints on the proposed Plio-Pleistocene boundary stratotype at Vrica, Italy. Nature 298, 55-59, 1982.

Page N.J., Pentlandite and pyrrhotite from the Stillwater complex, Montana: iron-nickel ratios as a function of associated minerals. Econ. Geol. 67, 814-820, 1972.

Pasini G., Selli R., Tampieri R., Colalongo M.L., d'Onofrio S., Borsetti A.M. and Cati F., The Vrica section, in: The Neogene-Quarternary boundary, II Symp. Bologna-Crotone, Excursion Guide-book, R. Selli, ed., pp. 62-72, 1975.

Pruysers P.A., de Lange G.J. and Middelburg J.J., Geochemistry of eastern Mediterranean sediments: Primary sediment composition and diagenetic alterations. Marine Geol. 100, 137-154, 1991.

Rochette P., Fillion G., Mattéi J.-L. and Dekkers M.J., Magnetic transition at 30-34 Kelvin in pyrrhotite: insight into a widespread occurrence of this mineral in rocks. Earth Planet. Sci. Lett. 98, 319-328, 1990.

Selli R., Accorsi C.A., Bandini Mazzanti M., Bertolani Marchetti D., Bigazzi G., Bonadonna F.P., Borsetti A.M., Cati F., Colalongo M.-L., d'Onofrio S., Landini W., Menesini E., Mezzeti R., Pasini G., Savelli G. and Tampieri R., The Vrica section (Calabria). A potential Neogene-Quarternary boundary stratotype. Giorn. Geol. 41, 181-204, 1977.

Schwarz E.J., Magnetization of Precambrian sulphide deposits and wall rocks from the Noranda district. Canada, Geophysics 31, 797-802, 1966.

Schwarz E.J. and Vaughan D.J., Magnetic phase relations of pyrrhotite. J. Geomagn. Geoelectr. 24, 441-458, 1972.

Schwarz E.J., Magnetic properties of pyrrhotite and their use in applied geology and geophysics. Geol. Surv. Can., Pap. 74-59, pp. 24, 1975.

Shimazaki H., Thermochemical stability of bravoite. Econ. Geol. 66, 1080-1082, 1971.

Shishkin N.N., Mitenkov G.A., Mikhaylova V.A., Rudashevsiy N.S. and Sidorov A.F., Nickel, cobalt and copper in pyrrhotite from massive ores of the Talnakh ore cluster. Geochem. Int., 76-84, Transl. from Geokhimiya 1, 95-104, 1974.

Snowball I., Magnetic hysteresis properties of greigite ($Fe_3S_4$) and a new occurrence in Holocene sediments from Swedish Lappland. Phys. Earth Planet. Int. 68, 32-40, 1991.

Snowball I. and Thompson R., A stable chemical remanence in Holocene sediments. J. Geoph. Res. 95, 4471-4479, 1990.

Stacey F.D. and Banerjee S.K., The physical principles of rock magnetism, 195 pp., Elsevier Scientific Publishing Company, Amsterdam, 1974.

Suttill R.J., Turner P. and Vaughan D.J., The geochemistry of iron in Recent tidal-flat sediments of the Wash area, England: a mineralogical, Mössbauer, and magnetic study. Geochim. Cosmochim. Acta 46, 205-217, 1982.

Sweeny R.E. and Kaplan I.R., Pyrite framboid formation: laboratory synthesis and marine sediments. Econ. Geol. 68, 618-634, 1973.

Tauxe L., Opdyke N.D., Pasini G. and Elmi C., Age of the Plio-Pleistocene boundary in the Vrica section, southern Italy. Nature 304, 125-129, 1983.

Taylor L.A., Smythite, $Fe_{3+x}S_4$, and associated minerals from the Silverfields Mine, Cobalt, Ontario. Amer. Mineral. 55, 1650-1658, 1970.

Thomson G.F., The anomalous demagnetization of pyrrhotite. Geophys. J. Int. 103, 425-430, 1990.

Thunell R.C., Pliocene-Pleistocene climatic changes: evidence from land-based and deep-sea marine records. Mem. Soc. Geol. It. 31, 135-143, 1986.

Vaughan D.J., Nickelian mackinawite from Vlakfontein, Transvaal. Amer. Mineral. 54, 1190-1193, 1969.

Vaughan D.J. and Craig J.R., Mineral chemistry of metal sulfides, 493 pp., Cambridge University Press, Cambridge, 1978.

Vaughan D.J. and Ridout M.S., Mössbauer studies of some sulphide minerals. J. Inorg. Nucl. Chem. 33, 741-746, 1971.

Vaughan D.J., Schwarz E.J. and Owens D.R., Pyrrhotites from the Strathcona Mine, Sudbury, Canada: a thermomagnetic and mineralogical study. Econ. Geol. 66, 1131-1144, 1971.

van Velzen A.J. and Zijderveld J.D.A., A method to study alterations of magnetic minerals during thermal demagnetization applied to a fine-grained marine marl (Trubi formation, Sicily). Geophys. J. Int. 110, 79-90, 1992.

van der Weijden C.H., Geochemical signatures preserved in sediments of the Semaforo and Vrica sections (Calabria, Italy) and their relations with variations of the sedimentary regime. Palaeogeog., Palaeoclimat., Palaeoecol. 103, 203-221, 1993.

Zijderveld J.D.A., Hilgen F.J., Langereis C.G., Verhallen P.J.J. and Zachariasse W.J., Integrated magnetostratigraphy and biostratigraphy of the upper Pliocene-lower Pleistocene from the Monte Singa and Crotone areas in Calabria, Italy. Earth Planet. Sci. Lett. 107, 697-714, 1991.

# 6 Rock magnetic properties of the Pliocene and Pleistocene marine marls from the Vrica section (Calabria, Italy)


## Abstract

Two groups of magnetic minerals are present in the marls of the Vrica section. The rock magnetic properties of the most important group with maximum blocking temperatures up to about 375°C indicate magnetic sulphides. The second group with lower coercivities and higher maximum blocking temperatures (550-600°C) consists of magnetite.

Based on remanent coercivities and thermal demagnetization of IRM and ARM it was not possible to choose between monoclinic pyrrhotite and greigite as main remanence carrier. Both minerals may be present in the marls. To explain the high maximum blocking temperatures of the sulphide remanence (330-375°C) it was either necessary to assume that impurities or oxygen in the crystal can enhance the Curie temperature of monoclinic pyrrhotite (suggested by Rochette et al., 1990) or that greigite can partly survive in the samples up to these temperatures (Snowball, 1991; Horng et al., 1992a; Roberts and Turner, 1993).

The NRM behaviour in marls from the Vrica section is quite variable. The rock magnetic results indicate that the NRM mainly resides in sulphides. Occasionally, a small magnetite component can be isolated, that likely predates the authigenic formation of the magnetic sulphides. In general this component could not be detected due to spurious magnetizations during thermal treatment.

The variation in rock magnetic properties is interpreted to be due to variations in the magnetic sulphide content. Small-scale variations appear to be caused by local conditions that have influenced the authigenic formation of sulphides. A decrease in NRM intensities 15 m below the Pliocene-Pleistocene boundary seems to be directly related to a decrease in sedimentation rate from about 40 cm/ky to 25 cm/ky.


## 1. Introduction

The marine marls of the Vrica section in Calabria (Southern Italy, figure 1) were deposited during the late Pliocene and the beginning of the Pleistocene. The section is formally designated as the Pliocene-Pleistocene boundary stratotype (Aguirre and Pasini, 1985) as proposed by Selli et al. (1977). The section was subject of a detailed integrated magnetostratigraphic and biostratigraphic study (Zijderveld et al., 1991). The interpretation of the natural remanent magnetization (NRM) in this study was not without problems. Throughout the section the NRM

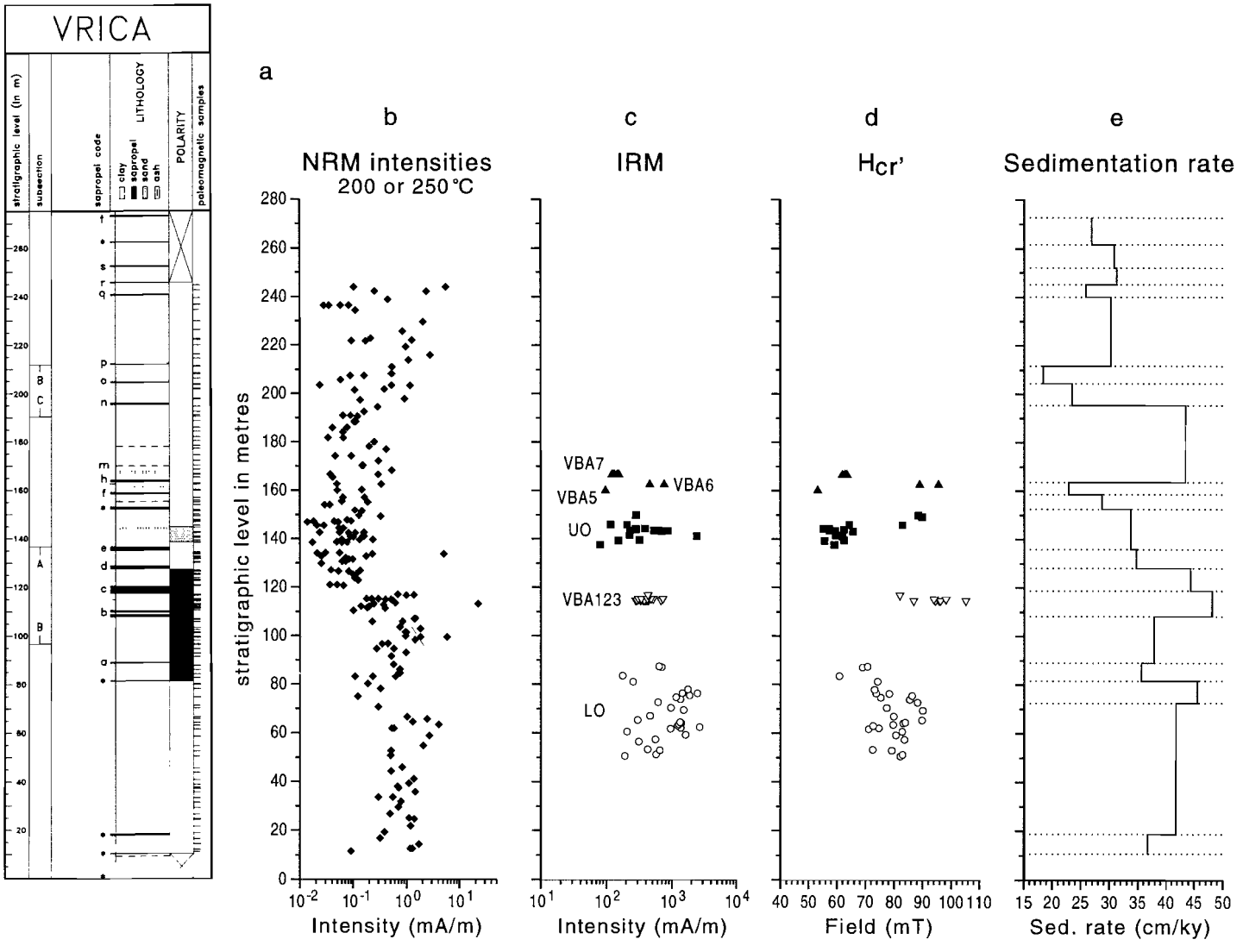
VRICA
stratigraphic level (in m)
subsection
sapropel code
LITHOLOGY
clay
sapropel
sand
ash
POLARITY
paleomagnetic samples
a
b
NRM intensities
200 or 250°C
c
IRM
d
Hcr'
e
Sedimentation rate
stratigraphic level in metres
VBA7
VBA6
VBA5
UO
VBA123
LO
Intensity (mA/m)
Intensity (mA/m)
Field (mT)
Sed. rate (cm/ky)

showed a considerable variety in intensity and behaviour during thermal demagnetization.

The blocking temperatures of NRM and isothermal remanent magnetization (IRM) and the high sulphide content of magnetic concentrates (van Velzen et al., 1993) pointed to a magnetic sulphide as the main remanence carrier. Remanent coercivities are in the range characteristic of monoclinic pyrrhotite, but the observed maximum blocking temperatures are too high compared to the values reported for monoclinic pyrrhotite. A rock magnetic study was undertaken to identify the magnetic minerals in the marls. The magnetic mineral content is very low, precluding other means of analysis. In this chapter the rock magnetic properties of the marls are discussed and compared with the properties of pyrrhotite and greigite. The relation between rock magnetic properties and variations in magnetomineralogy and the influence of sedimentation rate is discussed. The next chapter will focus on the influence of thermal alterations on the magnetic minerals.

## 2. Magnetic sulphides

Two ferrimagnetic iron sulphides may occur in sediments: pyrrhotite and greigite. Of the pyrrhotites only monoclinic pyrrhotite ($Fe_7S_8$) is ferrimagnetic. The iron-richer pyrrhotites are hexagonal and antiferromagnetic at room temperature. The Curie temperature of monoclinic pyrrhotite is reported between 305 and 325°C (Schwarz and Vaughan, 1972; Schwarz, 1975; Vaughan and Craig, 1978; Dekkers, 1989). Coercive forces are grain-size dependent. The remanent coercive force ($H_{cr}$) ranges from 10 mT for large grains to 110 mT in grains of 1 micron in synthetic and natural pyrrhotites, the coercive force ($H_c$) from 8 to 80 mT (Clark, 1984; Dekkers, 1988; Menyeh and O'Reilly, 1991). Greigite ($Fe_3S_4$) is reported to

---

**Figure 1.** (a) Vrica composite section. Polarities according to Zijderveld et al. (1991). Samples for the rock magnetic study were taken from an interval containing the Lower Olduvai transition record in subsection Vrica A (stratigraphic level 0-137 m), from six levels (VBA1, 2, 3, 5, 6 and 7) in subsection Vrica B (stratigraphic level 97-112 m). Samples from the interval containing the Upper Olduvai transition record were taken in the parallel San Leonardo section. See Table A for the stratigraphic level of the samples.
(b) Variation of NRM intensities in the Vrica composite section (after Zijderveld et al., 1991). The intensities were taken after thermal demagnetization at 200°C or 250°C, when secondary overprints are generally removed.
(c) IRM intensities in parts of the Vrica section and parallel section San Leonardo. Saturation IRM was induced in fields of 1.5 T. Open symbols refer to samples from the part with high NRM intensities below sapropel *c* (circles to Lower Olduvai (LO) samples; triangles to VBA1, 2 and 3). Closed symbols refer to the part with low NRM intensities above sapropel *c* (squares to Upper Olduvai (UO) samples; inverted triangles to VBA5, 6 and 7).
(d) Remanent acquisition coercivities of IRM ($H_{cr'}$). Symbols as in figure 1c.
(e) The sedimentation rate (cm/ky) in the Vrica section. Average values were calculated between the midpoints of the sapropels. Dating of the sapropels was done through astronomical tuning (Hilgen et al., 1993)

become unstable upon heating well below 300°C (Skinner, 1964; Uda, 1968; Coey et al., 1970; Spender et al., 1972). Direct measurement of the Curie temperature is therefore not possible. Values estimated by extrapolation are between 300 and 330°C (Uda, 1968; Coey et al., 1970; Spender et al., 1972). While synthetic greigites have low coercivities ($H_c$ = 10-30 mT; Uda, 1968; Coey et al., 1970; Spender et al., 1972; Snowball, 1991 and references therein), natural sedimentary greigites have considerably higher coercivities ($H_c$ = 41-57 mT, Snowball, 1991; $H_{cr}$ = 60-100 mT; Horng et al., 1992a). Possibly, differences in grain size are responsible for these discrepancies. These sedimentary greigites are reported to be thermally more stable, well above 300°C when heated in air and even close to 400°C in a nitrogen atmosphere (Snowball, 1991; Tric et al., 1991; Hoffmann, 1992; Horng et al., 1992a; Roberts and Turner, 1993).

## 3. Setting and sampling of the Vrica marls

The marls of the Vrica section are homogeneous on a large scale, except for a number of regularly occurring sapropelitic beds and some silty intervals. The sapropelitic beds consist of laminated marls deposited during oxygen-poor or anoxic conditions. Several distinct lithological levels in the section, among which most of the sapropels, have been labelled '*a*' to '*t*' (Selli et al., 1977; cf. figure 1a). The Pliocene-Pleistocene boundary (age 1.81 Ma; Hilgen, 1991) is defined at the top of sapropel *e*. The sequence of sapropels is interpreted in terms of interference patterns related to the Earth's orbital cycles (Hilgen, 1987, 1991). Outside the sapropels the carbonate content of the marls varies between 14 and 24% (van der Weijden, 1993). Clay minerals in the marls are smectite (40 - 70%), chlorite (20-30%), illite (30-40% and kaolinite (10-20%) (Combourieu-Nebout, 1987; van der Weijden, 1993). The relative contribution of smectite starts to decrease close to the Pliocene-Pleistocene boundary. Levels with a higher silt content incidentally occur, for example above sapropel *e* and between sapropels *h* and *n* (cf. figure 1a).

The Vrica section consists of subsections A, B and C. Geomagnetic polarities as recorded in the characteristic natural remanence are reversed, except for the interval of the Olduvai subchron. According to Zijderveld et al. (1991), the Olduvai subchron extends from the sapropel below sapropel *a* in subsection Vrica A to the base of sapropel *d* in subsection Vrica B with possibly another small normal interval above sapropel *e* (cf. figure 1a). The magnetostratigraphy of Tauxe et al. (1983) shows a reversed interval in the Olduvai subchron between sapropels *b* and *c*.

The rock magnetic properties of the marls vary considerably. The variations occur on a larger, stratigraphic scale, but also over small distances. One of the most notable variations is that in the NRM intensities (figure 1b). Up to sapropel *c* (i.e., the 120 m level) NRM intensities are relatively high (0.5-3.0 mA/m). The intensities are below 0.2 mA/m from sapropel *c* up to the 149 m level. Continuing upward in the section the NRM intensities recover slowly to higher values. The

small-scale variations, however, are also large and just as interesting from a rock magnetic point of view. These small-scale variations occur over distances of only a few cm, even within a stratigraphical level.

Samples used for the present rock magnetic study come from parts of the marl sequence with different NRM intensities (figure 1, Table A). Samples from an interval between the 50 m level and the 90 m level in subsection Vrica A, containing the Lower Olduvai transition, and samples from three closely spaced sites (VBA1, 2 and 3) around the 115 m level in subsection Vrica B are from the high-intensity part. The samples from a 13 m interval around the Upper Olduvai record (137 m to 150 m level) are in the low-intensity interval. This Upper Olduvai record was sampled in the parallel section of San Leonardo (Zijderveld et al., 1991), because the corresponding part in subsection Vrica B appeared to be too weathered to obtain meaningful paleomagnetic results. Samples from three sites (VBA5, 6 and 7) between the 160 and 167 m level in Vrica B are from the part where the intensity is increasing again (figure 1).

Cores were drilled with an electric drill and a portable generator. Before sampling, the weathered surface of each sampling site was removed to obtain samples from blue-coloured sediment, as fresh as possible. Cores from the Lower and Upper Olduvai transition were kept moist by packing in air-tight plastic bags to prevent oxidation. Two to four standard-sized specimens were obtained from each core.

| | LO | VBA 1 | VBA 2 | VBA 3 | UO | VBA 5 | VBA 6 | VBA 7 |
|---|---|---|---|---|---|---|---|---|
| **Strat. level (m)** | 50.3-88.7 | 114.6 | 115.2 | 116.8 | 36.5-15 | 160.1 | 162.6 | 166.6 |
| **Polarity** | R/N | N | N | N | N/R | R | R | R |
| **NRM int. (mA/m)** | 0.12-3.1 | 0.15-2.5 | 0.09-1.3 | 0.4-1.7 | 0.03-2.1 | 0.07-0.1 | 0.05-0.3 | 0.09-0.23 |
| **Typical** | 1000 | 500 | 500 | 600 | 300 | 110 | 200 | 200 |
| **ARM (mA/m)** | 3.5-13.8 | 4.8 | 4 | 3.5 | 1.9-13.6 | 2.2 | 4.5 | 2.5 |
| **Typical** | 6 | | | | 3 | | | |
| **IRM(1.5T) (mA/m)** | 180-2665 | 380/680 | 430 | 430 | 80-2380 | 100 | 460/760 | 130 |
| **Typical** | 1200 | | | | 350 | | | |
| **Hcr (mT)** | | 80/81 | 81 | 64 | | 43 | 73/78 | 49.5 |
| **Hcr' (mT)** | 62-90 | 87-105 | 94-98 | 82 | 55-89 | 53 | 89-96 | 62-63.5 |
| **Typical** | 80 | | | | 60 | | | |

**Table A.** Rock magnetic parameters for the samples from this study. Stratigraphic level refers to the position in the Vrica section (cf. figure 1a) and normal (N) or reversed (R) polarity of the characteristic NRM component is indicated. NRM intensities are initial intensities. ARM was acquired in AC fields of 300 mT with a DC field of 38 μT. $H_{cr}$ and $H_{cr'}$ are remanent coerce force and remanent acquisition coercive force, respectively. Ranges are indicated to illustrate variation within a level or interval. Averages indicate typical values.

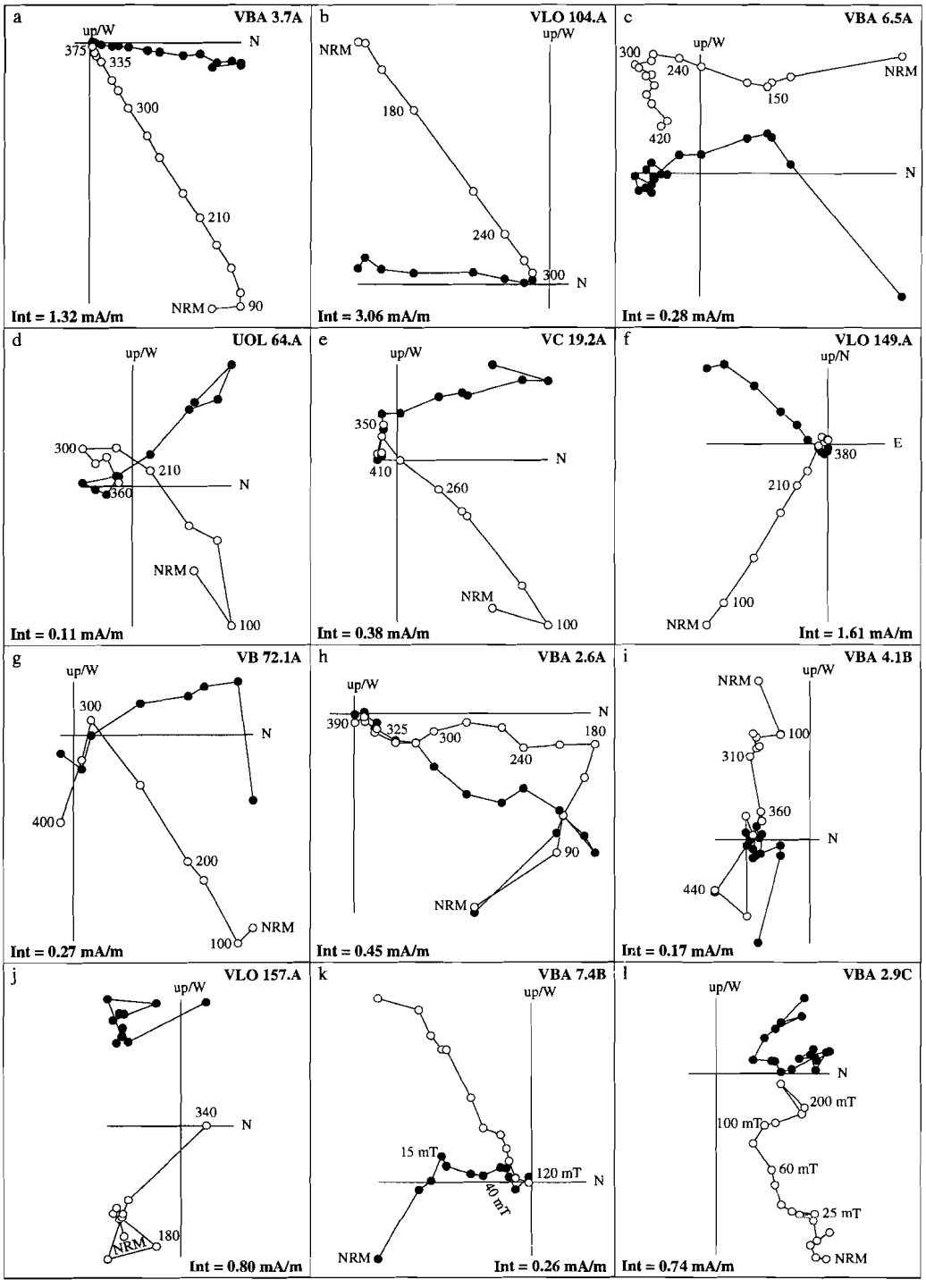
a
VBA 3.7A
up/W
N
375
335
300
210
NRM
90
Int = 1.32 mA/m
b
VLO 104.A
up/W
NRM
180
240
300
N
Int = 3.06 mA/m
c
VBA 6.5A
up/W
300
240
NRM
150
420
N
Int = 0.28 mA/m
d
UOL 64.A
up/W
300
210
N
360
NRM
100
Int = 0.11 mA/m
e
VC 19.2A
up/W
350
N
410
260
NRM
100
Int = 0.38 mA/m
f
VLO 149.A
up/N
E
380
210
100
NRM
Int = 1.61 mA/m
g
VB 72.1A
up/W
300
N
400
200
NRM
100
Int = 0.27 mA/m
h
VBA 2.6A
up/W
N
390
325
300
180
240
90
NRM
Int = 0.45 mA/m
i
VBA 4.1B
up/W
NRM
100
310
360
N
440
Int = 0.17 mA/m
j
VLO 157.A
up/W
340
N
NRM
180
Int = 0.80 mA/m
k
VBA 7.4B
up/W
15 mT
120 mT
N
40 mT
NRM
Int = 0.26 mA/m
l
VBA 2.9C
up/W
N
200 mT
100 mT
60 mT
25 mT
NRM
Int = 0.74 mA/m

## 4. Natural remanent magnetization

The demagnetization behaviour of the NRM is equally diverse as the NRM intensities. Samples from one level generally show the same demagnetization behaviour, but occasionally even in samples from one core the characteristic NRM directions can differ. All samples have in common that a major part of the initial NRM is removed after thermal demagnetization at 350°C. Examples of the varying demagnetization behaviour are shown in figure 2. A first group of samples, usually from the interval with higher NRM intensities, has a straightforward demagnetization behaviour. A characteristic normal or reversed direction is reached after removal of a viscous laboratory component at 150°C (figure 2a,b).

In a second group a characteristic direction is reached after demagnetization at about 300°C, after removal of a component with a different direction (figure 2c,d). Often it is only possible to determine the polarity of characteristic component, because components overlap (figure 2e,f). The maximum blocking temperatures of the characteristic NRM component are not always the same. The remanence can be almost demagnetized at 350°C (figure 2a,b,d), but in other samples the decay above 350°C is still significant (figure 2c,e,f). Even after heating to 400°C a part of the remanence still is present.

The demagnetization behaviour above 350°C can only be observed in samples that are not influenced by thermal alterations. From 300°C onwards, samples may become viscous or subject to spurious magnetizations acquired during heating. An increase of the initial bulk susceptibility ($\chi_o$), which in most samples starts at about 350°C (figure 3), corresponds with the occurrence of alterations producing a highly magnetic mineral phase. This alteration will be discussed in chapter 7. In the samples that are influenced by this alteration, the initial rectilinear decrease of remanence is interrupted and spurious remanences make further demagnetization useless (figure 2g).

A third group of samples shows a demagnetization path that deviates from the usual two-component demagnetization. In some samples the remanence first increases or moves in an apparently random direction between 150 and 300°C before decreasing along a curved trajectory towards the origin (Figure 2h). This behaviour is due to a low-temperature alteration of magnetic minerals, that has important consequences (see chapter 7). Some samples seem to behave randomly or show hardly any decay up to 300°C (figure 2i,j).

Alternating field (AF) demagnetization of the NRM was also attempted in order to avoid the thermal alterations (figure 2k,l). Demagnetization results are reasonable up to fields of 40 or 50 mT, but higher fields produce spurious magnetizations that are reminiscent of the effect of alternating fields on pyrrhotite

---

**Figure 2.** Examples of demagnetization diagrams of NRM after tectonic correction (strike 185°, dip 9°). Closed (open) symbols are horizontal (vertical) projections. Int = initial NRM intensity. (a-j) Thermal demagnetization, temperatures in °C.
(k,l) Alternating field demagnetization, alternating fields in mT.

and greigite (Schwarz, 1966; Thomson, 1990; Krs et al., 1990). During the three-axes, stationary AF procedure an increasing remanence was often produced (figure 2l).

The NRM intensities in figure 1b are given after thermal demagnetization at 200 or 250°C, dependent on the demagnetization behaviour. Generally, however, this intensity will be a good measure for the intensity of the characteristic component of the NRM, in spite of the diversity of the demagnetization behaviour.

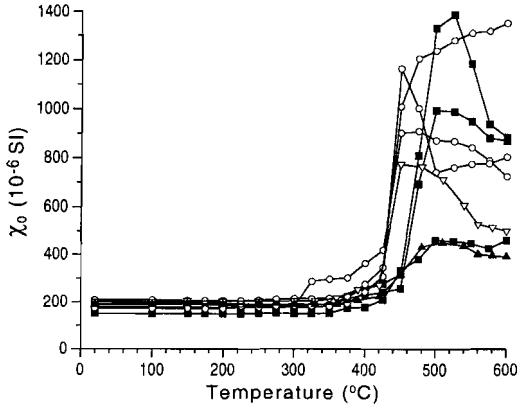


**Figure 3.** Changes in initial susceptibility ($\chi_0$) during thermal demagnetization. In most samples $\chi_0$ starts to increase above 350°C, but changes at lower temperatures occasionally occur. Symbols as in figure 1c.

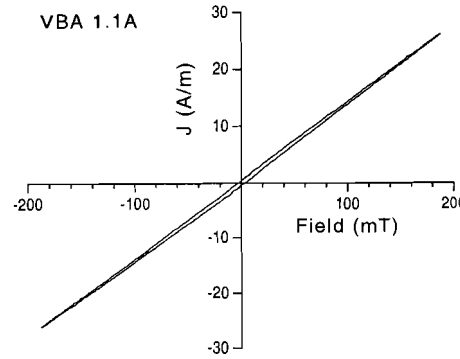


**Figure 4.** Hysteresis loop of sample VBA1.1A. The magnetization is dominated by paramagnetic clay minerals. Other samples showed similar loops.

## 5. Rock magnetic measurements

### *5.1. Methods and instrumentation*

The magnetic properties of the marls are dominated by clay minerals. Hysteresis curves and $\chi_0$ are strongly influenced by the presence of these paramagnetic minerals. Isothermal remanent magnetization (IRM) and anhysteretic remanent magnetization (ARM) are parameters that better represent the ferromagnetic minerals. IRM acquisition curves, remanent coercivity measurements and AF demagnetization are used to determine the coercivity spectra. The thermal decay curves of IRM and ARM yield the blocking temperature spectra (and alteration temperatures) of the magnetic minerals.

IRM acquisition curves and remanent coercivities were determined using DC coils with a maximum field of 1.5 T. ARM acquisition was performed in AC coils with a maximum field of 0.3 T and DC fields of 19 or 38 μT. The same coils were used for AF demagnetization. For hysteresis measurements a pair of balanced AC coils was used with a maximum field of 0.2 T. Initial susceptibility and anisotropy

of susceptibility were measured on a KLY-2 susceptibility bridge. Thermal demagnetization temperatures in a laboratory-built oven were accurate to within 2°C. Total heating times were chosen so that samples spent 5 to 10 minutes at the intended temperature. IRM and ARM intensities were measured on digitized Jelinek spinner magnetometers based on the JR3 drive unit, NRM partly on a 2G vertical cryogenic magnetometer (model 740 R). The detection limits of the magnetometers are $4*10^{-11}$ $Am^2$ and $2*10^{-11}$ $Am^2$ respectively, with the measuring protocols used.

### *5.2. Hysteresis parameters and anisotropy of the magnetic susceptibility*

The small amount of ferromagnetic minerals in the marls and the large contribution of paramagnetic clay minerals prevents accurate determination of the coercive forces and the remanent and saturation magnetization with hysteresis measurements (figure 4). Moreover, the maximum fields in the AC coils available for the hysteresis measurements were not sufficient to saturate the marls. The large high-field susceptibility of the samples ($160 \pm 10*10^{-6}$ SI) is mainly due to the clay minerals. This implies that also $160*10^{-6}$ SI of the initial susceptibility $\chi_o$ is contributed by clay minerals. This is 75% to 95% of the total $\chi_o$ of the marls.

When the clay content of the samples is assumed to be constant, $\chi_o$ only varies with the ferromagnetic content. Because IRM is a measure for the ferromagnetic content, linear extrapolation of $\chi_o$ versus IRM towards zero remanence (figure 5) yields another estimate for the paramagnetic susceptibility, provided that IRM and ferromagnetic susceptibility are proportional. That this value is $10\text{-}15*10^{-6}$ SI higher than $160*10^{-6}$ SI indicates that this condition might not be fulfilled, for example because several magnetic minerals with different $\chi_o$/IRM ratios contribute to the IRM.

The anisotropy of the magnetic susceptibility in the samples is low: the anisotropy factor P (=total anisotropy) measured in 10 samples is between 1.02 and 1.045. Foliation is dominant. The minimum axis of the anisotropy ellipsoid is always perpendicular to the bedding of the marls indicating a sedimentary fabric. Because such a large part of $\chi_o$ is due to the clay minerals, this anisotropy will be of paramagnetic origin, with only a minor (if any) influence of the remanence carrying minerals. Although the anisotropy ellipsoid shows a primary depositional fabric, this can therefore not be considered evidence of a primary origin of the remanence. Despite the small lineation (L is typically between 1.004 and 1.01), the maximum anisotropy axes concentrate reasonably well. The direction of the average lineation is (350°, 0°) is almost antiparallel to the average declination for the reversed polarity primary component of the NRM as calculated for the Vrica marl sequence by Scheepers (1994). It is unlikely, however, that this slight lineation is an expression of the anisotropy of the small amount of remanence carrying minerals in the marls. In similar sediments of the same age and with similar magnetic fabrics the lineation was demonstrated to originate from deformation (Scheepers and Langereis; 1994).

### 5.3. IRM acquisition

Although the variation in IRM intensity in the section is less than that of the NRM intensity, nevertheless a range of values between 0.1 and 2.5 A/m is measured for the IRM induced in a 1.5 T field (figure 1c and Table A). Over distances of less than a meter the intensity may vary an order of magnitude. Even within a single core the IRM can vary a factor of 2. Comparison of different rock magnetic parameters measured in separate specimens of the same core can therefore be less reliable.

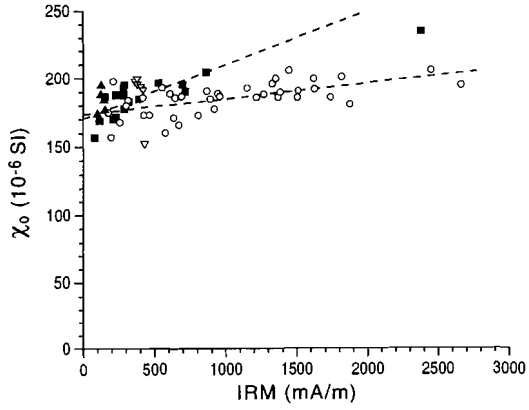


**Figure 5.** Initial susceptibility ($\chi_0$) versus IRM. Linear regression lines for LO samples and UO samples (sample with extremely high intensity excluded) are plotted. A linear relationship will only exist, however, for a simple magnetic mineralogy.

The efficiency of the NRM is low: the IRM/NRM ratio is generally between 500 and 1500 (figure 6), but IRM and NRM intensities do not show a simple linear relationship. The scatter in Lower and Upper Olduvai data may be partly due to the fact that in these intervals NRM and IRM were not measured in the same specimen, but in adjacent specimens from the same core.

The IRM acquisition curves (figure 7) show that the IRM is already close to saturation at 0.3 T. At 0.5 T more than 97% of the IRM intensity obtained

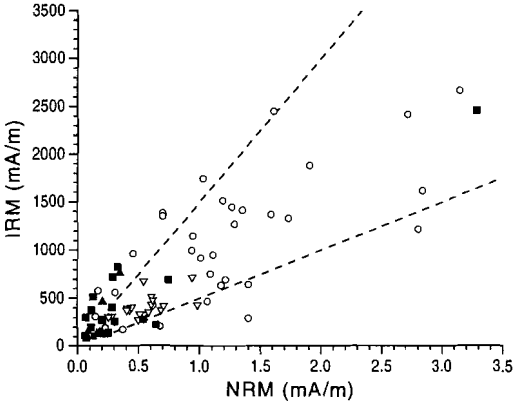


**Figure 6.** IRM intensity versus NRM intensity. In this case initial NRM intensities were taken. Lines indicate IRM/NRM ratios of 500 and 1500, respectively. Symbols as in figure 1c.

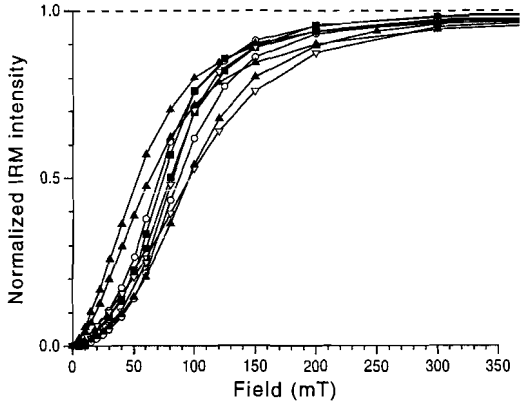


**Figure 7.** Initial part of IRM acquisition curves normalized to the intensity acquired at 1.5 T. Samples saturate in relatively low fields, but the remanent acquisition coercivities show a large variation. Compare figure 1d. Symbols as in figure 1c.

after applying fields of 1.5 T is reached. The coercivities of the magnetic minerals nevertheless show a considerable variation throughout the sequence. The remanent acquisition coercive force ($H_{cr'}$, i.e. the DC field needed to induce a remanence that is half the saturation IRM) varies between 53 and 105 mT, and $H_{cr}$ between 43 and 81 mT (Table A). The existence of such a range can indicate variations in magnetic mineralogy or grain size. The observed coercive forces are higher than those of magnetite (e.g. Dunlop, 1986). They are in a range typical of pyrrhotite (Clark, 1984; Dekkers, 1988; Menyeh and O'Reilly, 1991) or greigites found in sediments (Snowball, 1991; Horng et al., 1992a).

The IRM intensity and the coercive forces are both related to the magnetomineralogy. Plotting the IRM intensity versus $H_{cr}$ and $H_{cr'}$ (figure 8a,b) might therefore reveal whether the variation in magnetomineralogy in the section is due to the varying amount of one mineral phase with specific properties or to an overall variation of magnetic mineral content. $H_{cr}$ values were only determined in VBA samples, $H_{cr'}$ in all samples (figure 8). $H_{cr}$ increases with the IRM intensity, especially for IRM values $<400$ mA/m. In the VBA samples $H_{cr'}$ shows a similar relation as $H_{cr}$, but the trend in the Lower Olduvai (LO) and Upper Olduvai (UO) samples is not so clear. The LO samples suggest a slight increase of $H_{cr'}$ for IRM intensities $>400$ mA/m. The UO samples show $H_{cr'}$ values more or less independent of the IRM intensity. $H_{cr'}$ of UO samples is generally lower than that of LO samples, except for three samples with $H_{cr'}$ values between 80 and 90 mT. During sampling no differences were noted for the appearance of these three samples. The lower $H_{cr'}$ values could indicate larger grain sizes of the same magnetic sulphide or the presence of another magnetic mineral phase with lower coercivities.

### *5.4. Thermal demagnetization of IRM*

Thermal demagnetization of the remanent magnetization shows blocking temperatures of the magnetic carriers, indicative of magnetic mineral phases and grain sizes of the magnetic particles. Due to the low intensities of the NRM and the occurrence of spurious magnetizations or viscous behaviour, it is difficult to determine the thermal decay of the NRM in the Vrica samples. The IRM is in the order of 1000 times stronger than the NRM, and is consequently less affected by these problems. The thermal decay curves of the IRM (figure 9a,b) indicate that there are at least two magnetic minerals with different blocking temperature spectra. The most important mineral has blocking temperatures below 400°C. Above 400°C only a small part of the remanence remains, which apparently resides in another mineral (figure 9b).

The greater part of the thermal decay of the IRM occurs in fact below 325°C, i.e. below the Curie temperature of monoclinic pyrrhotite and in the temperature range where greigite becomes thermally unstable in air. However, the decay of the low-temperature remanence apparently continues above this temperature. The maximum blocking temperature of this remanence is indicated by an inflection in

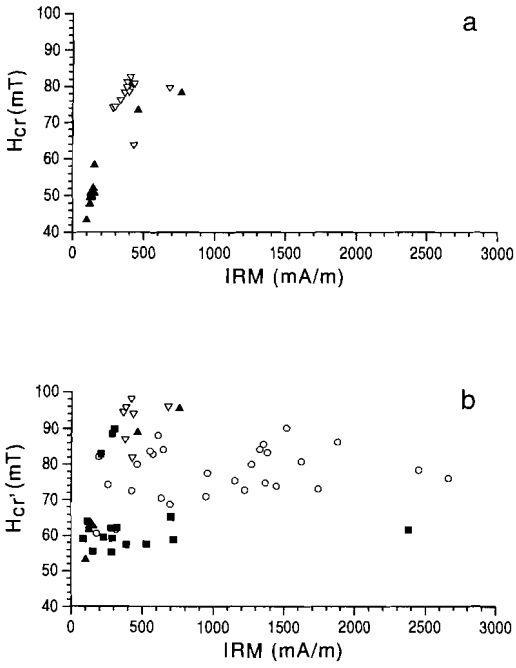


**Figure 8.** (a) Remanent coercivities ($H_{cr}$) and (b) remanent acquisition coercivities ($H_{cr}'$) as a function of the IRM intensity. Symbols as in figure 1c.

the decay curve, which can be found somewhere between 330 and 375°C in all samples. This could either mean that the mineral phase that carries the majority of the remanence has maximum blocking temperatures of around 360°C or that this remanence is carried by several mineral phases, one of which has these blocking temperatures higher than 325°C. It should be noted, however, that from these results it is not clear whether the demagnetization is due to unblocking of remanence or to alteration of the minerals involved. In fact, it can be shown that a small part of the decay is due to alteration (see chapter 7).

In view of the demagnetization temperatures the possibility should be considered that maghemite is an important remanence carrier. The inversion of maghemite to hematite can start at about 300°C. This inversion of this highly magnetic mineral (about 70 $Am^2/kg$) to the much less magnetic hematite (about 0.5 $Am^2/kg$) would be

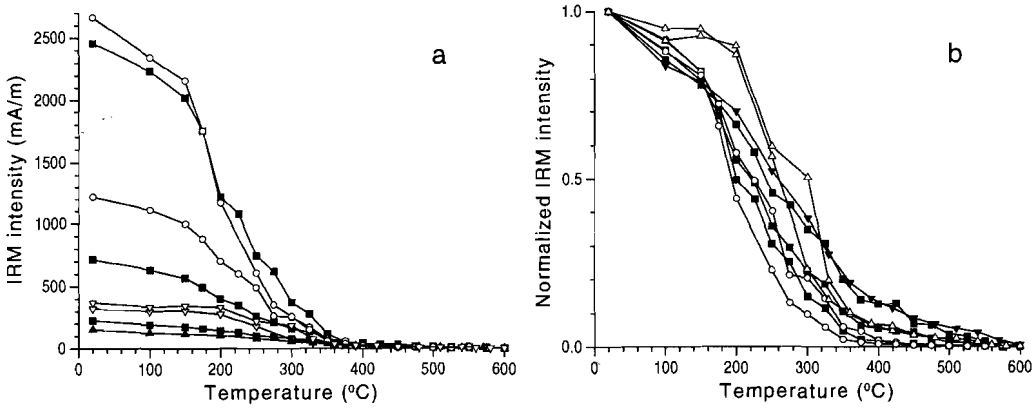


**Figure 9.** Thermal demagnetization of IRM. (a) Absolute values. (b) The same samples after normalization to the initial IRM intensity. Two magnetic phases are apparent. The decay up to 375°C is mainly attributed to sulphides. Above this temperature the remaining IRM is carried by magnetite. Symbols as in figure 1c.

accompanied by a decrease of the susceptibility. Also a decrease of low-coercivity remanence and an increase of low-coercivity remanence would occur. Such changes are not observed in this temperature range (see also chapter 7).

Based on the coercivities and the blocking temperatures as well as the alteration temperatures, it is therefore likely that the mineral phases carrying this dominant part of the remanence are some kind of magnetic sulphides. The anomalously high maximum blocking temperatures of this remanence indicate that it can not only reside in stoichiometric monoclinic pyrrhotite. An attempt to identify the sulphides in magnetic concentrates by X-ray diffraction was not successful. Many reflections were found, but most peaks belonged to clay minerals, which are abundantly present in the concentrates. Although with the microprobe numerous sulphide grains were found in the concentrates (van Velzen et al., 1993), the amount of sulphides was apparently too low to be detected with XRD.

To investigate the presence of monoclinic pyrrhotite, a sample with an IRM was cooled to liquid helium temperature, but it did not show the characteristic magnetic transition at 30-34 K (Rochette, pers. com.) found in many monoclinic pyrrhotites (Rochette et al., 1990). The absence of the transition does not prove that monoclinic pyrrhotite is not present. It is conceivable that the transition is suppressed when for example the pyrrhotite grains have an oxidized surface, analogous to the absence of the Verwey transition in slightly oxidized magnetite grains (Özdemir et al., 1993).

After heating to 375°C usually only a small part of the initial IRM remains. This part of the remanence decays almost linearly above this temperature and has maximum blocking temperatures between 550 and 600°C (figure 9b). The maximum blocking temperatures clearly point to magnetite. A linear decay can occur when the grain-size spectrum of a magnetic mineral is continuous between super paramagnetic (SP) and single domain (SD) sizes, from small grains with low blocking temperatures to larger grains with higher blocking temperatures. Whereas the IRM carried by the sulphide phases shows a large variation in intensity, the intensity of the magnetite IRM after heating to 375°C is more constant. It only varies between 15 and 60 mA/m (figure 10). The IRM remaining after demagnetization at 375°C is slightly higher in samples with higher initial IRM. All samples show this increasing trend. It should be noted that for samples with low IRM intensities the

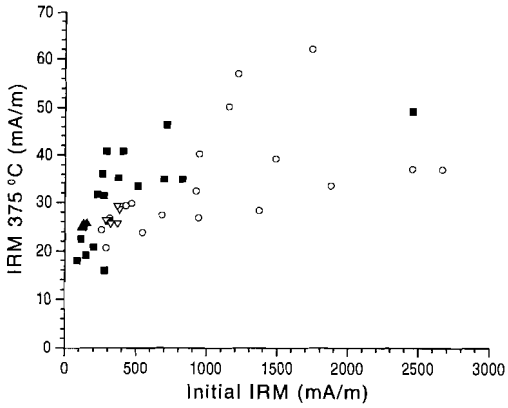


**Figure 10.** IRM remaining after thermal demagnetization at 375°C as a function of the initial IRM intensity. The IRM(375°C) varies between 20% of the initial IRM in samples with low intensities to 2% in samples with high intensities. Symbols as in figure 1c.

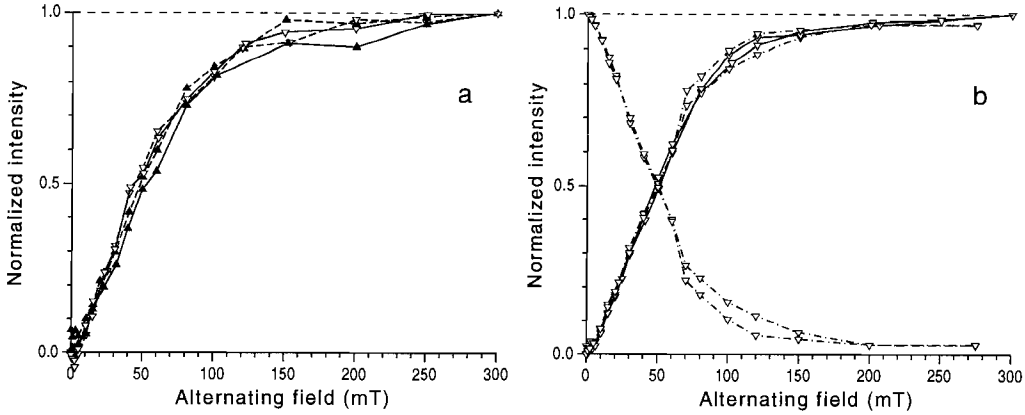


**Figure 11.** (a) Normalized ARM acquisition curves in alternating fields up to 300 mT and DC fields of 38 μT (solid lines) and 19 μT (dashed lines). Final ARM intensities are proportional to the DC fields. (b) Normalized ARM acquisition and AF demagnetization of the ARM. AF demagnetization curves are shown as well as their complement 1-AF (both dash-dot lines). Symbols as in figure 1c.

IRM(375°C) can be 20% of the total IRM, for the highest IRM intensities it is less than 2%.

### *5.5. ARM acquisition*

Only a small part of all magnetic minerals will contribute to an ARM induced in DC fields comparable to the Earth's magnetic field. ARM acquisition curves were measured with a constant DC field and increasing maximum AC fields (figure 11a). Comparison of the first part of the ARM acquisition curves with the corresponding part of the IRM acquisition curves reveals that the relative contribution of the magnetic fraction with coercivities $<100$ mT is higher for the ARM than for the IRM. The low coercivities are not enough to explain this. Differences in the nature of the anisotropy in different magnetic minerals are an important factor in ARM acquisition.

The normalized curves of ARMs induced in 19 μT and 38 μT DC fields are very similar and the remanences are proportional to the DC field. Intensities of the ARM induced in 38 μT fields are about 10 times the NRM intensity (Table A). At 100 mT, the AC field commonly used to induce an ARM, the ARM reaches 80 to 90% of the intensity obtained with 300 mT AC fields. Irregularities in the acquisition curves are due to the spurious magnetizations that also disturb the AF demagnetization of the NRM in fields $>40$ mT. For the same reason it was not always possible to demagnetized a sample completely before ARM acquisition (figure 11). AF demagnetization of the ARM, using stationary demagnetization along one axis, is complementary to the acquisition, showing that the process of ARM introduction is reversible (figure 11b). This indicates that there is no magnetic

interaction between magnetic grains (Dankers, 1981).

The different nature of the ARM and the IRM can help to distinguish the two groups of magnetic minerals in the marls. For low IRM intensities the ARM is relatively large (figure 12), as if in all samples a basic level of ARM can be induced. For higher IRM intensities the ARM increases starting from this level. This confirms the presence of a relatively constant amount of low-coercivity (<100 mT) mineral that easily acquires an ARM and a varying amount of higher-coercivity minerals that have a relatively less effective ARM acquisition. Figure 12 confirms indirectly that the variation in IRM intensity is mainly due to the mineral phase with higher remanent coercivities.

### *5.6. Thermal demagnetization of ARM*

Thermal demagnetization of the ARM shows the same two-phase behaviour as that of the IRM (figure 13), but the relative contribution of low-blocking-temperature (sulphide) ARM is smaller. At 340°C in LO samples still 25 to 40% of the initial ARM remains, both for the samples with a low intensity and with a high intensity. Both the part of the ARM acquired in low AC fields and the high-unblocking-temperature are relatively large. It supports the suggestion that, compared to the IRM, relatively a large part of the ARM is carried by magnetite.

## 6. Discussion

The magnetic minerals in the Vrica marls consist of two groups. The rock magnetic properties of the first group (relatively high remanent coercivities and maximum blocking temperatures below 375°C) point to a magnetic iron sulphide, possibly monoclinic pyrrhotite in combination with other magnetic sulphides. The second group has lower remanent coercivities and maximum blocking temperatures between 550 and 600°C, both characteristic of magnetite.

The large range of blocking temperatures indicate that the magnetite grains are SD, varying in size from larger SD to smaller grains close to SP size. The amount of magnetite present can be approximated by backward extrapolation of the IRM decay above 375°C to room temperature, assuming that the grain-size spectrum produces an approximately linear thermal decay of the magnetite remanence not only above 375°C but also between room temperature and 375°C. In that case, the total magnetite remanence is about twice the IRM(375°C). The maximum contribution of magnetite to the total IRM is then about 40% in samples with the lowest IRM. The IRM(375°C) varies between 15 and 60 mA/m (figure 10). Therefore the amount of magnetite in the marls is only very small: in the order of 1 ppm. Even in the samples with a low IRM intensity, the remanent coercivities are mainly determined by the sulphides (figure 8a,b).

### *6.1. Magnetic sulphides*

The magnetic sulphide is the major remanence carrier. It determines the intensity variations in the section and governs the ferromagnetic properties. It is not clear, however, whether there is just one magnetic sulphide phase or a combination of sulphide phases with slightly different magnetic properties. The thermal decay curves of the IRM show that a large part is demagnetized below the Curie temperature of pyrrhotite (305-325°C). This seems to confirm the role of monoclinic pyrrhotite as principal remanence carrier. A smaller part of the low-temperature remanence, however, has higher maximum blocking temperatures (or alteration temperatures), varying between 330 and 375°C. Other magnetic sulphides seem to be present as well. The bulk coercivities are in the range determined for small grain-size fractions of pyrrhotite (Clark,1984; Dekkers, 1988; Menyeh and O'Reilly, 1991). For greigite the grain-size dependence of $H_{cr}$ and $H_{cr'}$ is not yet known. Supposing one sulphide phase is predominant in the entire Vrica section, the $H_{cr}$ and $H_{cr'}$ of this mineral can be estimated from the high-intensity samples (IRM >0.5 A/m). $H_{cr}$ is between 70 and 85 mT and $H_{cr'}$ is between 70 and 95 mT, except for the UO samples. According to the three references mentioned above, for monoclinic pyrrhotite this would indicate grain sizes of 3-15 μm, 5-10 μm and 1-5 μm, respectively. This larger than the SD size range for pyrrhotite (<3 μm; Soffel, 1981) and the size of the sulphides observed with a microprobe in magnetic concentrates of the marls (<2 μm; van Velzen et al., 1993). The $H_{cr'}$ values for the UO samples point to a somewhat different magnetomineralogy for that interval. With three exceptions these $H_{cr'}$ values are lower over the whole range of IRM intensities (52-65 mT). The relatively high IRM(375°C) of a number of UO samples (figure 10) points to a slightly higher

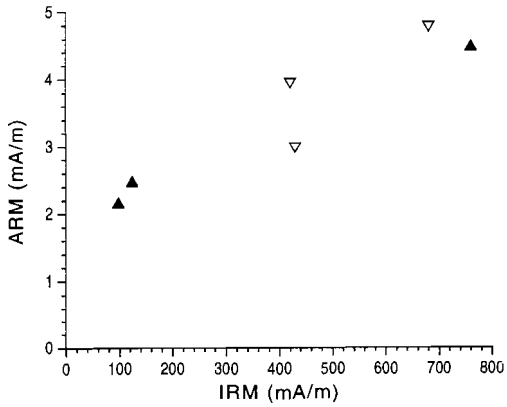


**Figure 12.** ARM versus IRM. IRM was acquired in a 1.5 T DC field, ARM in 300 mT AC fields with a 38 μT DC field. ARM is comparatively high in samples with a low IRM intensity. Symbols as in figure 1c.

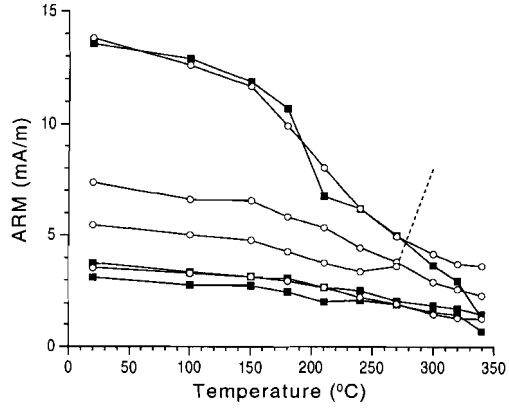


**Figure 13.** Thermal demagnetization of ARM. The increase at 300°C in one sample (dashed line) is accompanied by a considerable increase of $\chi_o$. Symbols as in figure 1c.

magnetite content, but this amount of magnetite remanence is not enough to explain the lower $H_{cr}$' values. The sulphide phase also seems to have lower $H_{cr}$' values than in other parts of the section. Such a difference can be produced by a different sulphide composition or by a larger grain size.

There are several possibilities to account for the anomalously high blocking temperatures of part of the sulphide remanence. One possibility is that partial oxidation may change the magnetic properties of pyrrhotite. Rochette et al. (1990) suggested oxidation could be the reason for the high maximum blocking temperatures (up to 350°C) observed in some monoclinic pyrrhotites. The magnetic ordering in pyrrhotite is dependent on its vacancy ordering and partial oxidation may hamper the redistribution of vacancies (Graham et al., 1987). On the other hand, the presence of other metal ions in the iron-sulphides may influence the Curie point. The Curie temperature of monoclinic pyrrhotite is slightly reduced by the presence of 1% Ni (Vaughan et al., 1971). A much larger amount of Ni-substitution was observed in the magnetic concentrates of the Vrica marls (van Velzen et al., 1993). The effects of such a large substitution on the magnetic properties and the Curie temperature of pyrrhotite are not known, nor the possible implications of the presence of Ni in other iron sulphides, like greigite.

The high blocking temperatures also suggest greigite ($Fe_3S_4$) is a possible contributor to the remanence. Greigites extracted from sediments of similar age and sedimentary environment as the Vrica marls seem to be thermally stable close to 400°C, at least in a nitrogen atmosphere (Snowball, 1991; Tric et al., 1991; Horng et al., 1992a; Roberts and Turner, 1993). Therefore, a similar greigite could also be the source of the maximum blocking temperatures between 330 and 375°C. Some of the sedimentary greigites in rapidly deposited Pliocene and Pleistocene marine sediments moreover have coercivities similar to those of the Vrica marls (Tric et al., 1991; Horng et al., 1992a; Roberts and Turner, 1993). Horng et al. (1992a) found that remanent coercivities in greigite-bearing layers (63-98mT) were on the average even higher than in pyrrhotite-bearing layers (51-88 mT), unlike the low coercivities for synthetic greigites. A review of the properties of greigite is given by Hoffmann (1992).

The fact that greigites with such different coercivities are found can be partly due to differences in grain size. The different thermal stabilities point to a more fundamental cause. The marine sedimentary greigites as well as other magnetic monosulphides may be very sensitive to the conditions of their formation. Depending on their formation history in their low-temperature environment they may be inhomogeneous or non-stoichiometric. In addition, they may have been subject to oxidation after uplift, when the reducing conditions were interrupted by meteoric water. All these circumstances will influence the vacancy distribution and oxygen content of the sulphides and consequently the magnetic properties and the thermal stability. Phase transitions and ordering temperatures during heating will also be influenced. For further discussion about this subject the reader is referred to chapter 7. Altogether it is likely that monoclinic pyrrhotite is one of the principle magnetic sulphide phases in these marls. Possibly non-stoichiometry, oxidation or

the presence of the relatively large amount of Ni in some sulphide grains are responsible for an increase of the Curie temperature. The sulphide remanence with blocking temperatures above 330°C, however, can also be carried by greigite. The possibility of inhomogeneous or mixed phases should also be considered.

### *6.2. Magnetite*

The $H_{cr}$ of the IRM carried by magnetite may be estimated by extrapolation of the $H_{cr}$ in figure 8 to lower IRM values. This yields a value of about 30-40 mT, somewhat below the lowest bulk remanent coercivities measured. This estimate is similar to $H_{cr}$ values reported for SD magnetite (e.g. Dunlop, 1986).

The magnetite in the marls may be of detrital origin or formed authigenically during an early stage of diagenesis. The redox conditions are favourable for the formation of magnetite, before the anoxic conditions for sulphate reduction are established (Karlin, 1990). In such conditions bacterially mediated, biogenic magnetite formation can occur as well (Lovley et al., 1987; Bazylinski et al., 1988). Although even in the sulphate reduction zone magnetite forming bacteria have been found (Sakaguchi et al., 1993), the detrital or authigenic magnetite starts to dissolve during prolonged sulphate reduction. The grain-size spectrum of the magnetite will first shift to larger grains, because the smaller grains are preferentially dissolved and then to smaller grains, when dissolution of the larger grains slowly reduces their size. Some magnetite apparently can survive the phase of sulphide formation, because the coexistence of magnetite and magnetic sulphides in sediments is common (e.g. Channel and Hawthorne, 1990; Hauger and Løvlie, 1992; Horng et al., 1992a,b; Torii et al., 1992; Mary et al., 1993). In the present study, a reliable NRM component after demagnetization up to 400°C could only be established in a few samples. Both normal and reversed directions were found for this magnetite component, excluding a recent origin of the magnetite.

### *6.3. The small scale variations*

The main magnetic carriers are sulphides which were formed authigenically. In this respect biogenic formation of magnetic sulphides by magnetotactic bacteria may be an important factor (Mann et al., 1990; Farina et al., 1990; Heywood et al., 1990). Magnetic sulphides have compositions in the range of monosulphides, which are intermediate products in a chain of reactions resulting in the formation of non-magnetic pyrite (Berner, 1984; Goldhaber and Kaplan, 1974). Whether intermediate phases are preserved depends on the presence of elemental sulphur or polysulphides, which are necessary for the reaction to pyrite (Middelburg, 1990; Mossmann et al., 1991). The limiting factor for the formation of elemental sulphur is the supply of oxidants. When reducing conditions are rapidly established, the supply of oxidants is limited, no elemental sulphur will be formed and monosulphides will not react to pyrite. Therefore, the amount of monosulphides can be determined by very local conditions like the availability of sulphate, iron and the

presence of organic material. The more easily metabolizable organic material disseminated throughout the sediment will have been exhausted after a relatively short time, whereas close to larger and less accessible organic particles reducing conditions may have favoured local sulphide formation and the preservation of a larger amount of monosulphides. An example of this replacement of organic material by sulphides was found in magnetic concentrates from the marls and analyzed with a microprobe (van Velzen et al., 1993). These processes can have been responsible for the local, small scale variations in NRM and rock magnetic properties occurring within a stratigraphic layer and even between specimens of one core.

### *6.4. Large-scale variations*

In contrast to the small-scale variations, the large-scale variations in the NRM intensities are likely influenced by long-term processes. Sedimentation rate and sedimentary input are important factors in the authigenic formation of sulphides. The availability of metabolizable organic matter and the porosity of the sediment influence the development of redox conditions shortly after deposition. The organic matter determines the reducing capacity and the porosity influences the transport of reactive agents.

The lithological variations in the Vrica marls are small. Between the sapropelitic layers the marls are quite homogeneous. Occasionally siltier layers occur. The average sedimentation rate between the midpoints of two consecutive sapropels can be calculated with the astronomically calibrated polarity time scale (Hilgen, 1991). The sedimentation rate at the bottom of the Vrica section appears to be higher than at the top (figure 1e, Hilgen et al., 1993; Lourens and Hilgen, in prep.). The changes in sedimentation rate have a similar pattern as the changes in paleoclimate indicated by temperature and humidity (Combourieu-Nebout, 1987; van der Weijden, 1993). The decrease of temperature and humidity coincides with the decrease in sedimentation rate below the Plio-Pleistocene boundary at sapropel *e*. The high sedimentation rate between sapropels *h* and *n* corresponds to a temporary increase of temperature and humidity. In this interval frequent thin sandy layers occur, that could explain the high sedimentation rate. Also the clay mineralogy shows a change below sapropel *e* (Combourieu-Nebout, 1987; van der Weijden, 1993). The smectite content, with 40-70% the most important clay mineral, varies in the same way as the NRM intensity: after a distinct drop close to the Plio-Pleistocene boundary it starts to recover higher in the section. Chlorite (20-30%), illite (30-40%) and kaolinite (10-20%) show a slightly increasing tendency above the boundary.

The drop in the NRM intensities occurs at sapropel *c*, just below the level where the first changes in sedimentation and climate occur. Goldhaber and Kaplan (1974; 1975) report that sedimentation rate in itself is an important factor in the preservation of intermediate (magnetic) monosulphides. More monosulphides are preserved when the sedimentation rate is high, because less elemental sulphur is

formed in the oxidizing conditions before burial or the availability of sulphate and sulphide is limited (Berner et al., 1979; Middelburg, 1990). Therefore the decrease in sedimentation rate above sapropel *c* may have been sufficient to cause the decrease in the amount of magnetic sulphides. The change in depositional conditions seems to have affected the magnetic minerals as deep as the top of sapropel *c*. The thick sapropel may have acted as a buffer, so that the changes did not affect deeper layers. Geochemical profiles show no major change in total Fe content in the marls above sapropel *c* (van der Weijden, 1993). Manganese does show a different profile above sapropel *c*. The Mn content increases in the homogeneous marls higher in the sediment column, while in the sapropels it stays the same as below sapropel *c*. One can only speculate how this may be related to the decrease in the amount of magnetic sulphides. It is likely, however, that the same change in climate that was the motive to locate the Pliocene-Pleistocene boundary at sapropel *e* is responsible for the decrease in NRM intensity at the top of sapropel *c*.

Another important factor are the sapropels themselves. During the deposition of sapropels conditions were anoxic, while generally the conditions were oxygenated (Howell et al., 1990; van der Weijden, 1993). It may therefore be more than a coincidence, that the NRM intensity reduction occurs in the middle of an interval with a number of very well developed, thick sapropels (*b*, *c*, *d* and *e*). The slightly different magnetomineralogy (lower coercivities) in the UO interval could be due to the fact that the marls are more silty in this particular interval. It causes a higher porosity which may induce a small change in grain sizes of the authigenic sulphides. Lower coercivities correspond with larger grain sizes.

Apart from processes during formation of the sulphides, also dissolution processes after uplift should be considered. Silty levels are more porous and accessible to meteoric water. Dissolution of magnetic sulphides would not only reduce the total IRM intensity, but would also produce a grain-size spectrum in which the smallest grains are underrepresented. This is an alternative explanation for the lower coercivities measured in the UO samples.

## 7. Conclusions

Rock magnetic properties indicate that magnetic iron sulphides are the main remanence carriers in the Vrica marls. Remanent coercivities ($H_{cr}$ and $H_{cr'}$) are similar to the values for monoclinic pyrrhotite (Clark, 1984; Dekkers, 1988; Menyeh and O'Reilly, 1991) and for greigite found in sediments of similar age as the Vrica section (Snowball, 1991; Horng et al. 1992a). Most of the remanence is thermally demagnetized in the temperature range where greigite becomes thermally unstable and below the Curie temperature of monoclinic pyrrhotite. The maximum blocking temperatures of this dominant remanence component (330-375°C) are remarkably high, however. Possibly the presence of oxygen in the sulphide crystal sustains the magnetic ordering of monoclinic pyrrhotite up to higher temperatures (Graham et al., 1987; Rochette et al., 1990). Alternatively, this remanence may be carried by greigite. Greigite was thought to be thermally

unstable below 300°C (Skinner, 1964; Uda, 1968; Coey et al., 1970; Spender et al., 1972), but some sedimentary greigites are reported to be thermally stable well above 300°C (Snowball, 1991; Tric et al., 1991; Horng et al., 1992a; Roberts and Turner, 1993). Differences in thermal demagnetization curves indicate a variation in magnetic sulphide content. Possibly both monoclinic pyrrhotite and greigite are present in varying proportion.

In the marls also some magnetite is present. The estimated contribution of magnetite to the total IRM is from 4% in samples with higher IRM intensities up to 40% in samples with lower IRM intensities. The absolute amount of magnetite is relatively constant. In the NRM the magnetite, when detected, carries a component with higher blocking temperatures than the sulphide remanence. This component is usually not observed, however, due to the low intensity and the spurious magnetizations occurring after heating above 350°C. The magnetite component likely predates the sulphide component.

Variations in remanence intensities are almost completely due to variations in magnetic sulphide content. Sulphides are formed authigenically and availability of metabolizable organic material and elemental sulphide governs the preservation of magnetic and non-magnetic monosulphides (Middelburg, 1990; Mossmann et al., 1991). Local variations in the conditions are likely responsible for the inhomogeneity of magnetic properties over short distances.

An abrupt decrease in NRM intensities occurs at sapropel *c*. The decrease seems to be related to the occurrence of a major change in climate, which was the reason to position the Pliocene-Pleistocene boundary at the top of sapropel *e*. A decrease in temperature and humidity already starting below sapropel *e* is related to a reduction in sedimentation rate. A lower sedimentation rate is accompanied by less preservation of monosulphides (Goldhaber and Kaplan 1974; 1975; Berner et al., 1979; Middelburg, 1990). The amount of magnetic monosulphides seems to be affected down to sapropel *c*. This thick sapropel apparently acted as a buffer against influence of the changing conditions to levels deeper in the sediment column. A change in the amount of magnetic sulphides rather than a change in sulphide mineralogy appears to be responsible for the decrease in NRM intensity. With the available data it was not possible to demonstrate a correlation between differences in magnetic properties and the subtle changes in lithology.

## References

Aguirre E. and Pasini G., The Plio-Pleistocene boundary. Episodes 8, 116-120, 1985.

Bazylinski D.A., Frankel, R.B. and Jannasch H.W., Anaerobic magnetite production by a marine, magnetotactic bacterium. Nature 334, 518-519, 1988.

Berner R.A., Baldwin T. and Holdren G.R.Jr., Authigenic iron sulfides as paleosalinity indicators. Jour. Sed. Pet. 49, 1345-1350, 1979.

Berner R.A., Sedimentary pyrite formation, An update. Geochem. Cosmochim. Acta 48, 605-615, 1984.

Channel J.E.T. and Hawthorne T., Progressive dissolution of titanomagnetites at ODP Site 653 (Tyrrhenian Sea). Earth Planet. Sci. Lett. 96, 469-480, 1990.

Clark D.A., Hysteresis properties of sized dispersed monoclinic pyrrhotite grains. Geophys. Res. Lett. 11, 173-176, 1984.

Coey J.M.D., Spender M.R. and Morrish A.H., The magnetic structure of the spinel $Fe_3S_4$. Solid State Commun. 8, 1605-1608, 1970.

Combourieu-Nebout N., Les premiers cycles glaciaires-interglaciaires en region Méditerranéenne d'après l'analyse palynologique de série Plio-Pleistocène de Crotone (Italie Méridionale). Thèse, l'Université des Sciences et Techniques du Languedoc. 161 pp., 1987.

Dankers P.H., Relationship between median destructive field and coercive forces for dispersed natural magnetite, titanomagnetite and hematite. Geophys. J. R. Astr. Soc. 64, 447-461, 1981.

Dekkers M.J., Magnetic properties of natural pyrrhotite Part I: Behaviour of initial susceptibility and saturation-magnetization-related rock-magnetic parameters in a grain-size dependent framework. Phys. Earth Planet. Int. 52, 376-393, 1988.

Dekkers M.J., Magnetic properties of natural pyrrhotite. Part II. High- and low-temperature behaviour of Jrs and TRM as function of grain size. Phys. Earth Planet. Inter. 57, 266-283, 1989.

Dunlop, D.J., Hysteresis properties of magnetite and their dependence on particle size: a test of pseudo-single-domain remanence models. J. Geophys. Res. 91, 9569-9584, 1986.

Farina M., Motta de Esquivel D. and Lins de Barros H.G.P., Magnetic iron-sulphur crystals from a magnetotactic microorganism. Nature 343, 256-258, 1990.

Goldhaber M.B. and Kaplan I.R., The sulfur cycle, in: The Sea. Vol. 5, Marine Chemistry, E. D. Goldberg, ed. pp. 569-655, Wiley, 1974.

Goldhaber M.B. and Kaplan I.R., Controls and consequences of sulfate reduction in recent marine sediments. Soil Sci. 119, 42-55, 1975.

Graham J., Bennet C.E.G. and van Riessen A., Oxygen in pyrrhotite: 1. Thermomagnetic behavior and annealing of pyrrhotites containing small quantities of oxygen. American Mineralogist 72, 599-604, 1987.

Hauger E. and Løvlie R., Palaeomagnetic characteristics of drill cores from Middle Jurassic delta plain sediments, the Brent Grouop, North Sea. Phys. Earth Planet. Int. 71, 74-84, 1992.

Heywood B.R., Bazylinski D.A., Garrat-Reed A., Mann S. and Frankel R.B., Controlled biosynthesis of greigite ($Fe_3S_4$) in magnetotactic bacteria. Naturwissenschaften 77, 536-538, 1990.

Hilgen F.J., Sedimentary rhythms and high-resolution chronostratigraphic correlations in the Mediterranean Pliocene. Newslett. Stratigr. 17, 109-127, 1987.

Hilgen F.J., Astronomical calibration of Gauss to Matuyama sapropels in the Mediterranean and implication for the Geomagnetic Polarity Time Scale. Earth Planet. Sci. Lett. 104, 226-244, 1991.

Hilgen F.J., Lourens L.J., Berger A. and Loutre L.J., Evaluation of the astronomically calibrated time scale for the late Piocene and earliest Pleistocene. Paleoceanography 8, 549-565, 1993.

Hoffmann V., Greigite ($Fe_3S_4$): magnetic properties and first domain observations. Phys. Earth Planet. Int. 70, 288-301, 1992.

Howell M.W., Rio D. and Thunell R.C., Laminated sediments from the Vrica section (Calabria, S. Italy): evidence for Plio-Pleistocene climatic change in the Mediterranean region. Palaeogeogr. Palaeoclimat. Palaeoecol. 78, 195-216, 1990.

Horng C.S., Laj C., Lee T.Q. and Chen J.C., Magnetic characteristics of sedimentary rocks from the Tsengwen-chi and Erhjen-chi sections in southwestern Taiwan. T. A. O. 3, 519-532, 1992a.

Horng C.S., Chen J.C. and Lee T.Q., Variations in magnetic minerals from two Plio-Pleistocene marine-deposited sections, southwestern Taiwan. J. Geol. Soc. China 35, 323-335, 1992b.

Karlin R., Magnetic mineral diagenesis in suboxic sediments at Bettis site W-N, NE Pacific Ocean. J. Geophys. Res. 95, 4421-4436, 1990.

Krs M., Novak F., Krsova M., Pruner P., Zeman A., Novak F. and Jansa J., A petromagnetic study of Miocene rocks bearing micro-organic material and the magnetic mineral greigite (Sokolov and Cheb basins, Czechoslovakia). Phys. Earth Planet. Int. 63, 98-112, 1990.

Lourens L.J. and Hilgen F.J., Pleistocene chronology and paleoceanography of the Plio/Pleistocene boundary stratotype at Vrica, in prep.

Lovley D.R., Stolz J.F., Nord G.L.Jr. and Phillips E.J.P., Anaerobic production of magnetite by a dissimilatory iron-reducing microorganism. Nature 330, 252-254, 1987.

Mann S., Sparks N.H.C., Frankel R.B., Bazylinski D.A. and Jannach H.W., Biomineralization of ferrimagnetic greigite ($Fe_3S_4$) and iron pyrite ($FeS_2$) in a magnetotactic bacterium. Nature 343, 258-261, 1990.

Mary C., Iaccarino S., Courtillot V., Besse J. and Aissaoui D.M., Magnetostratigraphy of Pliocene sediments from the Stirone River (Po Valley). Geophys. J. Int. 112, 359-380, 1993.

Menyeh A. and O'Reilly W., The magnetization process in monoclinic pyrrhotite ($Fe_7S_8$) particles containing few domains. Geophys. J. Int. 104, 387-399, 1991.

Middelburg J.B.M., Early diagenesis and authigenic mineral formation in anoxic sediments of Kau Bay, Indonesia. Ph. D. thesis University of Utrecht, pp. 177, 1990.

Mossmann J.-R., Aplin A.C., Curtis C.D. and Coleman M.L., Geochemistry of inorganic and organic sulphur in organic-rich sediments from the Peru Margin. Geochim. Cosmochim. Acta 55, 3581-3595, 1991.

Özdemir Ö., Dunlop D.J. and Moskowitz B.M., The effect of oxidation on the Verwey transition in magnetite. Geoph. Res. Lett. 20, 1671-1674, 1993.

Roberts A.P. and Turner G.M., Diagenetic formation of ferrimagnetic iron sulphide minerals in rapidly deposited marine sediments, South Island, New Zealand. Earth Planet. Sci. Lett. 115, 257-273, 1993.

Rochette P., Metamorphic control of the magnetic mineralogy of black shales in the Swiss Alps: toward the use of "magnetic isograde". Earth Planet. Sci. Lett. 84, 446-456, 1987.

Rochette P., Fillion G., Mattéi J.-L. and Dekkers M.J., Magnetic transition at 30-34 Kelvin in pyrrhotite: insight into a widespread occurrence of this mineral in rocks. Earth Planet. Sci. Lett. 98, 319-328, 1990.

Sakaguchi T., Burgess J.G. and Matsunaga T., Magnetite formation by a sulphate-reducing bacterium. Nature 365, 47-49, 1993.

Scheepers P.J.J., van Dijk J.P., Langereis C.G., Zijderveld J.D.A., Hilgen F.J. and Raffi I., Paleomagnetic results from Neogene sediments of northern Calabria (Crotone and Crati basins): additional support for the middle Pleistocene 15° clockwise rotation phase of the Calabro-Peloritan block. In Thesis University of Utrecht, 175-208, 1994.

Scheepers P.J.J. and Langereis C.G., Magnetic fabric of Pleistocene clays from the Tyrrhenian arc: a magnetic lineation induced in the final stage of the middle Pleistocene compressive event. Tectonics, in press.

Schwarz E.J., Magnetization of Precambrian sulphide deposits and wall rocks from the Noranda district, Canada. Geophysics 31, 797-802, 1966.

Schwarz E.J., Magnetic properties of pyrrhotite and their use in applied geology and geophysics. Geol. Surv. Can., Pap. 74-59, 24 pp., 1975.

Schwarz E.J. and Vaughan D.J., Magnetic phase relations of pyrrhotite. J. Geomagn. Geoelectr. 24, 441-458, 1972.

Selli R., Accorsi C.A., Bandini Mazzanti M., Bertolani Marchetti D., Bigazzi G., Bonadonna F.P., Borsetti A.M., Cati F., Colalongo M.-L., d'Onofrio S., Landini W., Menesini E., Mezzeti R., Pasini G., Savelli G. and Tampieri R., The Vrica section (Calabria). A potential Neogene-Quarternary boundary stratotype. Giorn. Geol. 41, 181-204, 1977.

Skinner B.J., Erd R.C. and Grimaldi F.S., Greigite, the thio-spinel of iron; a new mineral. American Mineralogist 49, 543-555, 1964.

Snowball I.F., Magnetic hysteresis properties of greigite ($Fe_3S_4$) and a new occurrence in Holocene sediments from Swedish Lappland. Phys. Earth Planet. Int. 68, 32-40, 1991.

Soffel H.C., Domain structure of natural fine-grained pyrrhotite in a rock matrix (diabase). Phys. Earth Planet. Inter. 26, 98-106, 1981.

Spender M.R., Coey J.M.D. and Morrish A.H., The magnetic properties and mössbauer spectra of synthetic samples of $Fe_3S_4$. Can. J. Phys. 50, 2313-2326, 1972.

Tauxe L., Opdyke N.D., Pasini G. and Elmi C., Age of the Plio-Pleistocene boundary in the Vrica section, southern Italy. Nature 304, 156-158, 1983.

Thomson G.F., The anomalous demagnetization of pyrrhotite. Geophys. J. Int. 103, 425-430, 1990.

Torii M., Hayashida A., Vigliotti L. and Wippern J., Rock magnetic properties of sediments from site 797, Japan Sea. Proc. ODP 127/128, 947-957, 1992.

Tric E., Laj C., Jéhanno C., Valet J.P., Kissel C., Mazaud A. and Iaccarino S., High-resolution record of the Upper Olduvai transition from Po Valley (Italy) sediments: support for dipolar transition geometry?. Phys. Earth Planet. Inter. 65, 319-336, 1991.

Uda M., Synthesis of magnetic $Fe_3S_4$. Sci. Pap. Inst. Phys. Chem. Res. (Jpn) 62, 14-23, 1968.

Vaughan D.J. and Craig J.R., Mineral Chemistry of Metal Sulfides, 493 pp., Cambridge University Press, Cambridge, 1978.

Vaughan D.J. and Ridout M.S., Mössbauer studies of some sulphide minerals. J. Inorg. Nucl. Chem. 33, 741-746, 1971.

van Velzen A.J., Dekkers M.J. and Zijderveld J.D.A., Magnetic iron-nickel sulphides in the Pliocene and Pleistocene marine marls from the Vrica section (Calabria, Italy). Earth Planet. Sci. Lett. 115, 43-55, 1993.

van der Weijden C.H., Geochemical signatures preserved in sediments of the Semaforo and Vrica sections (Calabria, Italy) and their relations with variations of the sedimentary regime. Palaeogeogr. Palaeoclimat. Palaeoecol. 103, 203-221, 1993.

Zijderveld J.D.A., Hilgen F.J., Langereis C.G., Verhallen P.J.J.M. and Zachariasse W.J., Integrated magnetostratigraphy and biostratigraphy of the upper Pliocene-lower Pleistocene from the Monte Singa and Crotone areas in Calabria, Italy. Earth Planet. Sci. Lett. 107, 697-714, 1991.

# 7 Thermal alteration of magnetic sulphides in marine marls from the Vrica section and the influence on the demagnetization of the natural remanent magnetization


## Abstract

The magnetic sulphides in the marine marls from the Vrica section (Calabria, Italy) are subject to several alterations during heating. The influence of these alterations on the thermal demagnetization of the natural remanent magnetization (NRM) prompted a detailed investigation. The alterations are studied with the so-called IRM monitoring method (see van Velzen and Zijderveld, 1992) and by thermomagnetic analysis of sediment samples and magnetic concentrates. Thermomagnetic analysis was performed in air and in argon.

An alteration observed with the IRM monitoring method in standard paleomagnetic samples between 150 and 250°C is suggested to be related to the $\gamma$-transition typical of hexagonal pyrrhotite. In this temperature interval NRM demagnetization diagrams often show aberrant behaviour. During thermomagnetic analysis in an argon atmosphere the alteration is observed at about 190°C and in air at about 230°C. The presence of oxygen in the sulphide (e.g. a slightly oxidized surface layer) may enhance the $\gamma$-transition temperature. The observed high maximum blocking temperatures (higher than the 325°C typical of monoclinic pyrrhotite) could be explained in a similar fashion. Similar high blocking temperatures are also reported for greigite. The observed magnetic behaviour is more in agreement, however, with a mixture of hexagonal and monoclinic pyrrhotite than indicative of greigite. Both minerals may be present in the Vrica marls.

A chain of alteration reactions starting at about 350°C and causing spurious magnetizations during thermal demagnetization of the NRM was attributed to the oxidation of iron sulphides to grains with magnetite-like properties, eventually leading to the formation of hematite. The IRM monitoring method shows that magnetite formation mainly yields grains with alternating field (AF) coercivities $<50$ mT. Hematite formation is characterized by AF coercivity fractions $>100$ mT.


## 1. Introduction

In paleomagnetism, stepwise thermal demagnetization is a routine technique to separate the various components of the natural remanent magnetization (NRM). Especially in sediments, thermal demagnetization is often more effective than alternating field (AF) demagnetization. The disadvantage of thermal demagnetization, however, is the occurrence of thermal alterations. During the consecutive heating steps to increasingly higher temperatures the magnetic minerals in which the NRM

resides, may be destroyed or new magnetic minerals may be formed from non-magnetic or magnetic precursors.

The magnetomineralogy of the marine marls in the Vrica section is dominated by sulphides as was shown in a rock magnetic study (chapter 6) and a microprobe study of magnetic concentrates (van Velzen et al., 1993). In sulphide-bearing sediments thermal alterations are expected when the sediment is heated above 300°C. Monoclinic pyrrhotite ($Fe_7S_8$) will start to oxidize at that temperature (Dekkers, 1990) in a first step to the formation of magnetite and, finally, hematite at higher temperatures. Greigite ($Fe_3S_4$), another magnetic sulphide, is reported to be thermally unstable well below 300°C (Skinner, 1964; Uda, 1968; Coey et al., 1970; Spender et al., 1972). Greigite identified in various sediments, however, was shown to be stable above 300°C (Snowball, 1991; Tric et al., 1991; Horng et al.,1992; Roberts and Turner, 1993). A reliable Curie point of this sedimentary greigite could not be established.

Magnetic transitions in sulphides should also be considered when studying the impact of heating on the NRM. The $\gamma$-transition in hexagonal pyrrhotite is reported between 170 and 220°C (Schwarz, 1975; Vaughan and Craig, 1978). A reordering of vacancies in the sulphide yields a more magnetic pyrrhotite phase. Finally, non-magnetic pyrite, which is the most common iron sulphide in sediments, oxidizes to a magnetic phase with magnetite-like properties above 350°C (van Velzen and Zijderveld, 1992; Mullender et al., 1993). The formation of these alteration products of pyrite may cause spurious magnetizations and viscous behaviour in magnetic fields.

It is commonly thought that up to 300°C chemical alterations do not interfere with thermal demagnetization results. It was recently shown, however, that heating to temperatures as low as 150°C may already produce irreversible changes in slightly weathered magnetite grains (van Velzen and Zijderveld, 1992). The present study of the Pliocene-Pleistocene Vrica marls also documents alterations starting below 200°C. Here, magnetic sulphides are involved. The alterations influence the NRM behaviour during routine stepwise thermal demagnetization. The method described in van Velzen and Zijderveld (1992) is used to study the thermal alterations of the magnetic sulphides. These results are compared with thermomagnetic analysis of the sediment and of magnetic concentrates from the sediment.

## 2. Magnetic characteristics of the Vrica section

The Vrica section is situated in the Crotone-Spartivento basin of northern Calabria, Italy. It was formally designated as the Neogene-Quarternary boundary stratotype (Aguirre and Pasini, 1985). The section, divided in subsections Vrica A, B and C, consists of homogeneous open-marine marls intercalated with laminated sapropelitic layers. Numerous studies have been devoted to the Vrica section. Magnetostratigraphic studies demonstrated the presence of the complete Olduvai subzone in the composite section (Tauxe et al., 1983; Zijderveld et al., 1991). The

complex demagnetization behaviour of the NRM in many samples showed the necessity of a rock magnetic study (chapter 6) and in particular a study of the thermal alterations in the marls. In most samples above 350°C spurious magnetizations and viscous behaviour disturb the thermal demagnetization of the NRM (figure 1). This is caused by the formation of new magnetic grains. Up to 350°C many samples have a straightforward demagnetization behaviour (figure 1a), but a large number of samples shows complex behaviour in the temperature range between 150 and 330°C (figure 1b). Thermal alterations could be the cause for this. Heating and cooling the samples in vacuum did not improve the results (figure 1d). On the contrary, the spurious behaviour, usually occurring above 350°C, seemed to start at lower temperatures.

Rock magnetic properties (chapter 6) and a microprobe study of magnetic concentrates (van Velzen et al., 1993) indicate that the majority of the remanence

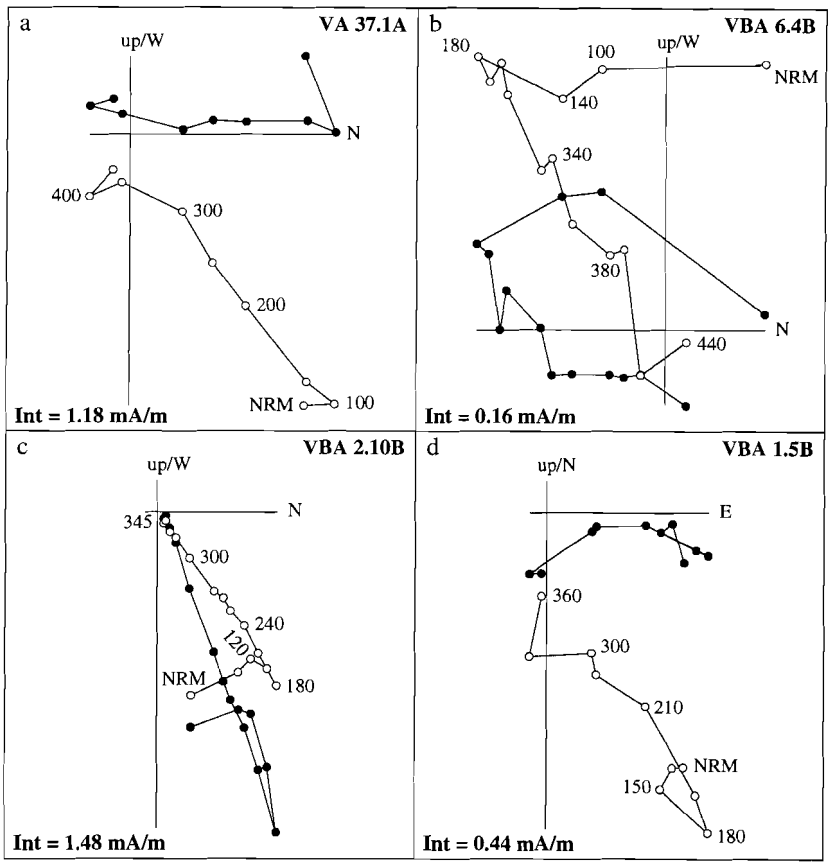


**Figure 1.** Stepwise thermal demagnetization of samples from the Vrica section. Examples a, b and c were heated in air, example d in vacuum. Closed (open) symbols are horizontal (vertical) projections, respectively. Temperatures in °C. Int = initial NRM intensity.

is carried by magnetic sulphides, but it could not be established by which kind of sulphide. The coercive forces are similar to those of monoclinic pyrrhotite, but the maximum blocking temperatures are higher than the Curie temperature of stoichiometric monoclinic pyrrhotite (305-325°C; Schwarz and Vaughan, 1972; Schwarz, 1975; Vaughan and Craig, 1978; Dekkers, 1989). There are indications that the Curie temperature of pyrrhotite can be higher (Rochette et al., 1990), possibly due to impurities, like oxygen.

Greigite could also carry (part of) the remanence in the present marls. The low coercive forces and the thermal instability that are generally reported for synthetic greigite argue against this sulphide as important remanence carrier. Greigites recently identified in various sediments, however, have higher coercive forces than synthetic greigites. These sedimentary greigites also are thermally more stable (Snowball, 1991; Tric et al., 1991; Krs et al., 1992; Horng et al., 1992; Roberts and Turner 1993). Therefore, observed rock magnetic properties would allow both monoclinic pyrrhotite and these sedimentary greigites as remanence carriers in the Vrica marls.

The microprobe study of magnetic concentrates from the Vrica marls (van Velzen et al., 1993) revealed a large number of sulphide grains with a large compositional range. Their sulphur content varies between that of pyrite ($FeS_2$) to that of pentlandite ($(Fe,Ni)_9S_8$). Moreover a high nickel content was observed in many grains, ranging from a few % to 35%.

### 3. Sampling and methods

For the present study, samples were chosen from different parts of the section. Samples from site VBA1 have a relatively high NRM intensity. They are taken from the Olduvai subzone. Sites VBA6 and 7 are situated above the Olduvai subzone in an interval with distinctly lower NRM intensities (cf. chapter 6). Care was taken to obtain samples as fresh as possible. The weathered surface was removed to reach blue-grey marls. Samples from VBA1 and VBA7 were used for the thermal alteration study. Magnetic concentrates were made of sediment from VBA1 and VBA6. Two magnetic concentrates were obtained from each sediment sample with a Frantz isodynamic separator (see van Velzen et al., 1993). First the minerals with the strongest magnetization were extracted with low magnetic fields. Then, with higher magnetic fields, the remaining magnetic fraction was extracted. In both concentrates clay minerals still are abundant.

Samples for the thermal alteration study were heated and cooled in a laboratory-built thermal demagnetizer with triple mu-metal shielding. Heating times were chosen to let the samples spend 5 to 10 minutes at the intended temperature, allowing for their thermal inertia. Temperatures are accurate up to ±2°C. Isothermal remanent magnetizations (IRM) were induced in DC coils. Stationary AF demagnetization was performed in AC coils in three orthogonal directions. Remanences were measured with a digitized Jelinek spinner magnetometer, based on the JR3 drive unit. A 2G cryogenic magnetometer (type 740 R) was used for NRM

measurements. Low-field susceptibilities were measured on a KLY-2 susceptibility bridge. Thermomagnetic analyses were performed with the improved horizontal translation Curie balance described in Mullender et al. (1993).

## 4. Magnetic monitoring of thermal alterations

The low-field or initial susceptibility $\chi_0$ is commonly used to monitor alterations of magnetic minerals during stepwise thermal demagnetization. This parameter, however, may not always be sensitive enough, in particular when only a minor part of $\chi_0$ is due to ferromagnetic minerals. An IRM, induced in the samples after every heating step, represents the remanence carrying minerals much better. In samples from site VBA1 and VBA7 both $\chi_0$ and the IRM show a large increase, which starts above 350°C and is most pronounced between 420 and 480°C (figures 2 and 3). The alterations causing the increase of the IRM at 150 and 200°C and the subsequent decrease above 300°C go unnoticed, however, when only $\chi_0$ is measured.

Van Velzen and Zijderveld (1992) suggested a method to monitor alterations of magnetic minerals during stepwise thermal demagnetization in more detail. The IRM that is induced after every heating step (and that will be referred to as the 'total IRM') is divided in six coercivity fractions using stepwise alternating field (AF) demagnetization. The selected demagnetization steps are 10, 25, 50, 100 and 300 mT. In this way changes in different coercivity fractions can be monitored separately, in the course of the stepwise thermal demagnetization. In addition, the IRM remaining after each heat treatment (referred to as the 'remaining IRM') and its coercivity fractions are measured. This remaining IRM represents the part of the total IRM with blocking temperatures higher than the

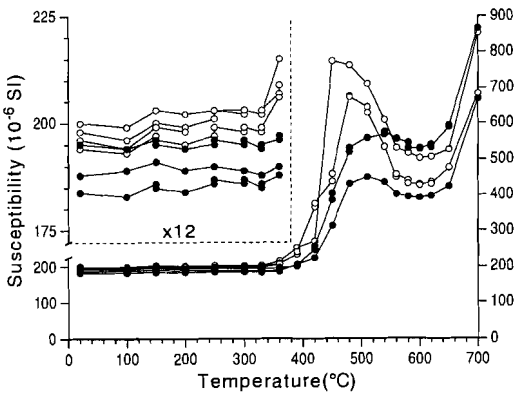


**Figure 2.** Changes in initial susceptibility $\chi_0$ during stepwise thermal demagnetization. Samples from VBA1 (open symbols) and VBA7 (closed symbols).

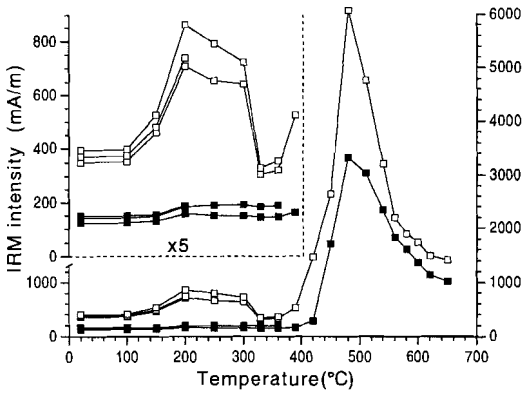


**Figure 3.** Changes in total IRM. Symbols as in figure 2.

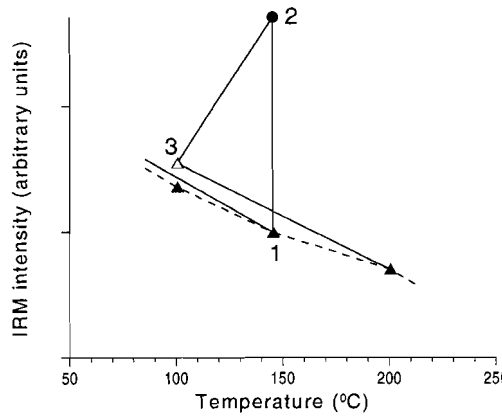


**Figure 4.** Schematic measuring cycle for the study of thermal alterations with the IRM monitoring method (Van Velzen and Zijderveld, 1992). The method is based on a stepwise thermal demagnetization of an IRM. After every heating, first the remaining IRM and its AF coercivity spectrum are determined (1). An new IRM is induced in the sample in the same direction as the original one. This total IRM and its AF coercivity spectrum are measured (2). Finally, the part of this IRM remaining after a control heating at the temperature of the previous temperature step is measured (3). The next step starts at the beginning of the measuring cycle at a higher temperature. The dashed line indicates the apparent decay curve, which will deviate from a normal decay curve because of the repeated IRM acquisition.

last heating step. In figure 4 a schematic representation of the complete cycle of measurements after each heating step is shown. This cycle also includes, after the acquisition of the total IRM, a control heating to the temperature of the previous heating step, followed by measurement of the remanence. For a complete description of the method the reader is referred to van Velzen and Zijderveld (1992). In this chapter it is referred to as the 'IRM monitoring method'. The results of all IRM measurements in the course of the procedure for the two sites of this study are given in figure 5. The initial part of the thermal decay curves of two samples only subjected to routine stepwise thermal demagnetization are included in the figure, for comparison.

## 5. Alterations at temperatures higher than 350°C

The $\chi_0$ increase above 350°C is well known in sulphide-bearing sediments. It is caused by magnetite-like grains formed from iron sulphides, like pyrite. A modest increase in $\chi_0$ is observed in the carbonate-rich sediments of the early Pliocene Trubi formation (van Velzen and Zijderveld, 1992). Sulphides are much more abundant in the present sediment. The formation of the new magnetic phases above 350°C is accordingly more prominent.

The alteration process of samples from site VBA1 and site VBA7 is essentially the same. The maximum in total IRM for VBA7, the site with the lower remanence intensities (and apparently lower sulphide content), is reached at a slightly higher temperature and it is less extreme (see figure 3).

*5.1. Changes in coercivity fractions of the total and remaining IRM*

Figure 6 shows the development of the separate coercivity fractions of the total IRM and of the remaining IRM. For the total IRM (figure 6a,b), initially only the low-coercivity fractions (<50 mT) increase above 350°C, reaching a maximum at 480°C. This maximum is a multiple of the original intensity. The 50-100 mT fraction shows a similar behaviour, but much less pronounced.

The blocking temperatures of the newly formed magnetic grains can be deduced from the coercivity fractions of the remaining IRM after each heating (figure 6c,d) and from the control heatings (figure 5). The small increase of the remaining IRM compared to the total IRM indicates that the blocking temperatures of the magnetite-like mineral formed between 350 and 500°C, are to a large extent (>95%) below the formation temperature. For instance after the heating at 480°C, the total IRM that can be induced in the sample shows its largest increase. The subsequent control heating at 450°C, however, removes most of the remanence of the newly formed magnetic grains. They apparently have blocking temperatures lower than 450°C. The part of this IRM surviving after the next heating step at 510°C, is even smaller. Figures 6c and 6d show that the coercivities of this remaining IRM are typically not below 10 mT, but mainly between 10 and 100 mT. It should be noted, however, that the thermal removal of remanence after heating at 510°C is not only due to unblocking. The magnetite-like mineral starts to alter to hematite, as can be deduced from the distinct increase of the >300 mT fraction that occurs at 510°C. The hematite formation starts at lower temperatures, but at 510°C the conversion of magnetite to hematite becomes more important than the formation of new magnetite, causing a decrease of total IRM. The low-coercivity fractions (<50 mT) of the total IRM consistently decrease until the last heating step, while the 50-100 mT fraction shows the combined effects of the decreasing low-coercivity fractions and increasing hematite fractions. After the 650°C heating step most of the low-coercivity IRM has vanished.

*5.2. Formation of a magnetite-like mineral*

The increase of the fractions with the lowest coercivities agree with the growth of submicron magnetite-like grains by oxidation of pyrite during prolonged heating (Nguyen and Pechersky, 1987). New magnetite grains are nucleated in different spots and develop simultaneously until the sulphide is completely oxidized. The lowest coercivities correspond to the smallest grains just above the superparamagnetic (SP) threshold size and the 50-100 mT fraction represents larger grains, which are magnetically more stable. The relatively low blocking temperatures of most of the grains agree with magnetite in the single (SD) size range just larger than SP grain size.

It is not likely that the new magnetic phase is stoichiometric magnetite. It starts to convert to hematite below 450°C, as indicated by the increase of the

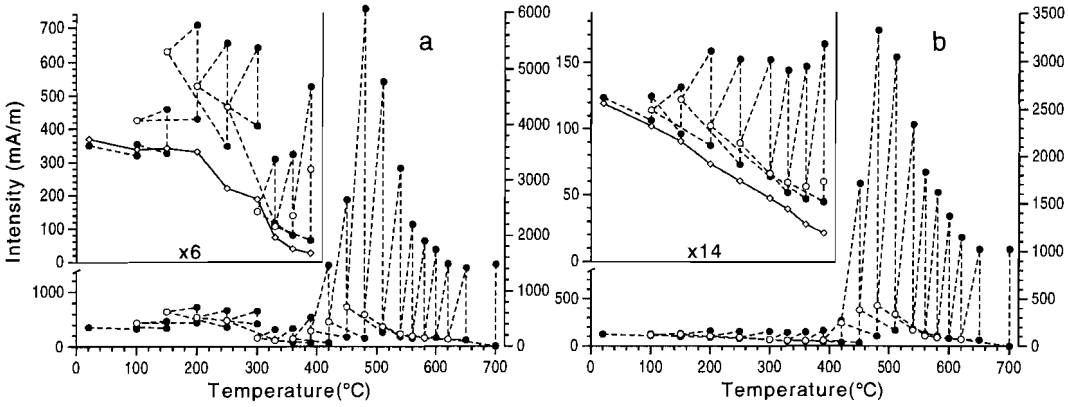


**Figure 5.** The measurement cycle of figure 4 repeated at every step of a thermal demagnetization procedure. Samples are from site VBA1 (a) and from site VBA7 (b). Closed circles are remaining IRM and (newly induced) total IRM. Open circles are control measurements. For each site the normal decay curve of another sample, obtained without the repeated IRM induction, is given for comparison in the low-temperature part of the curves (diamonds).

>300mT and the 100-300 mT fraction. The thermal instability of the magnetic grains points to a partly oxidized magnetite. There is no evidence for the formation of $\eta$-$Fe_2O_3$ (Levy and Quemeneur, 1968) as found by Krs et al. (1992) after thermal treatment of greigite at similar temperatures. This iron oxide is highly magnetic and it is reported to be thermally stable up to 700°C.

### *5.3. Aspects of the hematite formation*

The formation of the cation-deficient magnetite is relatively straightforward, its further oxidation to hematite, however, has several complex aspects. The increase of the two >100 mT fractions starts soon after the first magnetite is formed (above 450°C, figure 6a,b). The >300 mT fraction of the total IRM keeps increasing until the last heating at 650°C. The decrease of the >300 mT coercivity fraction of the remaining IRM in this temperature range is due to the approach of the hematite Curie temperature. The 100-300 mT fraction of the total IRM, which shows a similar behaviour as the >300 mT fraction, remains relatively small in the remaining IRM. Apparently, it has lower blocking temperatures than the >300 mT fraction. This likely is a 'grain size' effect: the fraction presumably consists of small hematite grains with relatively low coercivities and relatively low blocking temperatures (e.g. Néel, 1949; Stokking and Tauxe, 1987).

The $\chi_0$ increase above 620°C (figure 2) seems to be at odds with the relatively constant total IRM (figure 5a,b) and the conversion of the cation-deficient magnetite to hematite. It can be made plausible, however, if the conversion reaction of the magnetite-like grains to hematite is not completed (cf. van Velzen

and Zijderveld, 1992). The conversion of magnetite to hematite proceeds from the outside of a grain to the inside, possibly subdividing grains. If it stops before the conversion is completed (cf. Heider and Dunlop, 1987), it leaves tiny grains with a cation-deficient core and a hematite shell. If the core is sufficiently small, it will be superparamagnetic, i.e. unable to carry a stable remanence, but strongly contributing to the susceptibility. The still substantial soft remanence left after the 650°C step (figure 6a,b) may reside in somewhat larger remaining cation-deficient cores.

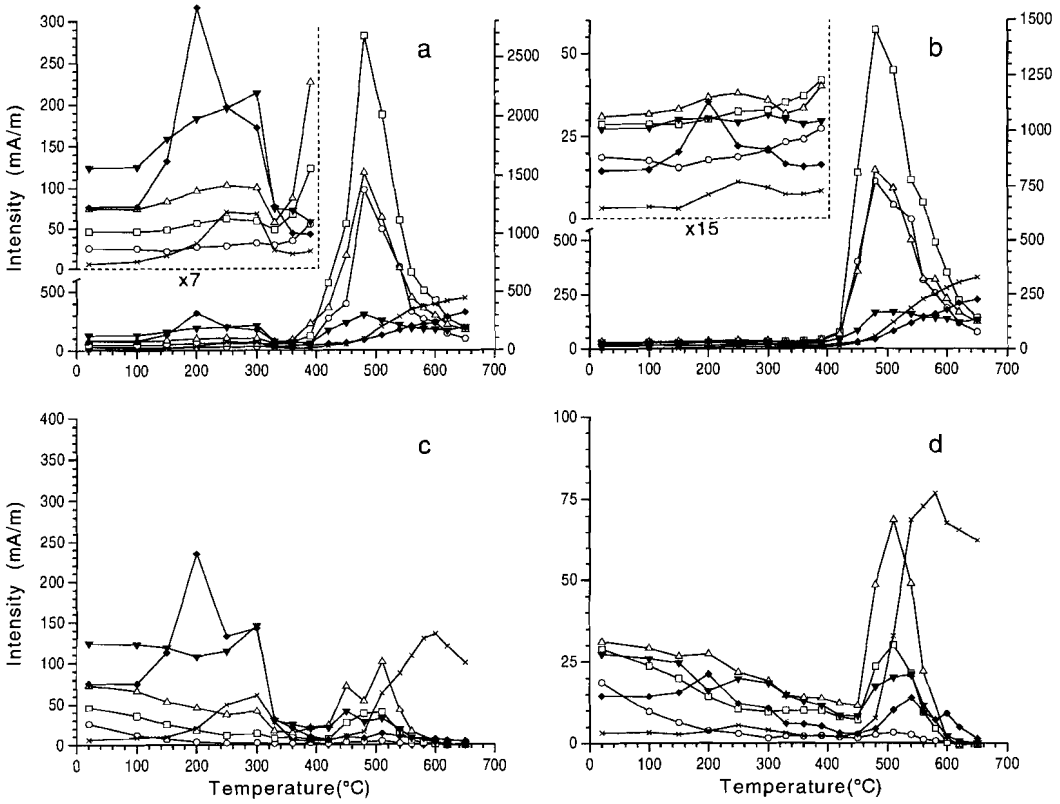


**Figure 6.** AF coercivity fractions of IRM(1.5 T).
(a,b) AF coercivity fractions of the IRM induced after every temperature step for sample VBA1.6A and VBA7.3B, respectively (total IRM, cf. figure 3).
(c,d) AF coercivity fractions of the part of the IRM remaining after every heating step for the same samples.
(a,b) represent the total IRM, (c,d) only the IRM with blocking temperatures higher than the heating temperature.

## 6. Alterations at temperatures between 150 and 350°C

The alterations below 350°C are of a different nature than the oxidative grain growth process above 350°C. The alteration is more subtle and not apparent from changes in $\chi_0$ (figure 2). Also the changes in total IRM are small compared to the changes above 350°C (figure 3). After heating at 200°C the total IRM doubles in VBA1 whereas the increase in total IRM is only 25% for VBA7. These changes are still significant, however, and the influence of this alteration on the NRM is just as important (see section 9). The alterations are essentially the same for both sites. In the following the changes in VBA1 will be discussed, because they are more evident those than in VBA7.

### *6.1. Changes in coercivity fractions of the total and remaining IRM*

In contrast to the alteration above 350°C, not the lowest coercivity fractions, but the >50 mT fractions are responsible for the rise in total IRM after heating at 150 and 200°C (figure 6a). The 100-300 mT fraction shows the largest increase, followed by a decrease at the subsequent heating steps at 250, 300 and 330°C. The 50-100 mT fraction increases in a more gradual manner up to 300°C, before collapsing at 330°C. The largest increase of the >300 mT fraction occurs at 250°C and its largest decrease at 330°C.

As mentioned before, the blocking temperatures of the original as well as the new remanence can be deduced from the control heatings and from the coercivity spectrum of the part of the newly induced total IRM at the next heating step. Comparison of the coercivity fractions of the total and remaining IRM for each temperature step shows that the blocking temperatures of the <50 mT fractions partly lie in the 100-250°C range (figure 6a,c). The higher-coercivity fractions also have blocking temperatures in this range, but a significant part of that remanence has blocking temperatures higher than 300°C. The >300 mT remanence, which is almost completely formed by alteration, hardly unblocks below 300°C.

When the control heatings are considered, the phenomenon can be further substantiated. The control heating at 100°C after the 150°C step shows that a large part of the new remanence has blocking temperatures higher than 100°C (figure 5a). The next heating is at 200°C and one would expect the remanence to decrease, because the remanence of grains with blocking temperatures between 100 and 200°C must be randomized. In contrast, the remanence seems to remain unchanged (figure 5a). In fact even a small remanence increase occurs. This likely is an effect of the alteration which causes the increase of total IRM. Comparison of the coercivity fractions of the total IRM induced after the 150°C heating step and the remaining IRM after the 200°C step (figures 6a,c) shows that this is not a marginal effect. The two >100 mT fractions of the total IRM induced after the 150°C heating increase during the heating at 200°C. The 100-300 mT fraction increases no less than 75%. Figures 6a and 6c also show that this coercivity fraction had already increased in a similar way in during the heating at 150°C.

After heating to 330°C, a distinct decrease of total IRM show that magnetic minerals are altered to non- or less magnetic phases. All three coercivity fractions between 25 and 300 mT decrease to values lower than their values before any thermal treatment. This indicates that not only the newly formed magnetic phase is affected by this alteration, but also the original remanence carriers. This conclusion has important implications: above 300°C the thermal decay of an IRM induced in an unheated sample and treated with normal stepwise thermal demagnetization is partially due to alteration of remanence carriers.

After heating at 360°C the alteration continues, as evidenced by the continuing decrease of the >50 mT coercivity fractions. The behaviour of the <50 mT fractions is difficult to evaluate, because they are already influenced by the formation of the magnetite-like mineral that becomes apparent at this temperature.

*6.2. IRM behaviour during routine thermal demagnetization*

In a routine stepwise thermal demagnetization of an IRM the remanence is only induced once, before the first heating step. The procedure used in the previous paragraphs required the acquisition of a new IRM after every heating step. To study the effect of the alteration at 150 and 200°C during normal thermal demagnetization a number of specimens from site VBA1 was given an IRM and subjected to routine thermal stepwise demagnetization (figure 7). In one specimen an IRM(1.5 T) was induced along one of the orthogonal specimen axes (the b-axis) and subsequently partly AF demagnetized with 50 mT along all three axes, leaving only the coercivity fractions that showed a distinct increase at 150°C and 200°C. The thermal decay curve of this remanence (figure 7a) indeed shows an increase at 150°C. The remanence increase is only in the same direction as the existing remanence. In another specimen an IRM(1.5 T) was induced along the a-axis and subsequently an IRM(60 mT) along the perpendicular b-axis (figure 7b), similar to the method introduced by Lowrie (1990). The remaining high-coercivity remanence along the a-axis behaves in the same way as the IRM of the first specimen (figure 7a). 0The low-coercivity IRM(60 mT) decreases almost linearly up to 300°C. Both the high- and the low-coercivity IRM is carried by magnetic sulphides and magnetite, as indicated by the two-phase thermal decay.

In two other samples the coercivity fractions of the IRM were measured before and after thermal demagnetization up to 200°C. Figure 7c shows the AF demagnetization of an IRM(1.5 T) with 50 mT AC fields and the subsequent thermal demagnetization at 100, 150 and 200°C. After these treatments the remaining IRM is harder than the original total IRM (cf. the remanences after 100 mT AF in figure 7c). Finally, the AF coercivity spectrum of an IRM(60 mT) after heating at 200°C (figure 7d) indicates that some higher-coercivity remanence has developed parallel to this low-coercivity IRM, but to a much lesser degree. After applying alternating fields of 100 mT, still part of the remanence remains.

In all cases the IRM remanence increase upon heating occurred at 150°C. The increase was only in the direction of the existing IRM, mainly coupled to the high-coercivity fractions (>50 mT) of the IRM. Apparently, it really is an increase of remanence of these IRM fractions, rather than the formation of a new high-coercivity mineral phase. With the IRM monitoring method the maximums of the

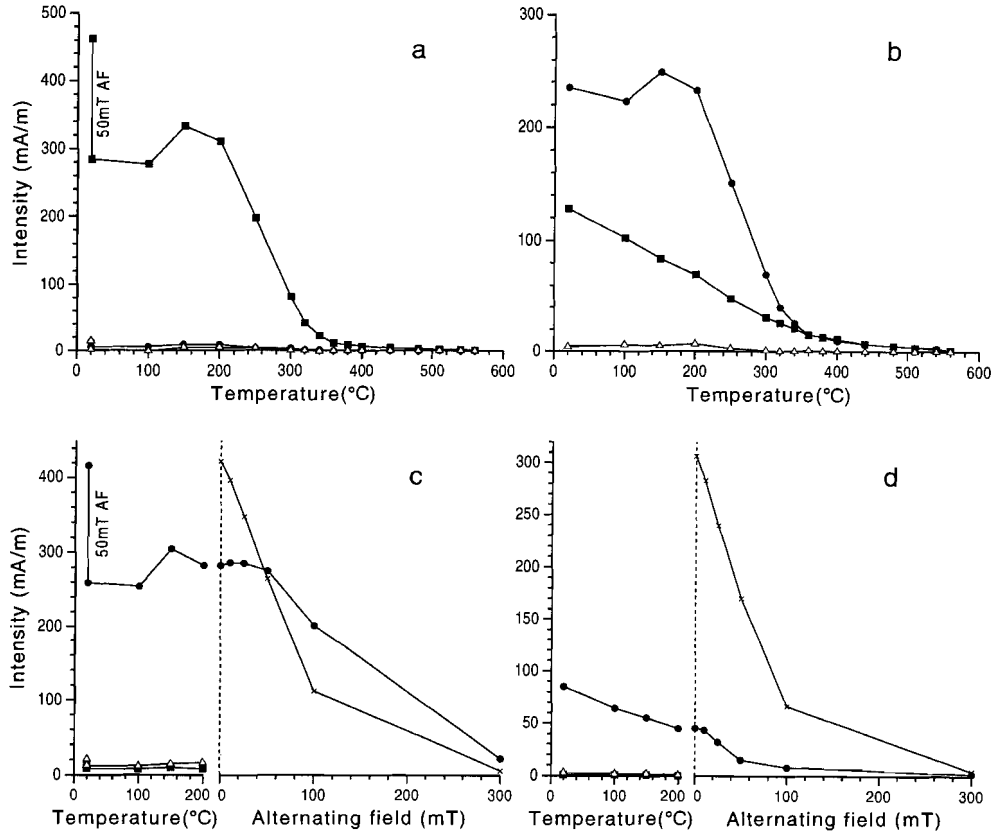


**Figure 7.** Thermal decay curves of partial IRMs. The complete remanence vectors were measured: the three remanence components along the orthogonal a-, b- and c-axis of the specimen are represented by circles, squares and triangles, respectively. The experiments show that the new remanence is formed in the direction of the existing remanence. AF demagnetization was performed in three orthogonal directions.
(a) IRM(1.5 T) after 50 mT AF demagnetization.
(b) IRM(1.5 T) along the a-axis combined with IRM(60 mT) along the b-axis.
(c) Thermal demagnetization of IRM(1.5 T) after 50 mT AF, up to 200°C. The subsequent AF demagnetization of the remaining remanence shows more > 50 mT remanence than the AF demagnetization of the original IRM(1.5 T) before heating (crosses).
(d) Thermal demagnetization of IRM(60 mT) up to 200°C. AF demagnetization of the remaining remanence shows some high-coercivity remanence. Crosses show AF demagnetization of original IRM(1.5 T) before heating.

total IRM and of the remaining IRM were observed after the 200°C step. This higher temperature is due to the repeated IRM acquisition used in that method. With the IRM monitoring method the alteration of the magnetomineralogy is observed. In the routine thermal demagnetization experiments the combined change due to this alteration and the thermal decay of the remanence during heating is observed.

## 7. Thermomagnetic analysis

Thermomagnetic measurements are carried out with the improved horizontal translation Curie balance described in Mullender et al. (1993). A novel measuring procedure involving the sinusoidal cycling of the applied field strength between two values results in a continuous drift correction and a very low noise level. In addition to the output of a conventional Curie balance, the ferromagnetic and the para- and diamagnetic contributions can be calculated separately, provided that saturation of the ferromagnetic part is achieved. When saturation is not complete in the maximum field used, the calculated paramagnetic magnetization will be higher than the actual paramagnetic contribution. The signal to noise ratios of the calculated curves depend strongly on the relative intensity of both contributions.

To distinguish between Curie temperatures and alterations, samples were heated and cooled in a number of runs, each time to a higher temperature. Routine heating and cooling rates were moderate, 6 and 10°C/min., respectively. The magnetic field is cycled between 200 and 400 mT or between 150 and 300 mT. Unless stated otherwise, analyses were performed in air. Measurements in an argon flow were performed after air was removed from the samples by evacuating and flushing with argon. Thermomagnetic analyses were performed on untreated sediment and on magnetic concentrates from sites VBA1 and VBA6 (cf. van Velzen et al., 1993).

### *7.1. The untreated sediment*

The thermomagnetic curves of the untreated sediment are dominated by clay minerals (figure 8, 9). The 1/T temperature dependence of the conventional signal, typical of paramagnetism, is evident. The amount of magnetic minerals in the marls is very small; even this very sensitive balance hardly detects a ferromagnetic contribution. The behaviour of the VBA1 sample is more pronounced (figure 8) than that of VBA6 (figure 9). The heating curve is reversible up to 200°C. After heating to 360°C the cooling curve is slightly below the heating curve. The next run to 500°C shows the expected increase of ferromagnetic magnetization at 400°C. After cooling to room temperature (RT) the ferromagnetic magnetization is much higher than the original value. Above 500°C, in the next heating run, a large part of the newly formed minerals is destroyed again. These observations are not in agreement with the results of the IRM monitoring method, because the alteration in the range 150 to 250°C is not detected. This can be related to the

low concentration of ferromagnetic minerals, however, which could make detection impossible. The sediment of VBA6 shows the same behaviour, but the changes are smaller (figure 9).

### *7.2. Magnetic concentrates in air*

The ferromagnetic magnetization of the magnetic concentrates is sufficient to distinguish it from the paramagnetic contribution (figures 10-13). The low-field concentrates and the remaining high-field concentrates of VBA1 have a ferromagnetic saturation magnetization of 1.2 and 0.02-0.03 $Am^2/kg$, respectively. The ferromagnetic contribution of the concentrates of VBA6 also differ about a factor 100 in intensity: 1.3 $Am^2/kg$ and 0.005-0.01, respectively. The relatively high paramagnetic contribution (figures 10-13) illustrates that in the concentrates paramagnetic clay minerals are still abundant. This is in agreement with microprobe observations (van Velzen et al., 1993) and X-ray diffraction. For comparison, the typical saturation magnetization for the untreated marl, calculated from the saturation remanence of standard paleomagnetic samples, assuming that approximately $J_{rs}/J_s = 0.5$, is about $0.5*10^{-3}$ $Am^2/kg$. It can be concluded that the ferromagnetic magnetization of the low-field magnetic concentrates is about 2500 times larger than that of the original sediment.

The magnetic concentrates of sites VBA1 and VBA6 show distinct differences. The concentrates of VBA6 are reversible up to 200°C, but heating of the low-field concentrate above 300°C shows an irreversible decrease of magnetization (figure 11), which occurs in the ferromagnetic magnetization. This decrease is compatible with the results of the IRM monitoring method. A magnetization increase corresponding to the increase of IRM observed with that method between 150 and 250°C is only marginally visible in the total magnetization of the high-field concentrate, at about 250°C (figure 10). The noise in the ferromagnetic signal is unfortunately too large to establish that the increase is related to the ferromagnetic contribution.

Like the thermomagnetic curves of VBA6, the curves of the concentrates of VBA1 are reversible up to 200°C, but not far above 200°C an alteration of magnetic minerals causes an increase of ferromagnetic magnetization (figure 12,13). Both the ferromagnetic and paramagnetic contribution increase. The observed increase of paramagnetic magnetization is an artefact due to an increase in ferromagnetic magnetization with coercivities higher than the magnetic fields used. The unsaturated part of this magnetization contributes to the calculated paramagnetic magnetization (Mullender et al., 1993).

The newly created magnetization is thermally stable up to at least 360°C (figure 12). There is no visible Curie point below 360°C. A Curie point for this magnetization cannot be assessed in the next heating run to 500°C, because also in the magnetic concentrates another increase in magnetization occurs from 400°C upwards (figure 12,13). This agrees with the formation of magnetite-like grains. To avoid alterations as much as possible, fast heating and cooling runs

(30°C/min.) to stepwise higher temperatures were performed (not shown). These curves proved to be reversible at least up to 390°C. No Curie point was observed below that temperature.

The increase of paramagnetic magnetization that sometimes occurs above 360°C (see e.g., figures 8 and 13) can be explained by the formation of very small grains. Part of the magnetite-like grains that are formed will be superparamagnetic and they will approximately have the same 1/T dependent magnetization in a magnetic field as paramagnetic magnetization. The magnetic fields in the Curie balance are far below the fields needed to saturate (super)paramagnetic grains. They will therefore partly contribute to the paramagnetic component.

The alteration below 300°C shows up slightly differently when various heating rates are used. The magnitude of the magnetization increase varies and the increase of the 'paramagnetic' contribution at 250°C is not always observed (e.g. figure 14). There is no simple relation between heating rate and the observed changes. The increase of ferromagnetic magnetization is considerably smaller when a low heating rate of 2°C/min. is used (figure 14). During the subsequent cooling at an even lower rate (0.2°C/min.) a similar curve as during cooling at the routinely used rate of 10°C/min. was found. Apparently, the alteration is not reversible, not even at this very low cooling rate.

To determine the actual temperature of the alteration, during the thermomagnetic analysis of another sample of the high-field concentrate of VBA1 the temperature was increased stepwise (figure 15). At 220°C and 225°C no change was seen after 30 minutes. At 228°C, however, the alteration slowly began to evolve. After 12 hours the temperature was increased again, but then the reaction was apparently completed. The temperature needed for the reaction to evolve seems to be close to 228°C. The apparent higher starting point in the routine thermomagnetic runs is likely due to the low reaction rate as compared to the heating rate.

Because the alteration during stepwise thermal demagnetization in standard paleomagnetic samples sets in at a much lower temperature, the influence of the different experimental conditions in the Curie balance was subject of another test. A magnetic concentrate was heated and cooled in the field-free space of a thermal demagnetizer (furnace), in the same manner as the standard paleomagnetic samples. After heating at 150°C and 200°C in the thermal demagnetizer, no increase of RT ferromagnetic magnetization was measured in the Curie balance (figure 16). After 5-10 minutes at 250°C in the thermal demagnetizer, the magnetization had increased, but the subsequent thermomagnetic run shows that the alteration was only in an initial stage. Apparently, the heating time in the thermal demagnetizer was not sufficient to let the alteration go to completion. It can be concluded that the thermal demagnetizer in itself is not the cause of the lower alteration temperatures observed with the IRM monitoring method. A sample heated in the thermal demagnetizer at 265°C for 15 hours shows a different behaviour (figure 17). An increase in RT ferromagnetic magnetization is observed

after this treatment and no further increase is observed during the first thermomagnetic run to 300°C. On the contrary, a small decrease in magnetization occurs during the runs to 300°C and to 360°C.

### *7.3. Magnetic concentrates in argon*

The thermomagnetic runs in an argon atmosphere (figures 18, 19) are more in agreement with the results of the IRM monitoring method than the thermomagnetic runs in air. In absence of oxygen, the magnetization increase in the VBA1 concentrates occurs at a considerably lower temperature. With the standard heating rates, the alteration causes a maximum of the magnetization in the concentrates of VBA1 at 250°C. In air it occurs at 300°C. Heating with routine rates up to 190°C and further with a low heating rate (0.5°C/min.) between 190 and 240°C, shows that the alteration is already in progress at 190°C (figure 20). Also in argon slow cooling (0.5°C/min.) shows that the alteration is not reversible. The concentrates of VBA6 reveal only a very small increase at the same temperature as the concentrates of VBA1 (figures 21). The decrease of magnetization after heating to 360°C is the same as in air.

---

**Figures 8-21**.Thermomagnetic analyses.
Thermomagnetic analyses were performed with an improved horizontal translation Curie balance (Mullender et al., 1993). Heating (cooling) curves are indicated with solid lines (lines with open circles). Routine heating (cooling) rates are 6 (10) °C/min. Heating was performed in air or in an argon atmosphere.
The signal of the balance is filtered before the three output signals shown are calculated (Mullender et al., 1993). The Total magnetization (top panel in the figures) is the signal a conventional Curie balance would yield, but with a much higher sensitivity. This signal can be separated in a ferro-/ferrimagnetic component (Ferromagnetic) and a paramagnetic/diamagnetic component (Paramagnetic), which is equal to the high-field susceptibility when the ferromagnetic minerals are saturated. When saturation is not achieved, the calculated paramagnetic contribution is too high. The maximum fields used in the measurements are 300 or 400 mT, in which fields the samples are close to saturation (see chapter 6).
The noise in the Ferromagnetic and Paramagnetic panels is due to vibrations in the soil and the foundation of the laboratory. The frequency spectrum of these minute movements extends to the operating frequency of the secondary signal which is used to calculate these contributions separately (see Mullender et al., 1993). Differences in noise level also appear as a result of variations in absolute magnetizations and due to the necessity to switch to a lower sensitivity for samples that go beyond the dynamic range of the most sensitive position.
'Low-field' and 'high-field' concentrates are separated with lower and higher magnetic fields corresponding to currents of 0.25 and 1.5 A in the Frantz isodynamic separator. Magnetization and High Field Susceptibility (Susc.) are given partly in units per mass, partly in absolute units when the mass of the sample was not exactly known. Typical sample weights are 5-50 mg for the concentrates and 150 mg for the sediment.

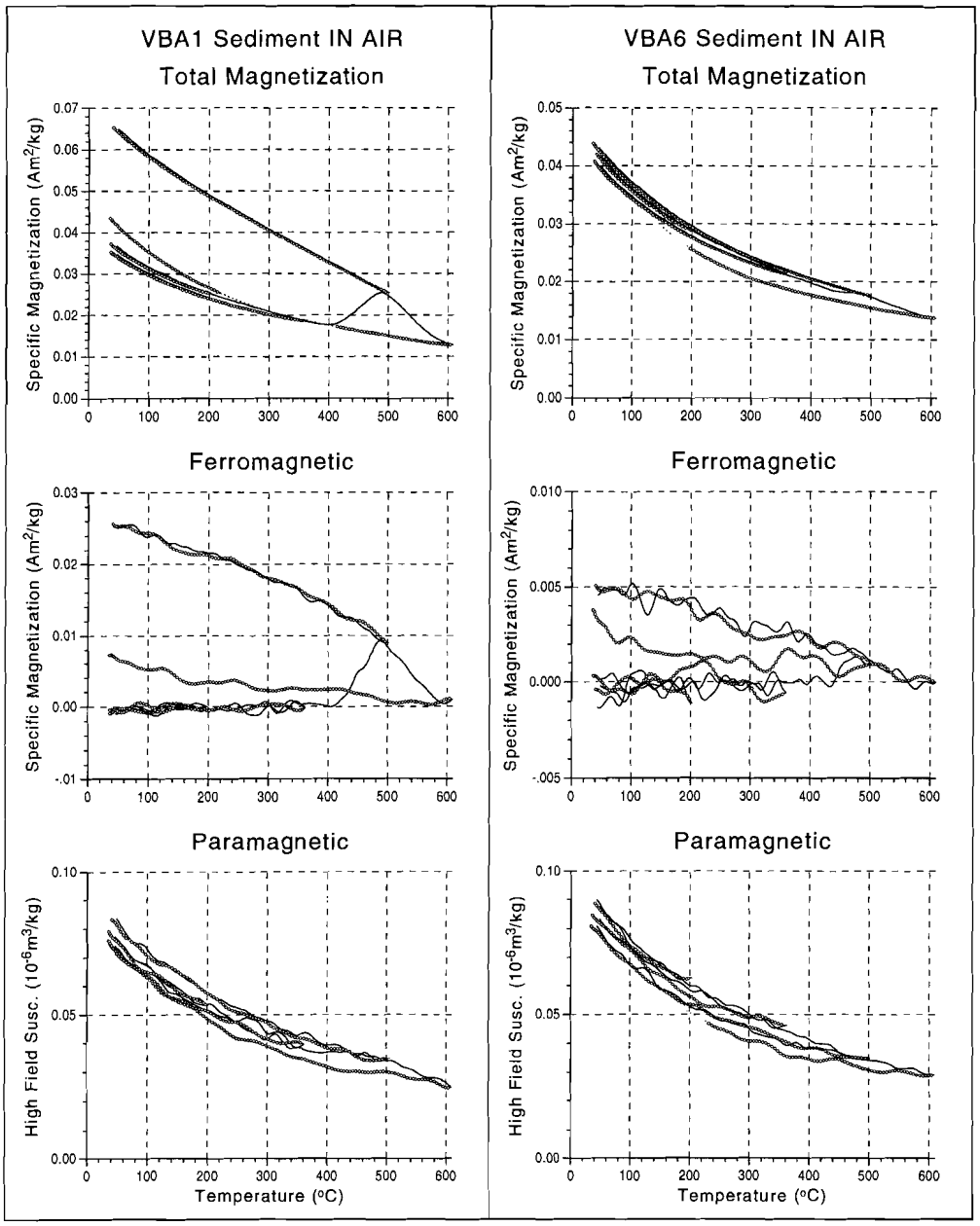


**Figure 8.** Sediment of VBA1. Four runs to increasing temperatures of 200, 360, 500 and 610°C. The dotted line segment indicates part of the cooling of the 610°C run.

**Figure 9.** Sediment of VBA6. Four runs to 200, 360, 500 and 610°C, respectively. The dotted line indicates where the last cooling curve was left out for reasons of clarity.

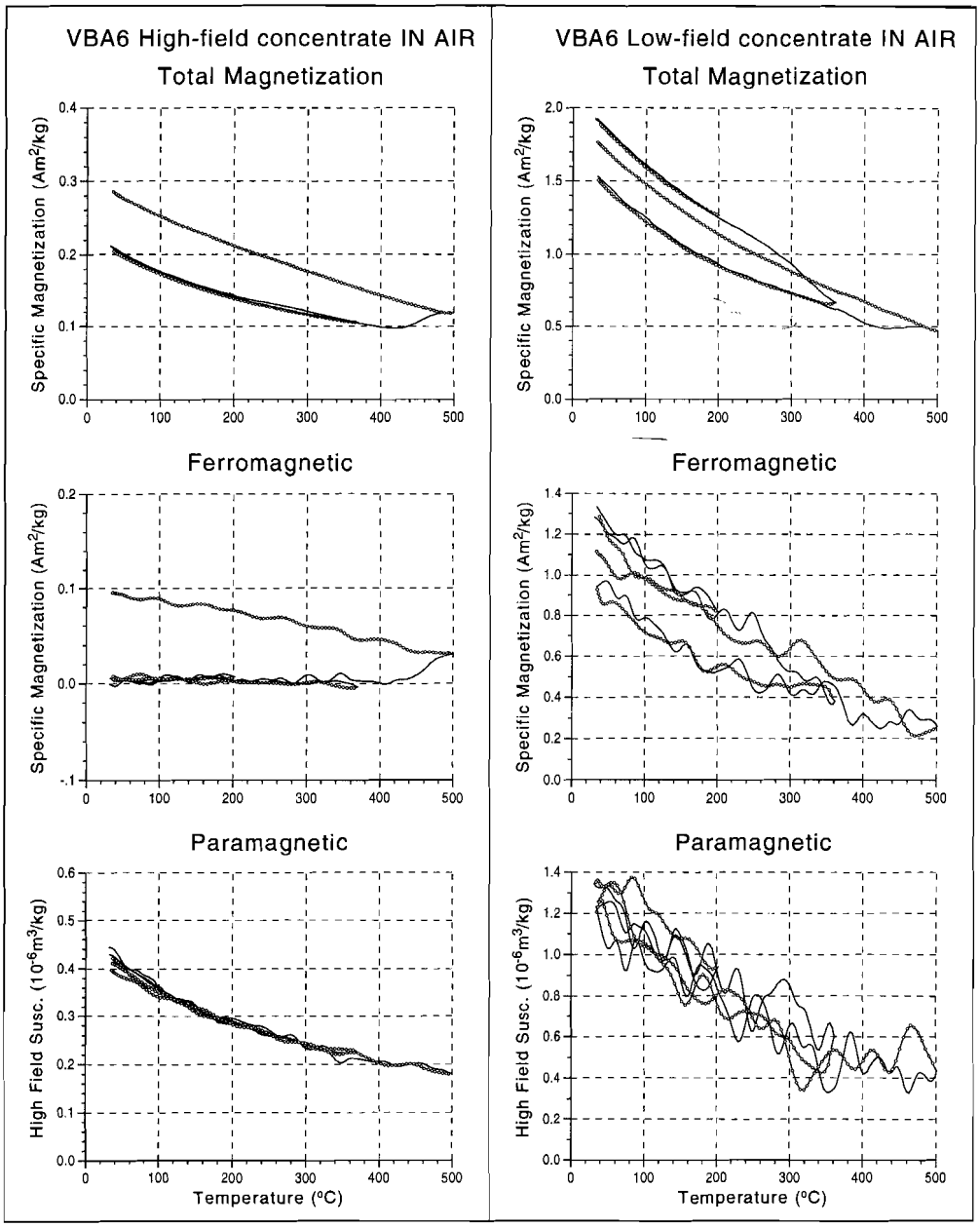


**Figure 10.** High-field concentrate of VBA6. Three runs (200, 360 and 500°C).

**Figure 11.** Low-field concentrate of VBA6. Three runs (200, 360 and 500°C).

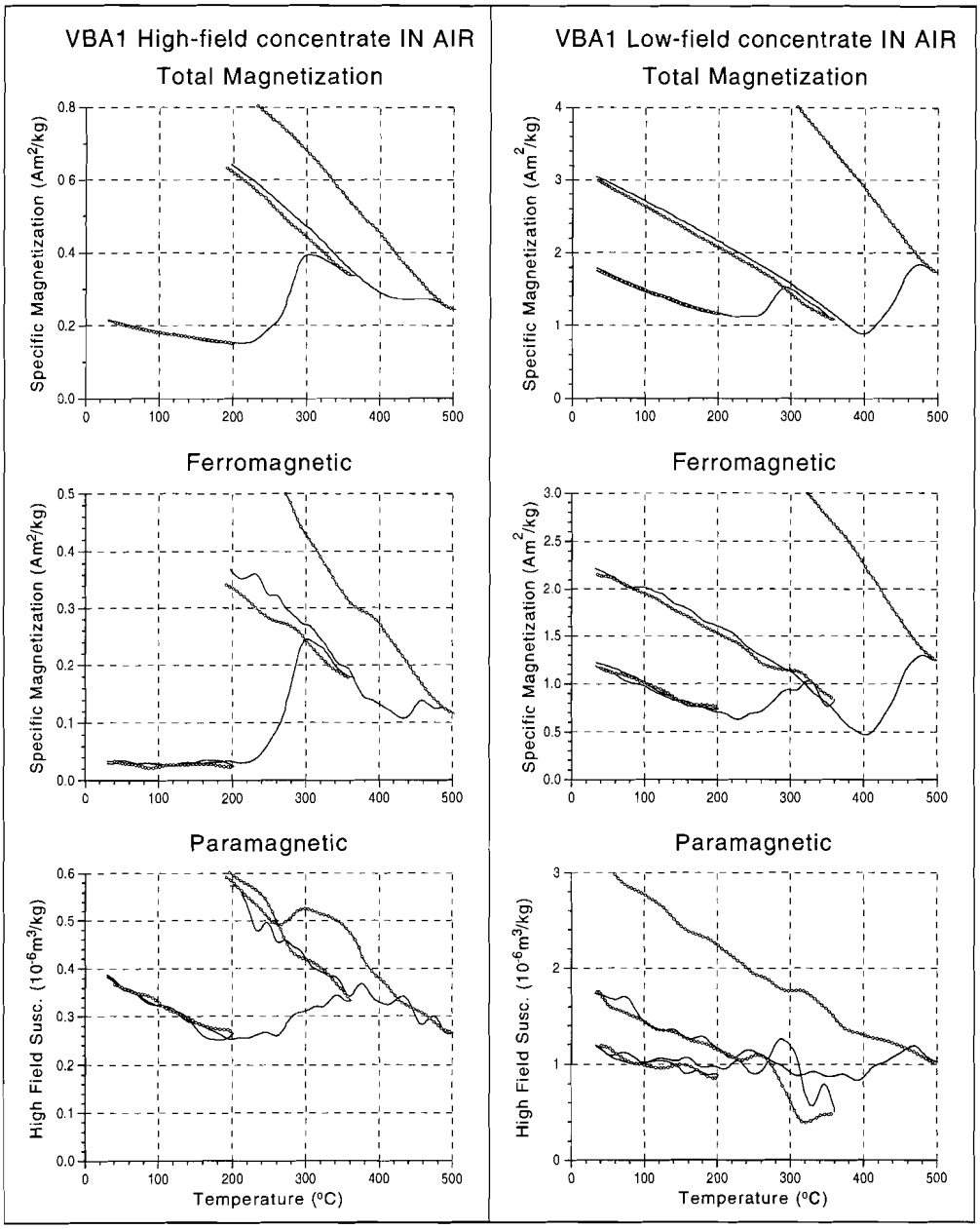


**Figure 12.** High-field concentrate of VBA1. Three runs (200, 360 and 500°C). Due to a large increase of magnetization parts of the curves were beyond the dynamic range of the balance.

**Figure 13.** Low-field concentrate of VBA1. Three runs (200, 360 and 500°C).

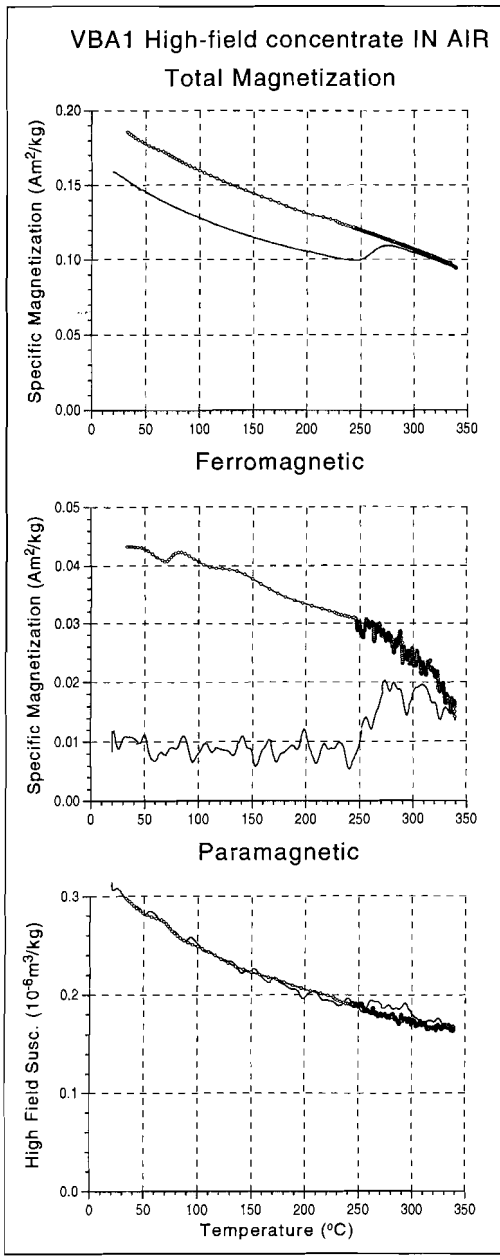


**Figure 14.** High-field concentrate of VBA1. Low heating and cooling rates: 2 and 0.2 °C/min., respectively.

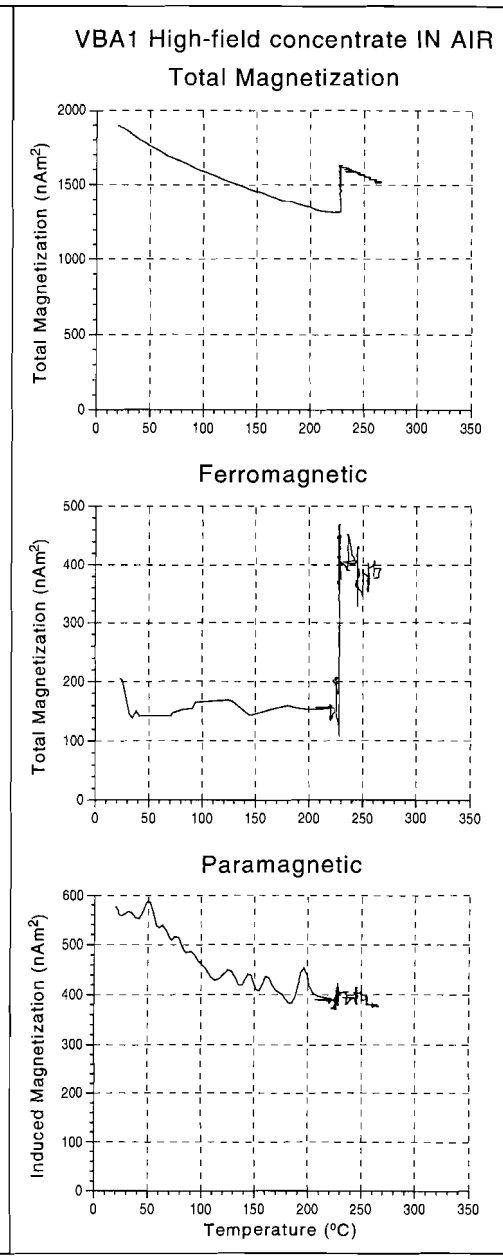


**Figure 15.** High-field concentrate of VBA1. Stepwise increase of temperatures. 30 minutes heating at 220 and 225°C, 12 hours at 228°C.

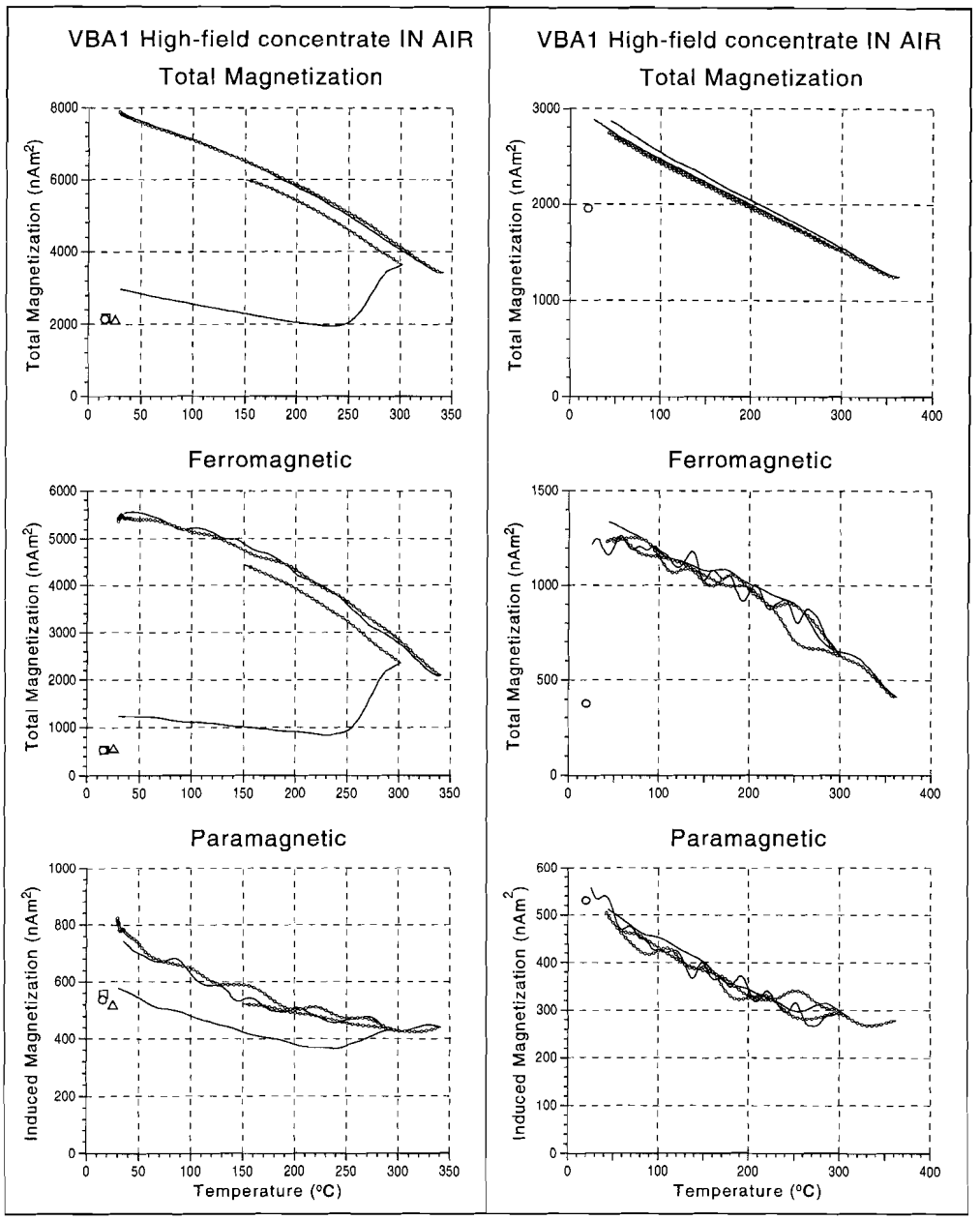


**Figure 16.** Measurements before heating in a field-free furnace (circles), after heating at 150°C (squares) and 200°C (triangles) and the thermomagnetic run after heating to 250°C in the furnace. During cooling after the 300°C run the magnetization went out of range. For the next run to 340°C the sensitivity was reduced.

**Figure 17.** High-field concentrate of VBA1. Circles denote magnetizations before heating. Thermomagnetic run after heating at 265°C in a furnace for 15 hours. A small decrease of total magnetization occurs after the runs to 300°C and to 360°C.

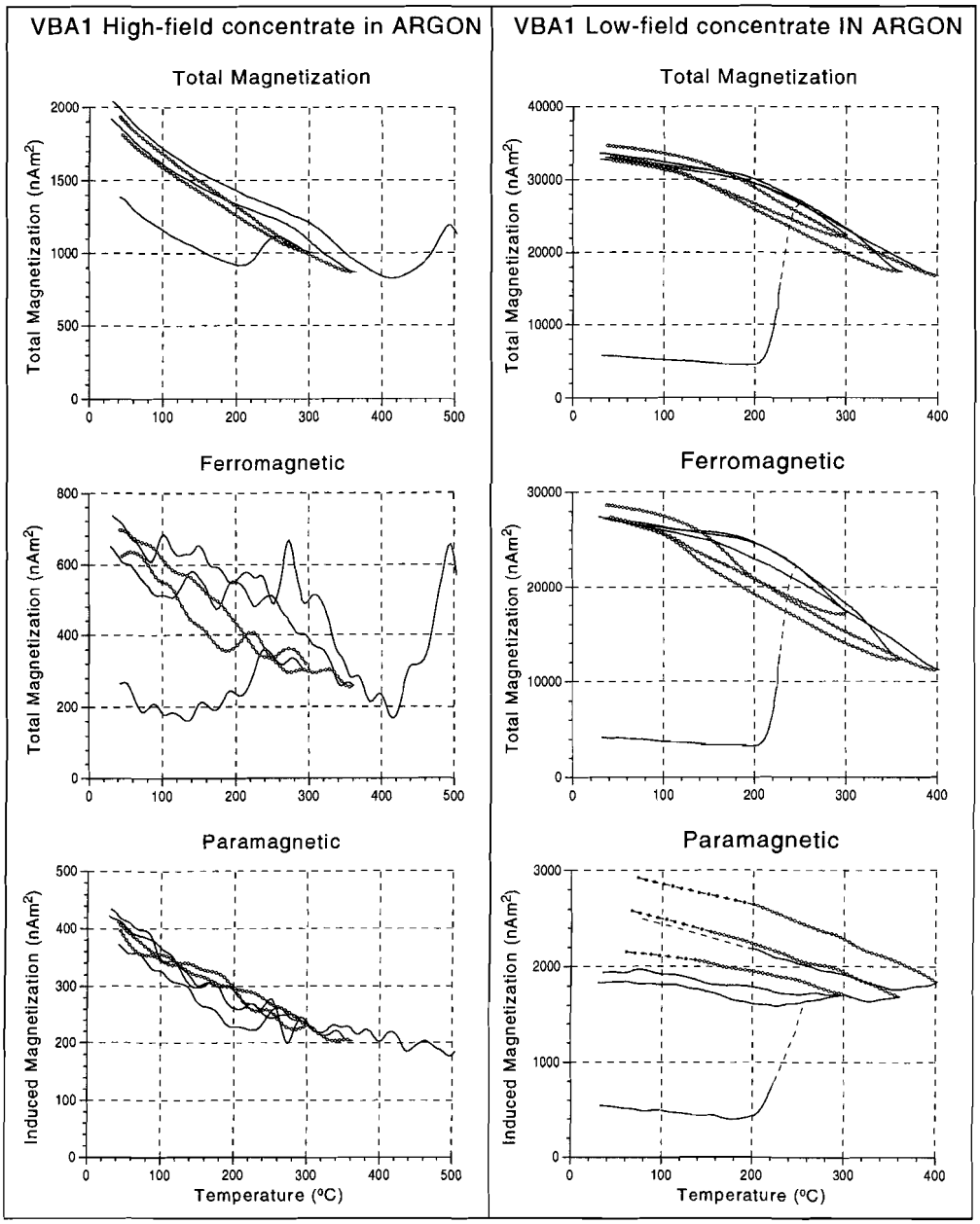


**Figure 18.** High-field concentrate of VBA1 in argon. Three runs to increasing temperatures of 300, 360 and 500°C. Only the heating part of the last run is shown.

**Figure 19.** Low-field concentrate of VBA1 in argon. Four runs (250, 300, 360 and 400°C). The first run was stopped when the magnetization went out of range. The second run was measured with a lower sensitivity. The cooling and heating curves show a remarkable hysteresis.

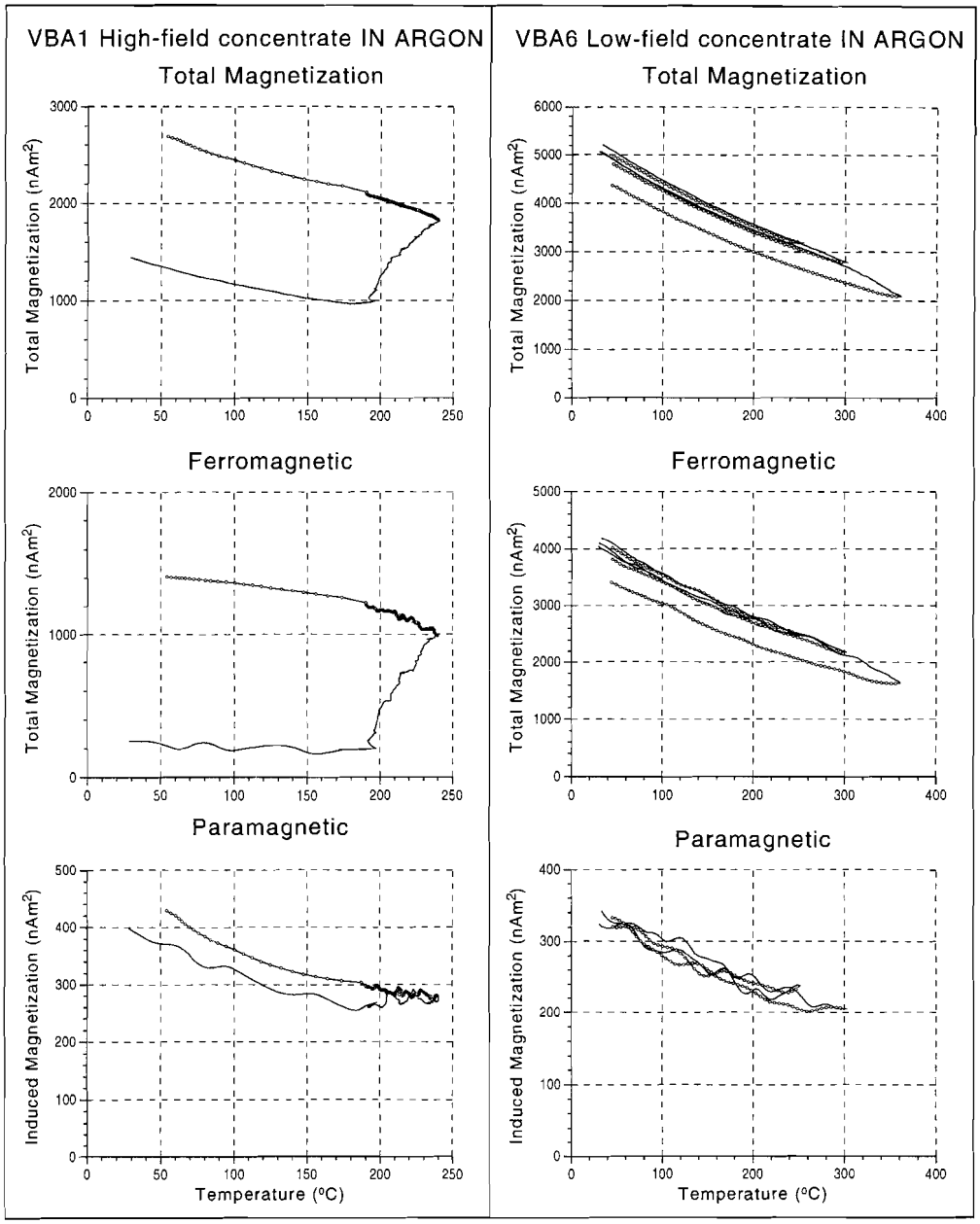


**Figure 20**. High-field concentrate of VBA1 in argon. Routine heating and cooling rate below 190°C. Slow heating and cooling (0.5°C/min.) above 190°C.

**Figure 21**. Low-field concentrate of VBA6 in argon. Three runs to increasing temperatures of 250, 300 and 360°C.

The thermal stability of the newly formed magnetization in the magnetic concentrates of VBA1 is different from that in air (figures 18,19). The ferromagnetic magnetization shows a decrease after heating to 300°C and higher temperatures. The curves also show a hysteresis in time or temperature: the heating curves are always above the cooling curves of the preceding run. This is a mysterious observation. A cooling curve is beneath the preceding heating curve when an alteration to a less magnetic phase has occurred and above the heating curve when a more magnetic phase is formed. The heating curve of the next thermomagnetic run, however, should be the same as the preceding cooling curve, because no alteration is expected during cooling and truly magnetic behaviour is reversible. We have no explanation for the hysteresis effect in the present curves, which moreover seems to be repeatable (figure 19). One could think of metastable behaviour and low reaction rates. Graham et al. (1987) observed such hysteresis at much higher temperatures (between 400 and 550°C), when investigating oxygen solubility in pyrrhotite.

## 8. Discussion: Alterations below 350°C

In the following several aspects of the magnetic behaviour below 350°C will be addressed. These include (1) an evaluation of the influence of different conditions during thermal demagnetization as employed in the IRM monitoring method and the thermomagnetic experiments, (2) a short overview of the thermal properties of possible magnetic sulphides in sediments, (3) a comparison of the observed magnetic behaviour with the $\gamma$-transition in hexagonal pyrrhotite and a discussion about the possible influence of oxygen on that transition, (4) a discussion about the thermal stability of the newly formed sulphide magnetization and (5) a summary of the arguments in favour of mixed phase pyrrhotite and in favour of greigite.

### *8.1. Differences between IRM monitoring method and thermomagnetic analysis*

The results of the IRM monitoring method and the thermomagnetic analysis of magnetic concentrates do not concur for the temperature interval between 150 and 350°C. With the IRM monitoring method an increase of the total IRM was observed after the 150 and 200°C steps. The increase occurred mainly in the high-coercivity fractions, some of which continued to increase at 250 and 300°C. The new high-coercivity remanence decreased again due to alteration at 300 and 330°C. The alterations occur both in samples of VBA1 and of VBA7, although much less pronounced in the latter. The thermomagnetic curves of the magnetic concentrates from VBA1 measured in air are reversible up to over 200°C. An increase of saturation magnetization starts at 228°C. The resulting magnetic phase is stable at least up to 390°C. In an argon atmosphere the increase of saturation magnetization in VBA1 occurs about 40°C lower than in air. The subsequent decrease of magnetization occurs some 50°C lower than in air. In the

concentrates of VBA6 in argon only a very small increase of magnetization occurs at the same temperature as in the concentrates of VBA1. Above 250°C the magnetization decreases due to alteration.

The most obvious difference in experimental conditions between the IRM monitoring method and the thermomagnetic analyses is the availability of oxygen. Before the influence of oxygen on the alteration process will be discussed, other differences will be evaluated (Table A).

**Table A.** Differences between IRM monitoring method and thermomagnetic analyses

| | IRM in 10 $cm^3$ marl samples | thermomagnetic analysis of magnetic concentrates |
|---|---|---|
| 1. | RT measurement of remanence | magnetization measured at elevated temperature |
| 2. | heating/cooling in zero field | heating/cooling in >150 mT magnetic field |
| 3. | all magnetic minerals in the marls | possibly biased selection of magnetic minerals |
| 4. | no previous treatment | after concentration procedure |
| 5. | in air? | in air or argon atmosphere |

(1) The remanence for the IRM monitoring method is measured at RT and the magnetization during thermomagnetic analyses is measured at elevated temperatures. The values observed at RT between the successive thermomagnetic heating runs to 200°C and 300 or 350°C demonstrate that the changes measured at elevated temperatures are comparable to the changes measured at RT. So the different measuring temperature is not a serious effect. (2) In case the alteration is an order-disorder effect, the presence of an external magnetic field could be important. In pyrrhotite, for example, a magnetic field causes magnetostrictive deformation which may facilitate the diffusion of cations (Schwarz, 1967). The values observed after heatings of concentrates in a field-free thermal demagnetizer before thermal analysis in a magnetic field (figures 16,17) do not indicate such an effect.

The concentration procedure may create another difference. (3) The magnetic mineral content of the concentrates is likely biased to the more magnetic grains, but this could only explain differences in the magnitude of the changes, not the observed differences in alteration temperature. (4) Furthermore, the surface of the sulphide grains may be slightly oxidized during the concentration procedure, in spite of precautionary measures. An oxidized surface layer may have a decisive influence on alterations during heating. It may hinder further oxidation (Freke and Tate, 1961), but possibly also impede reordering of vacancies and iron in the lattice (Graham et al., 1987).

(5) The presence or absence of oxygen, however, is the crucial difference between the experiments. It is not known to what extent the standard marl

samples are open to air, but the NRM of samples that where heated and cooled in vacuum showed the same alteration effects as the samples that were heated in air (figure 1d). Also the results of the IRM monitoring method indicate that during heating oxygen has no access to the magnetic sulphides in the marls. During thermomagnetic analyses in air, the alteration in VBA1 starts at 228°C. In argon, after oxygen has been removed as much as possible from the concentrates, it starts below 190°C. Apparently the presence of oxygen delays the alteration. In the standard marl samples the reaction temperature is even lower, about 150°C. Possibly surface oxidation of the sulphides in the concentrates forms an additional obstruction for the alteration. The absence of such oxidation of the sulphides in the standard marl samples could then explain the difference.

The different results of the three experiments indicate that the presence of oxygen influences the alteration. This may help to identify the sulphide phase responsible for the alteration, although the observed behaviour of the magnetization during heating is not a known characteristic of one specific magnetic sulphide.

### *8.2. Thermal properties of magnetic sulphides in sediments*

Ferrimagnetic properties of iron sulphides are restricted to the range of the monosulphides in the range from FeS to $Fe_3S_4$. Monoclinic pyrrhotite ($Fe_7S_8$) and greigite ($Fe_3S_4$) are both ferrimagnetic, but the (thermo-)magnetic properties of monoclinic pyrrhotite are much better known than those of greigite. The magnetic properties and phase transitions of monosulphides in the range FeS to $Fe_7S_8$ are complex and strongly composition dependent. Monoclinic pyrrhotite ($Fe_7S_8$) is ferrimagnetic at RT due to vacancy ordering and has a Curie temperature between 305 and 325°C. Hexagonal pyrrhotite ($Fe_9S_{10}$-$Fe_{11}S_{12}$) is antiferromagnetic at RT. It becomes ferrimagnetic between 170 and 220°C due to a change in the distribution of vacant iron positions over layers with antiparallel spin-coupling ($\gamma$- or $\lambda$-transition). Ferrimagnetic hexagonal pyrrhotite has a lower Curie temperature between 270 and 290°C. The ferrimagnetism is preserved upon quenching. The variation in $\gamma$-transition temperature and Curie temperature is related to the composition of the hexagonal pyrrhotite (for phase diagrams, see e.g. Schwarz, 1975; Vaughan and Craig, 1978; Kissin and Scott, 1982).

The formation of pyrrhotite in a sedimentary environment is not well-documented. Only Sweeny and Kaplan (1973) mention hexagonal pyrrhotite as a product of sulphate reduction reaction chain. Nevertheless pyrrhotite (also monoclinic pyrrhotite) is often found in sediments. Greigite ($Fe_3S_4$) is an intermediate phase in the sulphate reduction chain and is therefore more likely to occur in sediments. Until recently, however, greigite was considered a rare mineral. Usually greigite is reported to become thermally unstable starting at temperatures below 300°C and with coercivities considerably lower than pyrrhotite (Skinner, 1964; Hoffmann, 1992; Snowball, 1991; Krs et al., 1992). Recently, greigites were discovered in sediments of similar age and sedimentary environment as the Vrica marls (Tric et al., 1991; Horng et al., 1992) and in

Miocene/Pliocene sediments (Roberts and Turner, 1993). The amount of magnetic minerals in these sediments was much larger than in the Vrica marls, allowing identification of the greigite in magnetic concentrates with X-ray diffraction. The coercivities of these greigites are higher than reported hitherto for greigite (Horng et al., 1992) and they seem to be thermally stable up to 300°C.

Sulphide assemblages can be very complex. In sulphides of high-temperature origin intergrowths of hexagonal and monoclinic pyrrhotite, pyrrhotite and pentlandite ($(Fe,Ni)_9S_8$) and pyrrhotite and pyrite are very common. The ratios between the phases and the degree of exsolution depend on the original material, thermal history and in some cases the degree of oxidation. Although low-temperature equilibrium between phases differs from the high-temperature equilibrium, it can take a long time to be established. The processes involved, like structural changes and reordering of vacancies and metal ions, are much slower at low temperatures.

Authigenic sulphides, formed in a low-temperature sedimentary environment, are relatively unknown as far as the occurrence of different phases and intergrowths are concerned. It is conceivable that grains are inhomogeneous when changes in physico-chemical conditions occur during their growth, like changes in redox potential or availability of metal and sulphur. When in a grain the composition varies, different vacancy distributions may exist and grains may only be partly ferrimagnetic. Examples are hexagonal and monoclinic pyrrhotite phases or possibly Ni-rich and Ni-poor areas in a grain. In the microprobe study (van Velzen et al., 1993) such variations could not be established due to the small size of the sulphide grains. Furthermore low-temperature pyrrhotites are known to have complex superstructures due to partial vacancy ordering (Vaughan and Craig, 1978). An additional factor in sediments may be low-temperature oxidation (e.g. weathering), which will create a relatively sulphur-poor grain surface. For example, a so-called "anomalous" pyrrhotite on the surface of hexagonal pyrrhotite may occur (Clark, 1970). These deviations from stoichiometric phases in natural sulphides can cause complex (magnetic) behaviour. At RT, homogenization, redistribution of vacancies and metal ions and diffusion of oxygen will be very slow so that the sulphides may not reach a state of true thermodynamic equilibrium. During heating these processes will be accelerated and alterations influencing the magnetic properties may occur.

The changes in magnetic properties observed with the IRM monitoring method indicate that such processes occur during heating of the Vrica marls. The increase of total IRM after the 150 and 200°C temperature step is attributed to the increase of magnetization in sulphides. It is likely that it resides in sulphides, because the maximum demagnetization temperatures of the new remanence are similar to those of the existing remanence and because the new remanence is in the same direction as the existing remanence with similar coercivities ($>50$ mT). This corresponding direction of the new remanence can be due to: (1) a remanence increase of grains carrying the existing remanence; (2) interaction between grains carrying the existing remanence and grains carrying the new

remanence; (3) the subdivision of larger grains into smaller grains. Examples of alterations that can occur in sulphides are: (1) a magnetic phase transition; (2) oxidation or reduction; (3) decomposition of the original sulphide phases. Oxidation of the sulphide is not likely to occur at a lower temperature in an argon atmosphere than in air and reduction is not likely to occur in air. Decomposition of a sulphide with lower magnetization into more phases with a higher total remanence is possible (the unmixing of greigite into pyrrhotite and pyrite for example), but the preservation of the remanence would then require continuous exchange interaction during the change from one magnetic phase to another. It is not known whether such interaction is possible in ferrimagnetic sulphides. Taking all experimental results into account, a magnetic phase transition resulting in an increase of remanence is considered the most likely mechanism. This transition is discussed in the following paragraphs.

### *8.3. Mechanism of the γ-transition*

The present alteration shows similarities with the γ-transition in hexagonal pyrrhotite. The different temperatures at which the magnetization increase occurs under different experimental conditions, however, requires an additional explanation. Several mechanisms have been proposed for the increase of magnetization at the γ-transition. One possibility is the reordering of vacancies in pyrrhotite over the two sublattices with opposite magnetization direction, giving a ferrimagnetic instead of an antiferromagnetic structure (Lotgering, 1956). A more likely mechanism is the transition of one superstructure (5C) to another superstructure (imperfect monoclinic 4C) with a larger number of vacancies in one of the two sublattices (Marusak and Mulay, 1979). Nakazawa and Morimoto (1971) demonstrated with single crystal X-ray methods at elevated temperatures that the γ-transition is a change from a superstructure repeating along the c-axis (NC) to a superstructure along the a-axis (NA). In this transition only short-range reordering of vacancies is involved, which requires a low activation energy and may start at lower temperatures than the commonly reported $T_\gamma$ (Bennet and Graham, 1981). Because of the slowness of the reordering process, the γ-transition is not reversible upon cooling, unless cooling is slow (in the order of 0.5°C/min.; Schwarz, 1968; Bennet and Graham, 1980).

It is also important to note that the 'Curie point' of hexagonal pyrrhotite is a phase transition rather than a magnetic transition. The reduction of magnetization is a order-disorder effect due to the diffusion of vacancies, distributing the vacancies more evenly over the two sublattices (Bennet and Graham, 1980), which can be described as a transition from an NA superstructure to a MC structure (Kissin and Scott, 1982). This reordering also starts at lower temperatures than the reported 'Curie temperature' of 270-290°C (Brodskaya and Gendler, 1979) and competes with the increase of ordering brought about by the γ-transition.

Oxygen plays a role in how these transitions show up. When oxygen is present in the sulphide crystal, the mobility of vacancies might be reduced and the

diffusion of vacancies is slowed down until oxygen can also move (Graham, 1987). The activation energy for the movement of oxygen is slightly higher than that of vacancies (106 kJ/mol and 86.8 kJ/mol, respectively; Graham et al., 1987), so that the transition may occur at a higher temperature when oxygen is present. During heating in air, the alteration in the Vrica magnetic concentrates occurs at 228°C. In argon the alteration starts at a much lower temperature, within the range generally cited for the γ-transition (170-220°C; Schwarz, 1975; Vaughan and Craig, 1978). The elevated transition temperature in air might be attributed to the influence of oxygen from the air. This oxygen can only have the alleged effect if it penetrates into the sulphide crystal. In the standard paleomagnetic samples the alteration starts as low as 150°C, indicating that vacancies can move more freely than in the sulphides in the magnetic concentrates. Along the same lines of reasoning, it may be supposed that the sulphides in the concentrates have a higher oxygen content than the sulphides in the sediment, due to surface oxidation during the concentration procedure.

Although the alteration in the standard paleomagnetic samples starts below the reported γ-transition temperature range, it can be related to the γ-transition. Changes in magnetic properties of pyrrhotites at temperatures close to 150°C have been reported by several authors. Thomson (1990) reported changes in magnetic properties in pyrrhotite-bearing rocks starting after heating to 156°C. One of the effects was an increase of the rotational remanent magnetization that could be induced in the rocks. It was proposed that hexagonal pyrrhotite was responsible for this phenomenon. In other reports reordering processes in hexagonal pyrrhotite are mentioned at temperatures more than 60°C below $T_\gamma$ (Bennet and Graham, 1980). Like in the present samples, both changes in coercivities and in magnetization can occur. They can even start below 100°C (Brodskaya and Gendler, 1979; Brodskaya, 1980).

Regarding possible low-temperature oxidation of the sulphides, the behaviour of so called "abnormal" or "anomalous" pyrrhotite should be mentioned (Clark, 1970; Taylor, 1971; Graham et al., 1987). Anomalous pyrrhotite can occur in low-temperature sedimentary environments as rims around monoclinic pyrrhotite after low-temperature oxidation (Clark, 1970). It has a low magnetization and very low Curie temperature (approximately 250°C), but heating to 240-250°C produces a material with a Curie temperature over 300°C and a magnetization close to that of monoclinic pyrrhotite, presumably through some kind of rearrangement in the crystal (Graham et al., 1987). This alteration has similarities with the alteration occurring in the present samples.

### *8.4. Thermal stability and Curie points*

The demagnetization temperature (or thermal stability) of the magnetization after alteration is also different in the present experiments. The influence of oxygen seems to be an important factor in this case as well. Remarkable is the absence of a distinct Curie temperature in the temperature range between 270 and

400°C. For magnetic sulphides this needs further explanation. It has been suggested that the Curie temperature of monoclinic pyrrhotite, like the Curie point of hexagonal pyrrhotite, is a structural order-disorder temperature as well, and not merely a collapse of magnetic exchange interaction (Graham et al., 1987). The β-transition which occurs slightly above or at the same temperature (320°C; cf. Schwarz and Vaughan, 1972) also involves the diffusion of vacancies and it constitutes the transition from MC superstructures to disordered pyrrhotite (1C superstructure). This change in superstructure occurs for a large range of compositions (Ward, 1970; Kissin and Scott, 1982) from monoclinic to troilite (FeS). Here as well foreign ions like oxygen may prevent the diffusion and the ferrimagnetic structure may be sustained up to higher temperatures (Graham et al., 1987). If the Curie temperature of monoclinic pyrrhotite is related to this β-transition, the temperature at which it occurs may be influenced. Rochette et al. (1990) suggested that this process could be responsible for the anomalously high maximum blocking temperatures (up to 350°C) of some pyrrhotites. In our case the presence of Ni could also have some influence, but oxygen seems to be a major factor in the alterations. The 'Curie temperature' of hexagonal pyrrhotite, which is known to be a structural transition, may be suppressed by the presence of oxygen in the same way, so that it would not show up in the thermomagnetic curves.

The thermomagnetic curves of the magnetic concentrates of VBA6 in air and in argon are not reversible above 250°C. In argon the magnetic minerals lose a part of their magnetization between 300 and 360°C, after a small increase between 200 and 250°C (figure 21). The concentrates of VBA1 seem to lose part of their magnetization after heating to 300°C in argon (figure 19), but as mentioned before, in the next heating run the magnetization has recovered. No plausible explanation was found for this hysteresis effect.

In the marl samples the IRM starts to decrease after heating to 250°C and is reduced to values below the original IRM after heating to 330°C. It is not unlikely that alterations of magnetic sulphides occur in this temperature range. Greigite is unstable in air and monoclinic pyrrhotite converts to hexagonal pyrrhotite and pyrite (Schwarz, 1975) or to magnetite and pyrite (Dekkers, 1990). It is therefore remarkable that the magnetic phase formed in the concentrates of VBA1 during heating in air is stable even above 360°C. The modifications of the magnetic sulphide, possibly the incorporation of oxygen, seem to make the phase thermally more stable.

Magnetic transitions are in principle reversible, but high cooling rates (in the case of the stepwise thermal procedure) or changes in the structure other than diffusion of vacancies may cause irreversible behaviour. A dependence of the magnetization increase on heating rate, as observed in the magnetic concentrates, was reported for the γ-transition by Schwarz (1967) and Zapletal (1993). It is caused by two competing ordering processes that have different activation energies and therefore different reaction rates. Their equilibrium depends on the temperature. This is illustrated by the thermomagnetic curve after annealing at

265°C for 15 hours (figure 17) and by the relatively small increase of magnetization when a low heating rate is used (figure 14). If oxygen has the suggested influence on the structural transitions near the 'Curie points' of hexagonal and monoclinic pyrrhotite, it could explain why the magnetization is best preserved during thermomagnetic analysis in air and why the IRM almost completely disappears in the paleomagnetic marl samples after heating to 330°C.

### *8.5. Arguments for pyrrhotite*

The thermal alterations indicate that hexagonal pyrrhotite or a similar sulphide may be present in the Vrica marls. Hexagonal pyrrhotite is antiferromagnetic in stoichiometric form and therefore not able to carry a remanence. Nevertheless the IRM increases during heating (e.g. figure 7), indicating a strong interaction between the original magnetic phase and the altered magnetic phase. Possibly the vacancy distribution in the pyrrhotite is not completely that of an ideal antiferromagnet, so that the hexagonal pyrrhotite is slightly ferrimagnetic at RT. At the $\gamma$-transition the magnetization of this pyrrhotite may increase.

Another possibility is the presence of more and less magnetic intergrowths in one sulphide grain. The remanence direction of the more magnetic part (the original remanence carriers e.g. monoclinic pyrrhotite) could then be transferred to the new remanence originating from the $\gamma$-transition in the part of the grain with the less magnetic vacancy distribution. The initial magnetization of the mixed-phase grains is low, but due to the $\gamma$-transition the magnetization increases (Ward, 1970; Brodskaya and Gendler, 1979). The remanence residing in this pyrrhotite may preserve the original direction during the increase. There are no reports to confirm this suggestion. More complex processes may occur, since natural iron sulphides in sediments may be inhomogeneous.

The high maximum blocking temperatures of the IRM in the marl samples (see chapter 6) might be explained by the proposed influence of oxygen on the vacancy reordering. It is possible that only the newly formed remanence, which is coupled to the existing remanence, has these high blocking temperatures. It was observed that an IRM induced after heating to 200°C tended to be thermally more stable than the original IRM, but even in samples where the alterations are not so pronounced, like VBA6 and VBA7, the high blocking temperatures occur. A high Ni content is not required for the alteration to occur. In the concentrates of VBA6 the highest Ni contents were found, but only a small increase of magnetization was found.

There is no obvious explanation for the observation that the new remanence has mainly coercivities $>50$ mT and is mainly coupled to remanence with the same coercivities. The coercivities might be related to the special structure of the sulphide grains, that is responsible for the observed behaviour.

*8.6. Arguments for greigite*

There are also arguments in favour of the presence of greigite in the marls, in particular a greigite similar to the sedimentary greigite with higher coercivities found by Horng et al. (1992). From the thermomagnetic behaviour the presence of greigite could not be confirmed, however, although the phase resulting after the alteration at 228°C in the VBA1 magnetic concentrates has a thermal stability that can only be compared to concentrates of greigites found in some sediments (Snowball, 1991; Tric et al., 1992; Horng et al., 1992).

A remarkable detail in the thermal analyses of those concentrates is a small increase of magnetization between 250 and 300°C, when performed in a nitrogen atmosphere (Tric et al.,1992, Horng et al., 1992). Although the remanence increase in the samples of the present study is much more pronounced, it indicates that the two magnetomineralogies may have something in common. In the latter two references only thermomagnetic runs up to 600°C are reported, so that the thermal stability of the greigites could not be assessed.

Therefore partial thermomagnetic runs in air of the greigite extracted by Horng et al. (1992) were performed with the very sensitive Curie balance at Fort Hoofddijk, with the routine heating rates. These curves show a small increase of magnetization starting at about 160°C and the thermal instability of the greigite starts at 250°C (Dekkers, pers. com.). Although there are similarities, this behaviour differs from thermomagnetic behaviour of the magnetic concentrates of the Vrica marls. The presence of greigite can therefore not be confirmed. The monoclinic pyrrhotites found by Horng et al. (1992) in the same section as the greigites are thermally much more stable and show a clear Curie point at about 320°C (Dekkers, personal communication). This behaviour has no similarities with the magnetization of the Vrica marls.

The thermal behaviour of sulphide magnetization appears to be complex and relatively unknown. Identification of magnetic sulphide phases using thermal stability and Curie temperatures is therefore difficult. Apparently, the properties of natural sulphides are influenced by their environment. Differences in formation conditions will obviously influence the final sulphide phases, but a change in redox conditions in a later stage in the geologic history may also affect the sulphides.

The thermomagnetic properties of the magnetic minerals from sites VBA1, VBA6 and VBA7 show distinct differences. The rock magnetic properties (chapter 6) also show that the magnetic sulphide content varies throughout the Vrica section. The variation in thermal decay curves of IRM, for example, confirms this view. The increase of IRM and $H_{cr}$ after heating to 200°C, however, seems to be a common phenomenon. In the stratigraphic interval between 50 and 90 m, for example, every sample that was heated to 200°C showed the alteration. Only the magnitude of the changes varies. Outside this interval no dedicated experiments were performed, but the occurrence of the alteration could be inferred from the demagnetization behaviour of the NRM in many samples from every part of the section.

## 9. The effect of the alterations on NRM behaviour

The enigmatic demagnetization behaviour of the NRM in many samples can be explained with the results of this alteration study. It is clear that thermal alterations influence the demagnetization behaviour above 350°C. The occurrence of these disturbances is not surprising. The thermal experiments of the present study show that the total IRM, which is already about 1000 times stronger than the NRM, increases by another factor of 10 during thermal treatment above 350°C. Viscous grains are also produced.

The more subtle alterations between 150 and 250°C have a notable influence on the thermal decay curves of different IRMs (figure 7). During heating a new remanence is formed with the same direction as the existing remanence causing an increase of remanence instead of the expected decrease. The same alteration reaction occurs in the magnetic minerals carrying the NRM. There are samples in with no signs of such an alteration (figure 1a). In these samples interpretation of the primary direction is straightforward. In a large number of samples distributed over the entire section, however, the influence of the alterations between 150°C and 250°C prevents the accurate determination of the separate NRM components (figure 1b,c,d). In some samples the remanence seems to increase in the same way as the IRM (figure 1c), but in general the direction of the changes appears to be random. No general relation between existing remanence components and the direction of the new remanence was found. This may be because the apparent 'demagnetized' directions are the combined effects of the demagnetization of existing remanence and the formation of new remanence. Alternatively, the explanation may be related to the occurrence of the alteration specifically in remanence carriers with higher AF coercivities. The high coercivities may point to a complicated sulphide structure and an accordingly complicated magnetization.

Interpretation of the NRM demagnetization results will strongly depend on the presence or absence of erroneous new remanence components after the heating steps between 150 and 250°C. When the alteration occurs, the demagnetization steps between 150 and 300°C have to be considered with caution. Because the much better known formation of spurious magnetizations already starts around 350°C and will usually give erroneous results well below 400°C, the temperature steps between 300°C and 350°C may be the most reliable in these samples.

The formation of similar deviating components at low temperatures during thermal demagnetization of NRM residing in magnetic sulphides was encountered by Krs et al. (1990) and Dinarés and Parès (1993). The NRM in the middle Miocene clay stones studied by Krs et al. is carried by greigite. In some samples a deviating demagnetization trajectory is observed in the same temperature range (150-300°C) as in the Vrica marls. This deviation has characteristics similar to the one observed in the present samples, but it is accompanied by a large increase in susceptibility. In the Vrica samples such an increase is not evident, although this may be due to the very low concentration of magnetic minerals compared to the paramagnetic clay minerals. Dinarés and Parès reported the occurrence of a

spurious component with a direction antiparallel to the characteristic direction in Jurassic to Eocene marly limestones. This component was only found during thermal demagnetization. The spurious component increased between 150°C and 300°C. In these marly limestones this was not accompanied by an increase of susceptibility. The phenomenon was attributed to an alteration in magnetic sulphides and thermal demagnetization of an IRM indicated maximum blocking temperatures close to 400°C.

## 10. Conclusions

The magnetic sulphides in the Vrica marls are subject to thermal alterations. With the IRM monitoring method (van Velzen and Zijderveld, 1992) the alterations can be studied in detail. Alterations starting at about 350°C are due to the oxidation of pyrite and other iron sulphides. The alterations start with the formation of magnetite-like grains. Subsequently these grains are converted to hematite.

The first alteration is observed at much lower temperatures. After heating at 150°C and 200°C, an increase is observed of the total IRM that can be induced in the samples. It is demonstrated that it is likely an increase in remanence of a part of the magnetic minerals. During heating to 250°C, the total IRM starts to decrease and the new remanence formed at 150°C and 200°C has completely disappeared after heating to 330°C. In part of the samples the alterations affect the thermal demagnetization of the NRM. Occasionally the NRM increase that occurs at 150°C and 200°C can be related to the characteristic NRM component. In other cases no relation between the direction of the remanence increase and existing NRM components is apparent.

Thermomagnetic analysis of magnetic concentrates yields different results. During heating in argon the magnetization starts to increase below 190°C, while in air the increase starts at about 230°C. It is suggested that the alteration is related to the $\gamma$-transition in hexagonal pyrrhotite. In agreement with other workers it is suggested that the diffusion of vacancies, responsible for the change in magnetization at the $\gamma$-transition, already starts below the transition temperature and that it affects the magnetization of the pyrrhotite at temperatures as low as 150°C (Brodskaya and Gendler, 1979; Brodskaya, 1980; Bennet and Graham, 1980).

The different alteration temperatures may be related to the presence of oxygen in the sulphides. Oxygen in the pyrrhotite crystal may hinder the diffusion of vacancies (Graham et al., 1987). The increasing alteration temperatures may then be explained by an increasing oxygen content of the sulphides. The least oxygen is assumed to be present in the magnetic sulphides in the standard paleomagnetic samples. Some oxygen can be introduced in the magnetic sulphides during the concentration procedure due to superficial oxidation. During heating in air oxidation may proceed.

In the same way the presence of oxygen can stabilize the increased magnetization. Because the 'Curie point' of hexagonal pyrrhotite is in fact a reordering of vacancies, the influence of oxygen could be the same as before. Following the suggestion of Rochette et al. (1990), also the Curie temperature of monoclinic pyrrhotite could be influenced by the reordering of vacancies which results in the β-transition at temperatures only slightly higher than the observed Curie temperature of monoclinic pyrrhotite. This could be an explanation for the high maximum blocking temperatures (330-375°C) of part of the remanence.

It is suggested that the magnetic sulphides are inhomogeneous, having partly the ferrimagnetic structure of monoclinic pyrrhotite, partly the more or less ideal antiferromagnetic structure of hexagonal pyrrhotite. Heating results in the γ-transition in the hexagonal pyrrhotites and the new remanence may adopt the remanence direction of the closely associated monoclinic pyrrhotite.

Possibly greigite carries part of the remanence. The thermomagnetic properties neither confirm nor exclude this. Since the described alteration does not occur in all samples with the same intensity, a varying amount of different magnetic sulphides may be present in different parts of the section.

**References**

Aguirre E. and Pasini G., The Plio-Pleistocene boundary. Episodes 8, 116-120, 1985.

Bennet C.E.G. and Graham J., New observations on natural pyrrhotites. Part III. Thermomagnetic experiments. American Mineralogist 65, 800-807, 1980.

Bennet C.E.G. and Graham J., New observations on natural pyrrhotites: magnetic transition in hexagonal pyrrhotite. American Mineralogist 66, 1254-1257, 1981.

Brodskaya S.Y., Pyrrhotite as a geothermometer of secondary heating of rock. Izvestiya Earth Phys. 16, 187-192, 1980.

Brodskaya S.Y. and Gendler T.S., Nature of the alteration of λ-pyrrhotite in the region of the γ-transition. Izvestiya Earth Phys. 15, 924-932, 1979.

Clark A.H., Quantitative determination of hexagonal and monoclinic pyrrhotites by X-ray diffraction: A discussion. Canadian Mineralogist 10, 278-280, 1970.

Coey J.M.D., Spender M.R. and Morrish A.H., The magnetic structure of the spinel $Fe_3S_4$. Solid State Commun. 8, 1605-1608, 1970.

Dekkers M.J., Magnetic properties of natural pyrrhotite. Part II. High- and low-temperature behaviour of Jrs and TRM as function of grain size. Phys. Earth Planet. Inter. 57, 266-283, 1989.

Dekkers M.J., Magnetic monitoring of pyrrhotite alteration during thermal demagnetization. Geoph. Res. Lett. 17, 779-782, 1990.

Dinarés J. and Parès J.M., Characterization of the NRM in some Mesozoic Pyrenean marly limestones. The role of the iron sulphides investigated by the temperature dependence of low-field susceptibility and standard rockmagnetic and XRD experiments. Abstract. European Union of Geosciences VII. Terra Abstracts, p. 84, 1993.

Freke, A. M. and Tate, D, 1961. The formation of magnetic iron sulphide by bacterial reduction of iron solutions. J. Biochem. Microbiol. Technol. Eng. 3, 29-39.

Graham J., Bennet C.E.G. and van Riessen A., Oxygen in pyrrhotite: 1. Thermomagnetic behavior and annealing of pyrrhotites containing small quantities of oxygen. American Mineralogist 72, 599-604, 1987.

Heider F. and Dunlop D.J., Two types of chemical remanent magnetization during the oxidation of magnetite. Phys. Earth Planet. Inter. 46, 24-45, 1987.

Hoffmann V., Greigite ($Fe_3S_4$): magnetic properties and first domain observations, Phys. Earth Planet. Inter. 70, 288-301, 1992.

Horng C.S., Laj C., Lee T.Q. and Chen J.C., Magnetic characteristics of sedimentary rocks from the Tsengwen-chi and Erhjen-chi sections in southwestern Taiwan. T. A. O. 3, 519-532, 1992.

Krs M., Novak F., Krsova M., Pruner P., Zeman A., Novak F. and Jansa J., A petromagnetic study of Miocene rocks bearing micro-organic material and the magnetic mineral greigite (Sokolov and Cheb basins, Czechoslovakia). Phys. Earth Planet. Int. 63, 98-112, 1990.

Krs M., Novak F., Krsova M., Pruner P., Kouklikova L. and Jansa J., Magnetic properties and metastability of greigite-smythite mineralization in brown-coal basins of the Krusne hory Piedmont, Bohemia. Phys. Earth Planet. Inter. 70, 273-287, 1992.

Levy L.W. and Quemeneur E., Sur la termolyse des sulfates ferriques basiques. Bull. Soc. Chim. Fr. 2, 495-503, 1968.

Lotgering F.K., On the ferrimagnetism of some sulphides and oxides, Thesis, University of Utrecht, 1956.

Lowrie W., Identification of ferromagnetic minerals in a rock by coercivity and unblocking temperature properties. Geophys. Res. Lett. 17, 159-162, 1990.

Marusak L.A. and Mulay L.N., Mössbauer and magnetic study of the antiferro to ferrimagnetic phase transition in $Fe_9S_{10}$ and the magnetokinetics of the diffusion of iron atoms during the transition. J. Appl. Phys. 50, 1865-1867, 1979.

Mullender T.A.T., van Velzen A.J. and Dekkers M.J., Continuous drift correction and separate identification of ferrimagnetic and paramagnetic contributions in thermomagnetic runs. Geophys. J. Int. 114, 663-672, 1993.

Nakazawa H. and Morimoto N., Phase relations and superstructures of pyrrhotite, $Fe_{1-x}S$. Mat. Res. Bull. 6, 345-358, 1971.

Néel L., Théorie du traînage magnétique des ferromagnétiques aux grains fins avec applications aux terres cuites. Ann. Geophys. 5, 99-136, 1949.

Nguyen T.K.T. and Pechersky D.M., Experimental study of chemical and crystallization remanent magnetizations in magnetite. Phys. Earth Planet. Inter. 46, 46-63, 1987.

Roberts A.P. and Turner G.M., Diagenetic formation of ferrimagnetic iron sulphide minerals in rapidly deposited marine sediments, South Island, New Zealand. Earth Planet. Sci. Lett. 115, 257-273, 1993.

Rochette P., Fillion G., Mattéi J.-L. and Dekkers M.J., Magnetic transition at 30-34 Kelvin in pyrrhotite: insight into a widespread occurrence of this mineral in rocks. Earth Planet. Sci. Lett. 98, 319-328, 1990.

Schwarz E.J., Dependence of magnetic properties on the thermal history of natural polycrystalline pyrrhotite, $Fe_{0.89}S$. J. Geomagn. Geoelectr. 19, 91-101, 1967.

Schwarz E.J, Magnetic phases in natural pyrrhotite $Fe_{0.89}S$ and $Fe_{0.91}S$. J. Geomagn. Geoelectr. 20, 67-74, 1968.

Schwarz E.J., Magnetic properties of pyrrhotite and their use in applied geology and geophysics. Geol. Surv. Can., Pap. 74-59, 24 pp, 1975.

Schwarz E.J. and Vaughan D.J., Magnetic phase relations of pyrrhotite. J. Geomagn. Geoelectr. 24, 441-458, 1972.

Skinner B.J., Erd R.C. and Grimaldi F.S., Greigite, the thio-spinel of iron; a new mineral. American Mineralogist 49, 543-555, 1964.

Snowball I.F., Magnetic hysteresis properties of greigite ($Fe_3S_4$) and a new occurrence in Holocene sediments from Swedish Lappland. Phys. Earth Planet. Inter. 68, 32-40, 1991.

Spender M.R., Coey J.M.D. and Morrish A.H., The magnetic properties and mössbauer spectra of synthetic samples of $Fe_3S_4$. Can. J. Phys. 50, 2313-2326, 1972.

Stokking L.B. and Tauxe L., Acquisition of chemical remanent magnetization by synthetic iron oxide. Nature 327, 610-612, 1987.

Sweeny R.E. and Kaplan I.R., Pyrite framboid formation: laboratory synthesis and marine sediments. Econ. Geol. 68, 618-634, 1973.

Tauxe L., Opdyke N.D., Pasini G. and Elmi C., Age of the Plio-Pleistocene boundary at Vrica, Italy. Nature 304, 125-129, 1983.

Taylor L.A., The Fe-S-O system. Oxidation of pyrrhotites and the formation of anomalous pyrrhotite. Carnegie Institution of Washington Year Book 70, 287-289, 1971.

Thomson G.F., The anomalous demagnetization of pyrrhotite. Geophys. J. Int. 103, 425-430, 1990.

Tric E., Laj C., Jéhanno C., Valet J.P., Kissel C., Mazaud A. and Iaccarino S., High-resolution record of the Upper Olduvai transition from Po Valley (Italy) sediments: support for dipolar transition geometry? Phys. Earth Planet. Inter. 65, 319-336, 1991.

Uda M., Synthesis of magnetic $Fe_3S_4$. Sci. Pap. Inst. Phys. Chem. Res. (Jpn) 62, 14-23, 1968.

Vaughan D.J. and Craig J.R., Mineral Chemistry of Metal Sulfides, 493 pp., Cambridge University Press, Cambridge, 1978.

van Velzen A.J. and Zijderveld J.D.A., A method to study alterations of magnetic minerals during thermal demagnetization applied to a fine-grained marine marl (Trubi formation, Sicily). Geophys. J. Int. 110, 79-90, 1992.

van Velzen A.J., Dekkers M.J. and Zijderveld J.D.A., Magnetic iron-nickel sulphides in the Pliocene and Pleistocene marine marls from the Vrica section (Calabria, Italy). Earth Planet. Sci. Lett. 115, 43-55, 1993.

Ward J.C., The structure and properties of some iron sulphides. Rev. Pure Appl. Chem. 20, 175-206, 1970.

Zapletal K., Effect of intergrowths of the ferrimagnetic and antiferromagnetic phases on the rock magnetic properties of natural pyrrhotites. Phys. Earth Planet. Inter. 76, 151-162, 1993.

Zijderveld J.D.A., Hilgen F.J., Langereis C.G., Verhallen P.J.J.M. and Zachariasse W.J., Integrated magnetostratigraphy and biostratigraphy of the upper Pliocene-lower Pleistocene from the Monte Singa and Crotone areas in Calabria, Italy. Earth Planet. Sci. Lett. 107, 697-714, 1991.

# Curriculum Vitae

Adrianus Johannes van Velzen werd geboren op 10 januari 1959 in Geleen. De middelbare schoolopleiding volgde hij aan het St. Michiel Lyceum te Geleen. In 1977 behaalde hij het diploma Gymnasium-β en begon vervolgens aan de studie Natuurkunde aan de Rijksuniversiteit te Utrecht. Zijn kandidaatsexamen met bijvak Geofysica kreeg hij in juni 1980 uitgereikt. Het doktoraal examen Experimentele Natuurkunde met bijvakken Theoretische Natuurkunde en Capita Selecta van de Wiskunde behaalde hij in augustus 1985.

Vanaf november 1987 werkte hij aan het onderzoek voor dit proefschrift als Assistent in Opleiding bij het Paleomagnetisch Laboratorium 'Fort Hoofddijk' van de Universiteit Utrecht.

In september 1994 gaat hij voor een jaar naar het Laboratoire de Géophysique et Tectonique te Montpellier en het Laboratoire de Géologie du Quaternaire te Marseille voor een onderzoek in het kader van een Europees samenwerkingsproject op het gebied van gesteentemagnetisme.

# Dankwoord

Het is een hele opgave zo'n tijd met iets bezig te zijn zonder direkt resultaat te zien. Twijfels over het nut zijn er volop. Belangstelling van anderen is dan een bron van inspiratie. Mijn dank aan iedereen die gedurende al die tijd binnen of buiten het werk op die manier iets aan dit proefschrift hebben bijgedragen.

Mijn promotor Prof. Zijderveld heeft met zijn heldere kijk de vinger op menige zwakke plek in mijn teksten gelegd. Het uiteindelijke manuscript is daardoor een stuk begrijpelijker geworden voor de argeloze lezer. Mark Dekkers heeft me ingewijd in het gesteentemagnetisme en alles wat daarbij komt kijken. Zijn brede geochemische kennis en zijn schat aan literatuur waren een houvast. Cor Langereis heeft me veel werk uit handen genomen door te zorgen voor uitstekende computerfaciliteiten en door de vele computerprogramma's van zijn hand. Met zijn drieën hebben ze me de veelzijdigheid van paleomagnetisme laten zien.

Tom Mullender is om meer dan één reden belangrijk voor me geweest. Hij heeft me op weg geholpen en in de loop der jaren is hij steeds een aanspreekpunt geweest. Het onderhoud de apparatuur en vooral ook zijn eigen verbeteringen en ontwerpen hebben een wezenlijke bijdrage geleverd tot mijn onderzoek. De ontelbare rondjes die we gezamenlijk hardlopend hebben afgelegd waren een welkome ontspanning van de dagelijkse beslommeringen.

Henk Meijer komt speciale dank toe voor de vele maanden gedurende welke hij met veel toewijding ontelbare metingen voor mij heeft gedaan. Hij weet hoeveel werk er in één zo'n grafiekje kan zitten.

De veldwerken waren een bijzondere belevenis. Piet-Jan Verplak heeft daar veel werk verzet (denk alleen al aan Vrica B). Ton van Hoof en Peter Scheepers hebben het gedurende een aantal weken met mij uit kunnen houden in Zuid-Italië en een aantal jaren op Fort Hoofddijk. We hadden ieder ons eigen werk, maar hun bijdrage is ook in mijn werk terug te vinden. Pieter Vlag ben ik erkentelijk, omdat ik zijn gesteentemagnetische resultaten mocht gebruiken.

Willy van Beek heeft veel kopieën voor me gemaakt, maar belangrijker waren haar interesse en haar eigen kijk op het leven op het Fort. Een aantal buitenlandse gasten hebben gezorgd voor een welkome afwisseling, met name François Lévèque, Thomas Pick en Teresa Juárez.

De belangrijkste kategorie vormen natuurlijk familie en vrienden. Werken is leuk, maar het moet wel een hobby blijven. Mijn ouders wil ik bedanken voor hun steun, evenals Jolanda, Bram en Rosemary. Tenslotte natuurlijk Ineke, Kine en Teresa.

# Samenvatting

De gesteentemagnetische eigenschappen van twee verschillende Pliocene en Pleistocene mariene mergels uit Zuid-Italië zijn onderzocht. Verschillen in sedimentatiemilieu hebben ertoe geleid dat de magnetische mineralen in deze mergels geheel verschillend zijn. De hoofdstukken 2, 3 en 4 zijn gewijd aan de gesteentemagnetische eigenschappen van de vroeg Pliocene mariene mergels van de Trubi formatie. Deze pelagische mergels, die gemonsterd werden bij Eraclea Minoa in het Caltanissetta bekken op Zuid-Sicilië, hebben een hoog kalkgehalte (60-80%), een sedimentatiesnelheid van 4-5 cm/1000 jaar en een cyclische lithology die verband houdt met de variaties van de baan van de aarde (foto 1, blz. 11). De primaire remanentie in de Trubi mergels wordt gedragen door magnetiet. In de hoofdstukken 5, 6 en 7 worden de magnetische resultaten van de laat Pliocene tot vroeg Pleistocene marine mergels van de Vrica sectie behandeld (foto 2, blz. 11). De Vrica sectie is de type sectie voor de grens tussen het Plioceen en het Pleistoceen en is gelegen in het Crotone-Spartivento bekken in Noord-Calabrië. De mergels zijn in ondieper water afgezet met een sedimentatiesnelheid tussen 25 en 50 cm/1000 jaar en hebben een kalkgehalte van slechts 15 tot 25%. Klimatologische fluctuaties tengevolge van variaties in de baan van de aarde hebben in deze mergels gezorgd voor veelvuldig voorkomende sapropelitische lagen. De belangrijkste magnetische mineralen in de Vrica mergels zijn magnetische sulfides.

In hoofdstuk 2 worden de gesteentemagnetische eigenschappen van de Trubi mergels onderzocht. Gebruikte meettechnieken zijn onder meer acquisitie van isotherme remanente magnetisatie (IRM), wisselveld demagnetisatie en thermische demagnetisatie van IRM, hysterese metingen en lage temperatuur metingen van IRM tot vloeibaar stikstof temperatuur. Zeer kleine magnetiet korrels met slechts één magnetisch domein (SD magnetiet) blijken de belangrijkste dragers van remanente magnetisatie te zijn in de Trubi mergels.

In hoofdstuk 3 wordt een methode gepresenteerd om omzettingen van magnetische mineralen tijdens stapsgewijze thermische demagnetisatie te bestuderen. De methode kijkt naar veranderingen in totale IRM en veranderingen in het coërciviteitsspectrum van deze IRM om te bepalen in welke magnetische fracties omzettingen optreden. De resultaten bevestigen dat magnetiet de belangrijkste remanentiedrager is. Tijdens verhitten tot temperaturen boven 390°C worden in de mergels nieuwe magnetische mineralen gevormd met eigenschappen vergelijkbaar met die van magnetiet. Omzetting van pyriet is hiervoor de meest waarschijnlijke bron. De vorming van de nieuwe magnetische mineralen blijkt uit een toename van de magnetische susceptibiliteit en de totale IRM en uit het optreden van viscueuze magnetisaties. Tevens wordt aangetoond dat de demagnetisatie boven 500°C gedeeltelijk het gevolg is van de omzetting van magnetiet naar hematiet. Dit heeft geen invloed op de analyse van de richtingen van de natuurlijke remanente magnetisatie (NRM).

Rond 150°C treedt een omzetting op die wel van invloed is op de juiste analyse van de NRM. Bij verhitten tot 150°C verdwijnt bijna alle IRM met wisselveld coërciviteiten hoger dan 100 mT, terwijl de IRM met wisselveld coërciviteiten lager dan 100 mT toeneemt. Deze omzetting wordt verklaart door aan te nemen dat de coërciviteit van SD magnetiet korrels afneemt tengevolge van de afname van mechanische spanning. In hoofdstuk 4 wordt uitgebreid aandacht besteed aan dit proces. Het blijkt dat de in de secties waargenomen variatie van remanente coërciviteiten vooral veroorzaakt wordt door verwering. Na verhitten tot 150°C zijn de hoge coërciviteiten gereduceerd tot waardes die normaal zijn voor magnetiet en daarmee zijn de oorspronkelijke verschillen in coërciviteit bijna verdwenen. Thermische demagnetisatie experimenten tonen dat magnetiet met abnormaal hoge coërciviteit verantwoordelijk is voor de waargenomen variatie. Als verklaring wordt voorgesteld dat tijdens verwering het oppervlak van de magnetiet korrels een lage temperatuur oxidatie heeft ondergaan. De resulterende mechanische spanning in de korrels veroorzaakt een toename van de coërciviteiten. Als de mergels verhit worden tot 150°C, neemt de spanning af, mogelijk door de diffusie van Fe-ionen en lege roosterplaatsen. Aangetoond wordt dat de toename van de coërciviteiten tengevolge van verwering een stabiliserend effect heeft op zowel de primaire component als ook op de secundaire component van de NRM. Na verhitten tot 150°C blijkt wisselveld demagnetisatie een veel effectievere methode om de NRM te analyseren dan zonder deze thermische behandeling.

Hoofdstuk 5 laat enige gesteentemagnetische parameters zien voor de Vrica mergels and presenteert de resultaten van microprobe analyses van magnetische concentraten van de mergels. In de magnetische concentraten bevinden zich kleine ijzersulfide korrels met een groot aantal verschillende samenstellingen. De composities variëren van pyriet tot monosulfides en zelfs sulfides met minder dan de helft zwavel. Opmerkelijk is de aanwezigheid van een aanzienlijke hoeveelheid Ni in veel van de sulfide korrels. Ni concentraties tot 35% van de totale gehalte aan metalen komen voor. Er wordt een overzicht gegeven van processen die zich afspelen tijdens vroeg diagenetische sulfaatreductie, om de aanwezigheid van magnetische monosulfides en de hoge Ni inhoud te verklaren. De gesteentemagnetische eigenschappen bevestigen dat magnetische sulfides de belangrijkste remanentiedragers zijn. De eigenschappen komen overeen met die van monocliene pyrrhotien, met uitzondering van de waargenomen hoge maximum blocking temperaturen.

In hoofdstuk 6 wordt de variatie in gesteentemagnetische eigenschappen in de Vrica sectie onderzocht. Met de waarnemingen worden de magnetische eigenschappen van de remanentie dragers verder geanalyseerd. De resultaten duiden op een magnetische mineralogie bestaande uit wisselende hoeveelheden monocliene pyrrhotien en greigiet en een kleinere hoeveelheid magnetiet. Een opvallende afname van NRM en IRM intensiteiten, die 15 m onder de Plioceen-Pleistoceen grens optreedt, wordt toegeschreven aan een afname van de sedimentatiesnelheid door veranderende klimaatomstandigheden.

De methode van hoofdstuk 3 wordt in hoofdstuk 7 gebruikt om het thermische gedrag te bestuderen van de magnetische sulfides in de Vrica mergels. Na

verhitten tot 150 en 200°C neemt de aanwezige remanentie in de monsters toe. In een aantal monsters veroorzaakt deze toename storende magnetisaties tijdens thermische demagnetisatie van de NRM. Tijdens thermomagnetische analyses van magnetische concentraten worden hogere omzettingstemperaturen gevonden. De omzetting begint in lucht bij ongeveer 190°C en in een argon atmosfeer bij 230°C. De kenmerken van de omzetting worden vergeleken met de $\gamma$-transition in hexagonale pyrrhotien. De variabele transitietemperaturen worden verklaard met de invloed van zuurstof op de diffusie van lege roosterplaatsen in het sulfide kristal. Inhomogene sulfide korrels of korrels met samenstellingen tussen hexagonale en monocliene pyrrhotien vormen mogelijk de belangrijkste magnetische sulfide fase. Greigiet is een andere mogelijke remanentiedrager. De coërciviteiten van sedimentaire greigiet komen overeen met die in de Vrica sectie, maar het waargenomen thermische gedrag komt niet overeen worden met bekende eigenschappen van greigiet.